5-2018

Dynamic Simulation and Neuromechanical Coordination of Subject-Specific Balance Recovery to Prevent Falls

Nicolas Antonio Vivaldi
University of Tennessee

Dynamic Simulation and Neuromechanical Coordination of Subject-Specific Balance Recovery to Prevent Falls

A Dissertation Presented for the
Doctor of Philosophy
Degree
The University of Tennessee, Knoxville

Nicolas Antonio Vivaldi
May 2018

Dedication

This dissertation is dedicated to my family. To my parents, Caroline and Noel, for raising me to be who I am, teaching me to think for myself, and supporting me no matter how many times I changed paths. To my sister, Angela, for setting an example of selflessness and kindness that I aspire to. And to my wife, Katelyn, who always sees the potential in others, especially when they do not, who encouraged me to reach higher when I was certain that I had already reached my peak, and who got me here by making me a better person every day. To everyone that I count as family, related or not, I love you and I appreciate your support through the years.

Acknowledgements

First, I would like to thank my advisor, Dr. Jeffrey A. Reinbolt, for offering me invaluable guidance in research and in life. I am grateful to have had the opportunity to pursue my PhD in such a phenomenal environment, and I hope to always approach research, learning, and teaching with the same enthusiasm that he brings to the lab.

I would like to thank the members of my dissertation committee, Dr. William Hamel, Dr. Eric Wade, and Dr. Joshua Weinhandl for their time and patience. They challenged me to always improve methods and solutions, and their feedback as well as what I learned from them significantly improved the quality of this work.

Thank you to Dr. Rod S. Barrett and Dr. Cyril Jon Donnelly for providing the experimental data without which this research would not have been possible. To Dr. Misagh B. Mansouri for piloting the MATLAB-OpenSim interface and for his advice and help throughout this project.

Finally, thank you to my family and friends who stood by me every step of the way. I would not have made it this far without all of you and your support has meant everything to me.

Abstract

Falls are the leading cause of fatal and nonfatal injuries in elderly people, resulting in approximately $31 billion in medical costs annually in the U.S. These injuries motivate balance control studies focused on improving stability by identifying prevention strategies for reducing the number of fall events. Experiments provide data about subjects' kinematic response to loss of balance. However, simulations offer additional insights, and may be used to make predictions about functional outcomes of interventions. Several approaches already exist in biomechanics research to generate accurate models on a subject-by-subject basis. However, these representations typically lack models of the central nervous system, which provides essential feedback that humans use to make decisions and alter movements. Interdisciplinary methods that merge biomechanics with other fields of study may be the solution to fill this gap by developing models that accurately reflect human neuromechanics.

Roboticists have developed control systems approaches for humanoid robots simultaneously accomplishing complex goals by coordinating component tasks under priority constraints. Concepts such as the zero-moment point and extrapolated center of mass have been thoroughly evaluated and are commonly used in the design and execution of dynamic robotic systems in order to maintain stability. These established techniques can benefit biomechanical simulations by replacing biological sensory feedback that is unavailable in the virtual environment. Subject-specific simulations can be generated by synthesizing techniques from both robotics and biomechanics and by creating comprehensive models of task-level coordination, including neurofeedback, of movement patterns from experimental data.

In this work, we demonstrate how models built on robotic principles that emulate decision making in response to feedback can be trained by biomechanical motion capture data to produce a subject-specific fit. The resulting surrogate can predict a subject's particular solution to accomplishing the movement goal of recovering balance by controlling component tasks. This research advances biomechanics simulations as we move closer towards the development of a tool capable of anticipating the results of rehabilitation interventions aimed at correcting movement disorders. The novel platform presented here marks the first step towards that goal, and may benefit engineers, researchers, and clinicians interested in balance control and falls in human subjects.

Table of Contents

Chapter 1: Introduction 1

1.1 Project Summary 2
1.2 Research Significance 3
1.3 Research Innovation 3
1.4 Research Methods 4
1.4.1 Specific Aim I: Synthesis of biomimetic stepping response to prevent falls after support surface perturbations 4
1.4.2 Specific Aim II: Development of neuromechanical models and evaluation of differences between single and multiple steppers 5
1.4.3 Specific Aim III: Evaluation of the predictive accuracy of subject-specific simulations of whole-body, step recovery strategies to prevent falls 6

Chapter 2: Literature Review 7

2.1 Background 8
2.1.1 Simulation in biomechanics 8
2.1.2 Operational space and prioritized task control 10
2.1.3 Applications to biomechanical simulations 12
2.1.4 Modeling decision making using robotics concepts 14
2.1.5 Identifying potential coordination strategies for balance recovery 17
2.1.6 Preliminary findings: ZMP based control of step response 20

Chapter 3: Aim I - Synthesis of Biomimetic Stepping Response to Prevent Falls after Support Surface Perturbations 24

3.1 Abstract 25
3.2 Introduction 25
3.2.1 Human balance and falls 25
3.2.2 Simulations advance balance research 26
3.2.3 Protective stepping response to loss of balance 26
3.2.4 Interdisciplinary approach to balance recovery research 27
3.3 Methods 27
3.3.1 Experimental data 27
3.3.2 MATLAB-OpenSim simulation framework 29
3.3.3 Zero-moment point 30
3.3.4 Prioritized task control 32
3.3.5 Biomimetic decision making 36
3.3.6 Simulation 37
3.4 Results 37
3.4.1 Response to 6 cm perturbation 37
3.4.2 Response to 12 cm perturbation 37
3.5 Discussion 41

Chapter 4: Aim II - Development of Neuromechanical Models and Evaluation of Differences Between Single and Multiple Steppers 45

4.1 Abstract 46
4.2 Introduction 46
4.2.1 Balance control and protective stepping 46
4.2.2 Task-based movement 47
4.3 Methods 47
4.3.1 Experimental data 47
4.3.2 Task space surrogate response surfaces 48
4.4 Results 51
4.4.1 Traditional biomechanical measures of balance recovery 51
4.4.2 Surrogate response surface models 51
4.5 Discussion 56
4.5.1 Instability projections of surrogate models 56
4.5.2 Biomechanically consistent differences between cohorts 56
4.5.3 Surrogate models in biomechanics simulations 57

Chapter 5: Aim III - Evaluation of the Predictive Accuracy of Subject-Specific Simulations of Whole-Body, Step Recovery Strategies to Prevent Falls 58

5.1 Abstract 59
5.2 Introduction 59
5.2.1 Factors impacting human balance 59
5.2.2 Simulation of dynamically changing tasks 60
5.3 Methods 61
5.3.1 Experimental balance recovery data 61
5.3.2 Compound surrogate response model 62
5.3.3 Prioritized task simulation of compound surrogate models of neuromechanics 64
5.4 Results 64
5.5 Discussion 70
5.5.1 Overview of results 70
5.5.2 Controller performance 74
5.5.3 Challenges and recommendations 74

Chapter 6: Conclusion 76

References 81

Appendix 89

Appendix A 90
A1: Response to 6 cm perturbation 90
A2: Response to 12 cm perturbation 93
Appendix B 96

B1: Surrogate response surfaces for step foot y and z components....96
B2: Surrogate response surfaces for posture y and z components....99
Appendix C 102
C1: Trial 0010....102
C2: Trial 0018....105
C3: Trial 0063....108
C4: Trial 0075....111
C5: Trial 0077....114
C6: Trial 0085....117

Vita 120

List of Tables

Table 1: Reports the results for subjects in each cohort. The instance where stepping foot overtakes ZMP is given as a percentage of step motion. Displacement between ZMP and step foot at the conclusion of the motion is reported in centimeters. 16
Table 2: Task prioritization hierarchy and definitions of behavior during balance recovery simulations. Locations are displayed in Figure 9, above. 33
Table 3: Table reporting traditional measures of the biomechanics of forward loss of balance: step length, forward lean, and center of mass height. Step length is reported both as a distance from both the ZMP and the plant foot. Forward lean angle is measured from the vertical y-axis (Fig. 18) to the posture task point using the subject's CoM as the origin point of rotation. 52
Table 4: Mean and standard deviation for biomechanical measures of balance recovery of each cohort displayed in Table 3. 52
Table 5: Table listing percent error values for each component of the three predicted task points located in the ground frame compared against the experimental data. Trial 64, displayed in Figures 28-31 above, was withheld from task point location mean calculation (bottom row) in order to remove outlier percentage error values. Mean error for all tasks in a single trial is diplayed in the right column. 69

List of Figures

Figure 1: Flowchart showing synthesis of techniques across multiple fields of study. Experimental motion capture data provides the basis for subject-specific surrogate modeling, which informs control strategy and decision making. Robotic task-based prioritization implements control outputs as biomechanical simulations of human movement..... 13
Figure 2: Depiction of the experimental setup before (left) and after (right) cable release with ground frame axis shown. The ZMP location is marked by the blue cylinder. 16
Figure 3: Depiction of before and after 12 cm posterior perturbation and subsequent step response. CoM, xCoM, ZMP, and swing foot locations were reported as displacements from the stance foot for model fitting..... 19
Figure 4: CoM plotted against swing foot for x-direction displacement. Data was separated by perturbation (anterior, posterior) and recovery (step, no step). Polynomial fits of order 1 to 5 were calculated for each control, perturbation, recovery, and direction. 19
Figure 5: (a) Comparison of experimental (green) and predictive simulation (red); (b) root-mean-square (RMS) error between experiment and predictive simulation task body center of mass positions. 23
Figure 6: Experimental data collection setup (left). Subjects were instructed whether to stand on one or two legs via directions on the screen. CAREN support surface perturbation was triggered after a randomized time interval. OpenSim scaled model (right). Models were scaled to the subject's body dimensions. Inverse kinematics was carried out on marker trajectory data to determine joint angle changes through time. 28
Figure 7: Flow chart of MATLAB-OpenSim platform. Beginning with a biomechanical model, the system outputs a motion file that is generated by using a closed-loop control system to minimize positional error between tasks and desired locations iteratively in time. 31
Figure 8: Side and front view of step response after forward loss of balance. Zero-moment point is displayed as a blue cylinder. The center of mass (green sphere) in human balance recovery closely follows the ZMP trajectory during stepping. ZMP is the point about which x and z moments sum to zero. 31
Figure 9: Task point definitions across the single-support model. Each task is fixed within its respective body's frame (e.g. Task #2 remains at the same position on the left foot relative to its frame of reference). 33
Figure 10: Plot of center of mass x-direction displacement from the support foot after 6 cm perturbation. 38
Figure 11: Plot of center of mass y-direction displacement from the support foot after 6 cm perturbation. 38
Figure 12: Plot of center of mass z-direction displacement from the support foot after 6 cm perturbation. 39
Figure 13: Plot of center of mass x-direction displacement from the support foot after 12 cm perturbation. 39
Figure 14: Plot of center of mass y-direction displacement from the support foot after 12 cm perturbation. 40
Figure 15: Plot of center of mass z-direction displacement from the support foot after 12 cm perturbation. 40

Figure 16: Time lapse showing 0 - 100% of response movement. (Above) Generic prioritized task, biomimetic decision, forward dynamics simulated response after 6 cm posterior perturbation. (Below) Subject 2, trial 31 response. 43
Figure 17: Time lapse showing 0 - 100% of response movement. (Above) Generic forward dynamics simulated response after 12 cm posterior perturbation. (Below) Subject 1, trial 46 response..... 44
Figure 18: Definition of task vectors for step trials. Task 1 defines vector V1 between whole-body center of mass and zero-moment point. Task 2 defines vector between whole-body center of mass and the center of mass of the step foot body (calcaneus). Task 3 defines vector between whole-body center of mass and the posture (C7 vertebrae). 49
Figure 19: Surrogate response surface models of step foot x direction task space from OMS cohort trials..... 53
Figure 20: Surrogate response surface models of step foot x direction task space from OSS cohort trials..... 53
Figure 21: Surrogate response surface models of step foot x direction task space from YSS cohort trials..... 54
Figure 22: Surrogate response surface models of posture x direction task space from OMS cohort trials..... 54
Figure 23: Surrogate response surface models of posture x direction task space from OSS cohort trials..... 55
Figure 24: Surrogate response surface models of posture x direction task space from YSS cohort trials..... 55
Figure 25: Depiction of K-Fold Cross Validation. In each iteration (K) a subset consisting of one trial is withheld from the modeling process (testing subset). The remaining N – 1 trials are used to build the model and train the system (training subset). The system is tested using the inputs that originally generated the test set. The output is compared to the test set in order to determine how well the model predicts the subject's response. The power behind this technique is that each trial is guaranteed use in both testing and training. 63
Figure 26: Definition and formulation of surrogate response surface. Task vectors were defined between CoM and plant foot (V1), CoM and step foot (V2) and CoM and posture (V3). Quadratic surfaces were used to model CoM and posture movement while a quintic fit was applied to the step foot. 63
Figure 27: Flow diagram describing system process. Initial states inform original task locations. Errors between task locations and compound surrogate models drive PID calculation of acceleration vector to move task points to desired positions by prioritized task calculation. Output movement prediction is compared to the testing subset movement. 65
Figure 28: Depiction of the lateral (top) and front (bottom) view of the predicted response (blue) to the 12 cm perturbation experienced by the subject in Trial 0064 and their experimental response (green). The predicted response was generated using the compound surrogate response surface of the other nine trials in the training set, while the experimental response was withheld in the testing set. 66
Figure 29: Displacement of center of mass in the x-direction from its initial position. Test line (green) represents experimental data collected from the subject during Trial 0064. Prediction line (blue) represents the system response to the same perturbation input. 67

Figure 30: Displacement of step foot in the x-direction from its initial position. Test line (green) represents experimental data collected from the subject during Trial 0064. Prediction line (blue) represents the system response to the same perturbation input. 67
Figure 31: Displacement of posture in the x-direction from its initial position. Test line (green) represents experimental data collected from the subject during Trial 0064. Prediction line (blue) represents the system response to the same perturbation input. 68
Figure 32: Predicted (Trial 0064) center of mass movement (blue) in the x-direction as a percentage of step response. Shaded (green) region represents one standard deviation about the mean experimental center of mass trajectory for all posterior perturbation trials. Both predicted and experimental trajectories are reported as displacements from the base of support (right, plant foot). 71
Figure 33: Predicted (Trial 0064) step foot movement (blue) in the x-direction as a percentage of step response. Shaded (green) region represents two standard deviations about the mean experimental step foot trajectory for all posterior perturbation trials. Both predicted and experimental trajectories are reported as displacements from the base of support (right, plant foot). 72
Figure 34: Predicted (Trial 0064) posture movement (blue) in the x-direction as a percentage of step response. Shaded (green) region represents one standard deviation about the mean experimental posture trajectory for all posterior perturbation trials. Both predicted and experimental trajectories are reported as displacements from the base of support (right, plant foot). 73
Figure 35: Plot of step foot x-direction displacement from the support foot (6 cm perturbation). 90
Figure 36: Plot of step foot y-direction displacement from the support foot (6 cm perturbation). 90
Figure 37: Plot of step foot z-direction displacement from the support foot (6 cm perturbation).91
Figure 38: Plot of posture x-direction displacement from the support foot (6 cm perturbation).. 91
Figure 39: Plot of posture y-direction displacement from the support foot (6 cm perturbation).. 92
Figure 40: Plot of posture z-direction displacement from the support foot (6 cm perturbation).. 92
Figure 41: Plot of step foot x-direction displacement from the support foot (12 cm perturbation). 93
Figure 42: Plot of step foot y-direction displacement from the support foot (12 cm perturbation). 93
Figure 43: Plot of step foot z-direction displacement from the support foot (12 cm perturbation). 94
Figure 44: Plot of posture x-direction displacement from the support foot (12 cm perturbation).94
Figure 45: Plot of posture y-direction displacement from the support foot (12 cm perturbation).95
Figure 46: Plot of posture z-direction displacement from the support foot (12 cm perturbation).95
Figure 47: Surrogate response surface models of step foot y-direction task space from OMS cohort trials. 96
Figure 48: Surrogate response surface models of step foot z-direction task space from OMS cohort trials. 96
Figure 49: Surrogate response surface models of step foot y-direction task space from OSS cohort trials. 97

Figure 50: Surrogate response surface models of step foot z-direction task space from OSS cohort trials..... 97
Figure 51: Surrogate response surface models of step foot y-direction task space from YSS cohort trials..... 98
Figure 52: Surrogate response surface models of step foot z-direction task space from YSS cohort trials..... 98
Figure 53: Surrogate response surface models of posture y-direction task space from OMS cohort trials..... 99
Figure 54: Surrogate response surface models of posture z-direction task space from OMS cohort trials..... 99
Figure 55: Surrogate response surface models of posture y-direction task space from OSS cohort trials..... 100
Figure 56: Surrogate response surface models of posture z-direction task space from OSS cohort trials..... 100
Figure 57: Surrogate response surface models of posture y-direction task space from YSS cohort trials..... 101
Figure 58: Surrogate response surface models of posture z-direction task space from YSS cohort trials..... 101
Figure 59: Depiction of the lateral (top) and front (bottom) view of the predicted response (blue) to the 6 cm anterior perturbation experienced by the subject in Trial 0010 and their experimental response (green). 102
Figure 60: Displacement of center of mass in the x-direction from its initial position. Test line (green) represents experimental data collected from the subject during Trial 0010. Prediction line (blue) represents the system response to the same perturbation input. 103
Figure 61: Displacement of step foot in the x-direction from its initial position. Test line (green) represents experimental data collected from the subject during Trial 0010. Prediction line (blue) represents the system response to the same perturbation input. 103
Figure 62: Displacement of posture in the x-direction from its initial position. Test line (green) represents experimental data collected from the subject during Trial 0010. Prediction line (blue) represents the system response to the same perturbation input. 104
Figure 63: Depiction of the lateral (top) and front (bottom) view of the predicted response (blue) to the 12 cm anterior perturbation experienced by the subject in Trial 0018 and their experimental response (green). 105
Figure 64: Displacement of center of mass in the x-direction from its initial position. Test line (green) represents experimental data collected from the subject during Trial 0018. Prediction line (blue) represents the system response to the same perturbation input. 106
Figure 65: Displacement of step foot in the x-direction from its initial position. Test line (green) represents experimental data collected from the subject during Trial 0018. Prediction line (blue) represents the system response to the same perturbation input. 106
Figure 66: Displacement of posture in the x-direction from its initial position. Test line (green) represents experimental data collected from the subject during Trial 0018. Prediction line (blue) represents the system response to the same perturbation input. 107

Figure 67: Depiction of the lateral (top) and front (bottom) view of the predicted response (blue) to the 6 cm anterior perturbation experienced by the subject in Trial 0063 and their experimental response (green). 108
Figure 68: Displacement of center of mass in the x-direction from its initial position. Test line (green) represents experimental data collected from the subject during Trial 0063. Prediction line (blue) represents the system response to the same perturbation input. 109
Figure 69: Displacement of step foot in the x-direction from its initial position. Test line (green) represents experimental data collected from the subject during Trial 0063. Prediction line (blue) represents the system response to the same perturbation input. 109
Figure 70: Displacement of posture in the x-direction from its initial position. Test line (green) represents experimental data collected from the subject during Trial 0063. Prediction line (blue) represents the system response to the same perturbation input. 110
Figure 71: Depiction of the lateral (top) and front (bottom) view of the predicted response (blue) to the 6 cm posterior perturbation experienced by the subject in Trial 0075 and their experimental response (green). 111
Figure 72: Displacement of center of mass in the x-direction from its initial position. Test line (green) represents experimental data collected from the subject during Trial 0075. Prediction line (blue) represents the system response to the same perturbation input. 112
Figure 73: Displacement of step foot in the x-direction from its initial position. Test line (green) represents experimental data collected from the subject during Trial 0075. Prediction line (blue) represents the system response to the same perturbation input. 112
Figure 74: Displacement of posture in the x-direction from its initial position. Test line (green) represents experimental data collected from the subject during Trial 0075. Prediction line (blue) represents the system response to the same perturbation input. 113
Figure 75: Depiction of the lateral (top) and front (bottom) view of the predicted response (blue) to the 12 cm posterior perturbation experienced by the subject in Trial 0077 and their experimental response (green). 114
Figure 76: Displacement of center of mass in the x-direction from its initial position. Test line (green) represents experimental data collected from the subject during Trial 0077. Prediction line (blue) represents the system response to the same perturbation input. 115
Figure 77: Displacement of step foot in the x-direction from its initial position. Test line (green) represents experimental data collected from the subject during Trial 0077. Prediction line (blue) represents the system response to the same perturbation input. 115
Figure 78: Displacement of posture in the x-direction from its initial position. Test line (green) represents experimental data collected from the subject during Trial 0077. Prediction line (blue) represents the system response to the same perturbation input. 116
Figure 79: Depiction of the lateral (top) and front (bottom) view of the predicted response (blue) to the 6 cm anterior perturbation experienced by the subject in Trial 0085 and their experimental response (green). 117
Figure 80: Displacement of center of mass in the x-direction from its initial position. Test line (green) represents experimental data collected from the subject during Trial 0085. Prediction line (blue) represents the system response to the same perturbation input. 118

Figure 81: Displacement of step foot in the x-direction from its initial position. Test line (green) represents experimental data collected from the subject during Trial 0085. Prediction line (blue) represents the system response to the same perturbation input. 118
Figure 82: Displacement of posture in the x-direction from its initial position. Test line (green) represents experimental data collected from the subject during Trial 0085. Prediction line (blue) represents the system response to the same perturbation input. 119

Chapter 1: Introduction

1.1 Project Summary

Falls are a leading cause of injury worldwide in the elderly population and people with conditions impacting neuromuscular control. This research aims to deepen fundamental understanding of the relationship between neurological control and balance recovery in human subjects. Balance is the most basic part of any coordinated movement in order to minimize risk of falling and subsequent injury. Therefore, it is necessary to accurately represent the complex decision making and execution that the human body displays in maintaining stability in a variety of situations. Simulations can be used to facilitate investigations on a subject-by-subject basis, and can provide insight into rehabilitation techniques by predicting clinical outcomes. Differences from person to person can dramatically impact the efficacy of prescribed interventions, so there is significant burden on researchers to provide accurate subject-specific modeling and simulation. A combination of techniques from the fields of biomechanics, robotics, and control systems engineering with *in vivo* experimental methods has been shown to provide quantifiable data related to human movement control and coordination. This information can be used to: investigate gaps in understanding of how the body's neuromuscular system makes decisions regarding stability; model an individual's loss of balance and predict his/her response; and simulate interventions aimed at improving stability in the virtual space, *in silico*. This research project seeks to: 1) link control systems and open-source software to simulate balance recovery in neuromechanical systems; 2) identify differences in coordination strategy employed by subjects that recover balance after a single step versus those that require multiple steps; 3) generate predictive simulations of subject-specific balance recovery.

1.2 Research Significance

This project is significant to advancing knowledge and understanding in more than one field of science and engineering. It bridges gaps existing between the experimental approaches used by physicians, physical therapists, and rehabilitation scientists and the computer simulation approaches used by engineers, mathematicians, and computer scientists. The proposed activities have combined techniques across different fields of study in order to create a new tool set for the evaluation of human movement control. This project is transformative because 1) simulations are be based on optimal, subject-specific models rather than generic, one-size-fits-all models, producing the best possible results for individual subjects and 2) a quantitative basis to discover effective treatments is enabled, providing evidence-based knowledge about which treatment options work best in which subjects. Although the described activities focus on neuroscience and rehabilitation, these activities may impact other areas, including ergonomics, sports performance, and injury prevention.

1.3 Research Innovation

This project advances discovery and understanding for the study of human balance and coordination, which is integral to fall risk detection and prevention. A set of models representing the experimental data have been generated which can now be used in other unique research studies. The described activities enhance the infrastructure for scientific investigation of neuromuscular disorders by further developing the computational and theoretical framework and tools for next-generation research and education. Results have been disseminated broadly through SimTK.org, a community-building website with over 10,000 members (more than 5,000 of whom will be directly impacted by the proposed activities). Its potential widespread use could benefit society by advancing core medical technology, enabling new discoveries in the neuroscience and medical rehabilitation communities.

In the spirit of National Science Foundation topic areas, one such discovery may be a fundamental theory of physically-interactive motor control. A step toward such discoveries is identifying effective rehabilitation strategies for patients that do not respond to traditional training as well as those with other movement disorders.

1.4 Research Methods

The objective of this research is to develop a novel platform for emulating subject-specific human balance recovery by simulating the coordinated neuromechanical response to include somatosensory informed decision making. To do this, we paired OpenSim [1] and MATLAB ® (MathWorks, Natick, MA, USA) two widely used software packages with unique advantages and limitations. This was done by bridging the gap between the two programs using C++ code to access OpenSim's API through MATLAB's native compiler. In this way, we had access to the extensive computational toolbox and robust control system design in MATLAB, in addition to the musculoskeletal models and biomechanical analysis functions of OpenSim. The resulting tool was used to investigate human balance recovery in the following three studies:

1.4.1 Specific Aim I: Synthesis of biomimetic stepping response to prevent falls after support surface perturbations

Goal: The purpose of specific aim I was to answer the following questions:

1) How accurate are *in silico* human balance recovery trials that use humanoid robotics principles to model and replace somatosensory feedback compared to experimental trials?

Methods: To accomplish this study, a novel forward-dynamics simulation platform was developed to model human balance recovery after experiencing support surface perturbations. Zero-Moment Point (ZMP) and capture point calculations were selected as

replacements for the feedback system that replaces sensory information in determining where and when to step in order to prevent a fall.

Significance: This work produced a computational tool that can be used in a wide array of moment analysis studies to investigate the relationship between identifying potential dangers and generating a coordinated response.

1.4.2 Specific Aim II: Development of neuromechanical models and evaluation of differences between single and multiple steppers

Goal: The purpose of specific aim II was to answer the following questions:

1) Can subject-specific models of balance recovery neuromechanics be developed for cohorts with different stability metrics?
2) What are the differences in coordinated response between single and multiple steppers during balance recovery?

Methods: To accomplish this study, surrogate response surface models of 15 subjects (5 young, single steppers; 5 elderly single steppers; 5 elderly multiple steppers) were generated from experimental motion capture data. Each model represented the subject's complete response from decision to execution of a step. The models were compared across cohorts to identify statistical differences in chosen coordination patterns.

Significance: This study identifies areas for targeted improvement efforts in subjects that have lower levels of stability.

1.4.3 Specific Aim III: Evaluation of the predictive accuracy of subject-specific simulations of whole-body, step recovery strategies to prevent falls

Goal: The purpose of specific aim III was to answer the following questions:

1) With what percent accuracy can trained models predict response outcomes in subject-specific simulations?

Methods: To accomplish this study, the generic balance recovery platform developed in specific aim I was merged with the subject-specific surrogate models developed in specific aim II. The model was trained using the K-fold cross validation technique in order to determine the accuracy of predictive simulations given new perturbation inputs.

Significance: This work produces a comprehensive platform for rapidly and efficiently modeling specific subjects and predicting their balance recovery coordination within a percent accuracy envelope.

Chapter 2: Literature Review

2.1 Background

Chronic medical conditions create significant physical, psychological, and financial burdens on those affected. Of the various types of disorders, musculoskeletal diseases have been estimated to affect the largest proportion of the United States population. For the year 2011 the Medical Expenditures Panel Survey of the US Department of Health and Human Services reported 126.6 million adults affected by musculoskeletal conditions, which accounts for a staggering $874 billion in cost of treatment and lost wages (5.7% GDP) [2].

Simulations of human movement still lack the necessary models of somatosensory and proprioceptive feedback to investigate neurodegenerative conditions.

Advances in research methods and technology have created new platforms for the analysis of human movement. There are now sophisticated equipment setups that include high precision motion capture [3]–[6], EMG signal acquisition [7], and force data collection [8], [9]. Although our understanding of biomechanical systems is improving due to this increase in the amount of information that can be characterized, the underlying neural control mechanisms are still not fully understood. This is particularly true in the case of neurodegenerative diseases resulting in loss of normal musculoskeletal function since experimental design parameters are often limited by the progression of deterioration. In order to define the mechanisms that drive physical activity, novel assessment tools must be developed.

2.1.1 Simulation in biomechanics

Simulations provide an alternative or complementary method for evaluating complicated systems as compared to traditional experimentation. The primary strengths of simulations include the high volume of trials that can be completed in a short amount of time, as well as the diminished

costs. Simulations can be broadly divided into two categories: data-tracking and predictive. The first approach involves minimizing the error between the position of simulated points on the human body and their corresponding points from motion tracking data. The second approach requires the definition of some output parameter and the minimization of a performance variable, such as energy expenditure, in order to achieve the desired results [10].

These types of simulations have been used to help analyze the mechanics of various situations, including non-contact injuries [11], blunt force impacts and vehicular collisions [12]–[14], and balance control strategies and fall dynamics [15], [16], in order to predict outcomes and develop counter-strategies from the clinical, rehabilitation, and manufacturing stand points. The described circumstances are challenging to evaluate since they are aimed at understanding and/or preventing injuries. Simulation techniques provide an avenue by which we can study scenarios that would otherwise be too difficult or dangerous to recreate in the lab setting.

Similarly, some data cannot be easily collected through traditional experimentation, e.g. muscle forces and joint torques, although they are essential to understanding the human body system. Simulating movement by tracking motion capture data has proven to be a powerful tool in determining such quantities [17]–[19]. However, this method has its limitations because following previously recorded point trajectories means that the system cannot react to changes in scenario for which there is no existing data.

Predictive simulations offer a potential solution to various unanswered questions in the field of biomechanics. Virtually any conceivable scenario can be evaluated through proper task definition and simulation architecture. Previous work has already demonstrated this utility in calculating movement patterns of simple (1-3 DOF) models [10], anticipating gait adaptations in

changing environments [20], evaluating patient-specific gait modifications [21], and predicting surgical outcomes [22].

2.1.2 Operational space and prioritized task control

The results of predictive simulations can be improved by synthesizing methods from other fields of study into biomechanical models. Operational space control, which is generating movement by relating body movement spaces and forces to one another, is a widely-used methodology in the field of robotics [23]–[25]. For robotic manipulators, it allows tasks to be carried out by coordinating motions between body linkages while considering the constraints added by shifting frames of reference. In humanoid robotics, the need to control multiple, complex tasks simultaneously led to the development of prioritized task control [26]–[28]. Systems with increasing complexity can efficiently carry out desired tasks while maintaining body integrity, e.g. joint limitations, velocity and acceleration constraints, etc. Assigning tasks to be carried out within a designated hierarchy prevents unexpected interference among tasks which gives this method a distinct advantage in controlling multibody systems with multiple operational goals.

Disciplinary overlap between robotics, control systems engineering, and biomechanics could significantly improve subject-specific simulations.

Previous work [28] showed that a simulated humanoid robot can accomplish specified tasks by following such a set of linear controls for accelerations and forces. A set of *N* prioritized task points were defined over the body with corresponding task objectives, i.e. desired locations in the ground frame of each task point, which are fixed to separate task bodies. The *N* tasks are prioritized into a multi-task control structure which is calculated as in Equation 1:

$$\Gamma = (J_1^{*T} F_1) + (J_{2|1}^{*T} F_{2|1}) + \ldots + (J_{N|prec(N)}^{*T} F_{N|prec(N)}) = \sum_{k=1}^{n} J_{k|prec(k)}^{*T} F_{k|prec(k)} \quad (1)$$

Where Γ [Gamma] represents the prioritized torque control vector to be applied to the joints on the body; $J^{*T}_{k|prec(k)}$ [subscript k|prec(k)] is the transpose of the support-consistent constrained Jacobian associated with the k^{th} task; and $F_{k|prec(k)}$ [subscript k|prec(k)] is a force based on acceleration-level control incorporating gravity and Coriolis/centrifugal compensating terms [28].

The support-consistent constrained Jacobian matrix is calculated using the aggregate of null space matrices for all tasks preceding *k, 'prec(k)'*. That is to say, for the first task:

$$J_1^* = J_1\overline{SN_s} \tag{2}$$

Where J_1 [subscript 1] is the Jacobian matrix of body to which task 1 is fixed, N_s [subscript s] is the null space matrix of the support body (or bodies) that is in contact with the ground, and S is a selection matrix that identifies which bodies are currently functioning as support. For inferior tasks, i.e. k greater than 1, the null space term becomes a combination of prior null spaces:

$$J_{2|1}^* = J_2\overline{SN_s}N_1^* \tag{3}$$

$$N_1^* = N_s - \overline{J_1^*}J_1^* \tag{4}$$

Where (*) indicates that a value is constrained by the support null space and ($\bar{}$) is a mass constraint that limits movement based on the inertial properties of the system.

The force (*F*) formulation is dependent on the acceleration level control output (a_{ref} [subscript ref]) from each task's controller which designates the required vector to accomplish each task in priority order, as well as the dynamically consistent generalized inverse of the current task's Jacobian matrix (Λ [gamma]). The equation includes compensating terms for centrifugal (μ [mu]) and gravity (p) forces acting on the body:

$$F_k = \Lambda^*_{k|prec(k)}a_{ref} + \mu^*_{k|prec(k)} + p^*_{k|prec(k)} \tag{5}$$

Constraining elements of lower priority tasks in Equation 1 to operate within the null spaces of higher priority tasks prevents each subordinate task from interfering with the system achieving any defined previously. In doing so, Γ [Gamma] becomes a [q x 1] torque vector that drives the whole-body system made up of q joints to move in such a way that it will accomplish all defined tasks, so long as they are feasible under the burden of constraints placed by all prior tasks.

2.1.3 Applications to biomechanical simulations

Previous work [22] has shown that operational space prioritized task control can be adapted to execute under the OpenSim-MATLAB interface developed in [29], thereby creating a novel, closed-loop control system that accurately predicts balance recovery. The closed-loop controller serves as a way to include neurological feedback, such as stretch reflexes, to existing mechanical models.

Research on the underlying mechanisms of goal achievement and balance control have been explored previously using the task based robotics approach [30]–[33]. Figure 1 gives a conceptual flow diagram of the methodology used. In [30] multiple tasks were successfully implemented on musculoskeletal simulations where control of the center of mass through a series of objective locations was accomplished while maintaining < 10mm position error. Surrogate subject-specific models were developed in [31]–[33] in order to compare the OpenSim-MATLAB platform's performance to data collected experimentally. Response surfaces (RS) were fit to the data in order to compare the subjects' and simulations' responses to the same perturbation requiring a coordinated balance control effort. The results showed that the simulation data

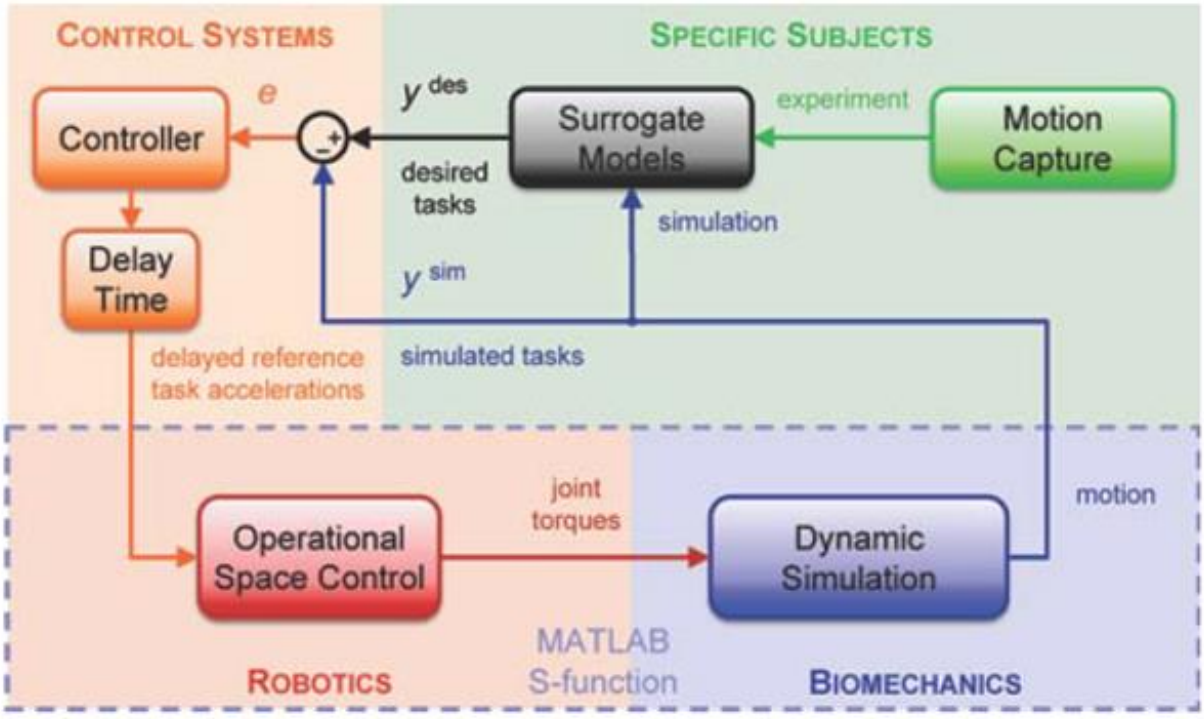

Figure 1: Flowchart showing synthesis of techniques across multiple fields of study. Experimental motion capture data provides the basis for subject-specific surrogate modeling, which informs control strategy and decision making. Robotic task-based prioritization implements control outputs as biomechanical simulations of human movement.

generated by the closed-loop controller could accurately predict subjects' response, and that the system itself did not pollute the data set with unnecessary noise [34].

While the methods described above have been used to evaluate balance control in specific subjects, these techniques have not yet been extended to include scenarios involving loss of balance that require expanding the base of support by taking a step in human systems. The literature shows that closed-loop control of balance recovery is feasible, therefore, the overall goal of the proposed work is to expand, improve, and apply this closed-loop framework in order to synthesize subject-specific balance recovery by predictive simulation.

2.1.4 Modeling decision making using robotics concepts

This section was originally published by Nicolas A. Vivaldi, Jeffrey A. Reinbolt, and Rod S. Barrett:

Vivaldi, N.A., Reinbolt, J.A., and Barrett, R.S. Using zero-moment point to predict single versus multiple step recovery from forward loss of balance. 8th World Congress of Biomechanics, Dublin, Ireland, July 8-12, 2018.

This section was accepted for presentation at the 8th World Congress of Biomechanics in Dublin, Ireland in July 2018. Nicolas Vivaldi conducted the investigation and wrote the abstract with feedback from Dr. Reinbolt and Dr. Barrett. Dr. Barrett provided the experimental data used for analysis.

Protective stepping is a natural response for preventing falls. Successful balance recovery is complex, and sometimes multiple steps are necessary [35]. *In silico* simulations could play a critical role in falls prevention since they can be used to investigate scenarios that are difficult to analyze experimentally [36]. It is a challenge to model the feedback-driven decision-making

processes involved in executing stepping response(s) in simulations of balance recovery [37]. In robotics Zero-Moment Point (ZMP) is used to measure stability [38] for AI decision-making regarding balance (for the complete formulation please see Chapter 3). We determined the utility of replacing biofeedback with ZMP by identifying differences in outcome measures between three cohorts: older multi steppers (OMS), older single steppers (OSS), and younger single steppers (YSS).

We used experimental data collected at 200 Hz from 14 subjects standing with feet shoulder width apart, tilted forward via cable in parallel with the floor until 20% of body weight was recorded by a series-connected load cell [35] (Figure 2). Subjects were then released and instructed to take a single step. We calculated the ZMP using pelvis residual forces and moments taken from inverse dynamics and body kinematics. We reported

stepping foot overtaking the forward component of the ZMP as a percentage of the step movement to normalize results across trials. Distance between the step foot placement at contact and ZMP was also calculated.

OMS brought the stepping foot past the ZMP later during balance recovery (92.9% ± 6.2) as shown in Table 1. Both single stepper cohorts overtook the ZMP with at least 20% of the step left to complete (older: 80.4% ± 1.9; younger: 73.8% ± 18.3). The OMS cohort was compared by *t*-test to both OSS and YSS and was statistically different at a 5% significance level with $p = 0.0049$ and $p = 0.0317$, respectively. OSS compared to YSS was not statistically different at this significance level. OMS had less than half the distance between step placement and ZMP as compared to single steppers.

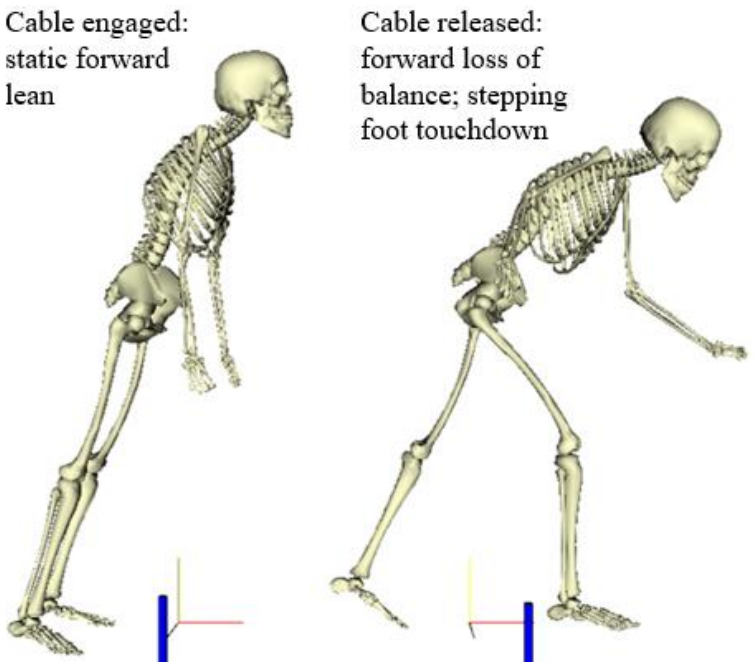

Figure 2: Depiction of the experimental setup before (left) and after (right) cable release with ground frame axis shown. The ZMP location is marked by the blue cylinder.

Table 1: Reports the results for subjects in each cohort. The instance where stepping foot overtakes ZMP is given as a percentage of step motion. Displacement between ZMP and step foot at the conclusion of the motion is reported in centimeters.

Cohort	***Subject***	***% Step***	***Mean***	***Displacement (cm)***	***Mean (cm)***
Older Multi Steppers	1	93.4	92.9 ± 6.2	15.8	12.8 ± 6.0
	2	92.4		18.7	
	3	81.7		17.4	
	4	100.0		2.7	
	5	96.9		9.1	
Older Single Steppers	6	81.8	80.4 ± 1.9	21.5	30.4 ± 5.7
	7	77.4		29.8	
	8	79.4		38.4	
	9	80.5		27.9	
	10	83.0		34.3	
Younger Single Steppers	11	81.0	82.9 ± 2.6	32.5	25.2 ± 6.4
	12	84.4		30.5	
	13	86.3		18.0	
	14	79.8		19.8	

In humans, somatosensory feedback provides recognition of failure to recover balance by single step and results in multiple steps. Simulations can be improved by modeling the recognition and adaptation process using a threshold trigger in lieu of biofeedback. ZMP is well suited to for this, since measures of swing foot position in relation to ZMP can predict when multiple steps are necessary. In future work, we will use ZMP to smoothly transition between control strategies for predicting single versus multi step responses.

2.1.5 Identifying potential coordination strategies for balance recovery

This section was originally published by Nicolas A. Vivaldi and Jeffrey A. Reinbolt:

Vivaldi, N.A. and Reinbolt, J.A. Identifying novel strategies for controlling step response during balance recovery simulations. 8th World Congress of Biomechanics, Dublin, Ireland, July 8-12, 2018.

This section was accepted for presentation at the 8th World Congress of Biomechanics in Dublin, Ireland in July 2018. Nicolas Vivaldi conducted the investigation and wrote the abstract with feedback from Dr. Reinbolt.

To reduce the incidence of falls worldwide, coordinated balance recovery simulations may offer new insights, but they need to be controlled in a complex, variable environment (e.g., perturbation, decision making, step response) [29], [37]. Center of mass (CoM), extrapolated center of mass (xCoM) [39], and Zero-Moment Point (ZMP) [38] are well-known in biomechanics and robotics and may fill this control strategy gap. We aimed to identify the relationships between these three measures and experimentally observed balance recovery to determine the best physiologically-consistent control strategy for simulations.

We collected experimental data at 250 Hz from 2 subjects (female 25 yrs | 1.72 m | 68.0 kg; male 25 yrs | 1.79 m | 84.5 kg) standing on one foot (Figure 3) during random anterior or posterior perturbation trials (6, 12 cm | 40 cm/s). We performed inverse kinematics, inverse dynamics, and body kinematics for each trial using OpenSim [1] and MATLAB® batch scripts. We calculated the ZMP using pelvis residual forces and moments and xCoM using an inverse pendulum model with the foot as the reference frame origin pivot point and the CoM as the mass load. We fit polynomial models (ranging linear to quintic) to determine the best fit (using R-squared values) between the three biomechanical or robotic measures and balance recovery after forward and backward loss of balance (Figure 4).

A combination of biomechanical and robotic measures using higher degree polynomial models fit the experimental data better with higher R-squared values (Figures 3 and 4). The CoM allowed the best overall fit to the step recovery in the ±X-direction ($0.67 \leq R2 \leq 0.71$). For posterior perturbations without stepping, the ZMP allowed best, but marginal, fit in the Z-direction ($R2 = 0.21$). For anterior and posterior perturbations with stepping, the xCoM allowed the best fit for the Z-direction ($R2 = 0.93$) and Y-direction ($R2 = 0.25$).

For generating simulations to study falls and fall-related injuries, we identified relationships using CoM, xCoM, and ZMP that may be used to control balance recovery simulations. Although one control strategy would be the simplest design, balance simulation is a complex, dynamic control problem that may benefit from hybrid control strategies using biomechanics and robotics measures. The stepping response can be controlled using the CoM (X-direction), xCoM (Y-direction), and ZMP (Z-direction); using other fits (sinusoidal, Fourier) did not change this control strategy ranking.

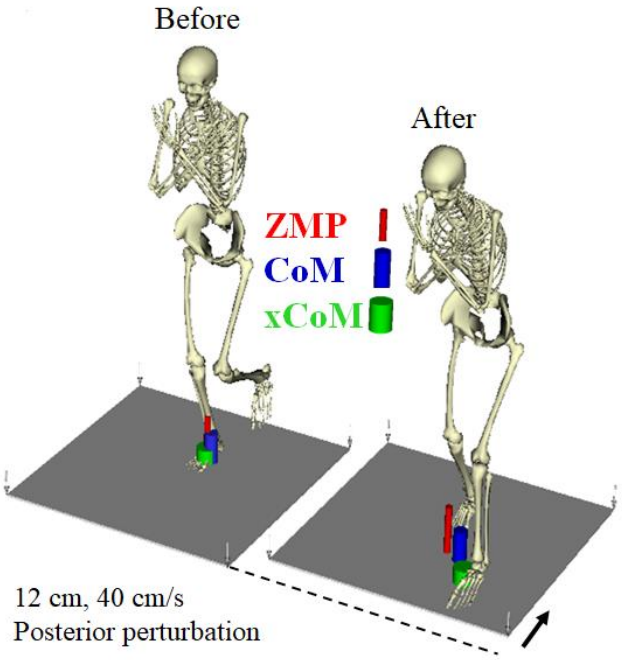

Figure 3: Depiction of before and after 12 cm posterior perturbation and subsequent step response. CoM, xCoM, ZMP, and swing foot locations were reported as displacements from the stance foot for model fitting.

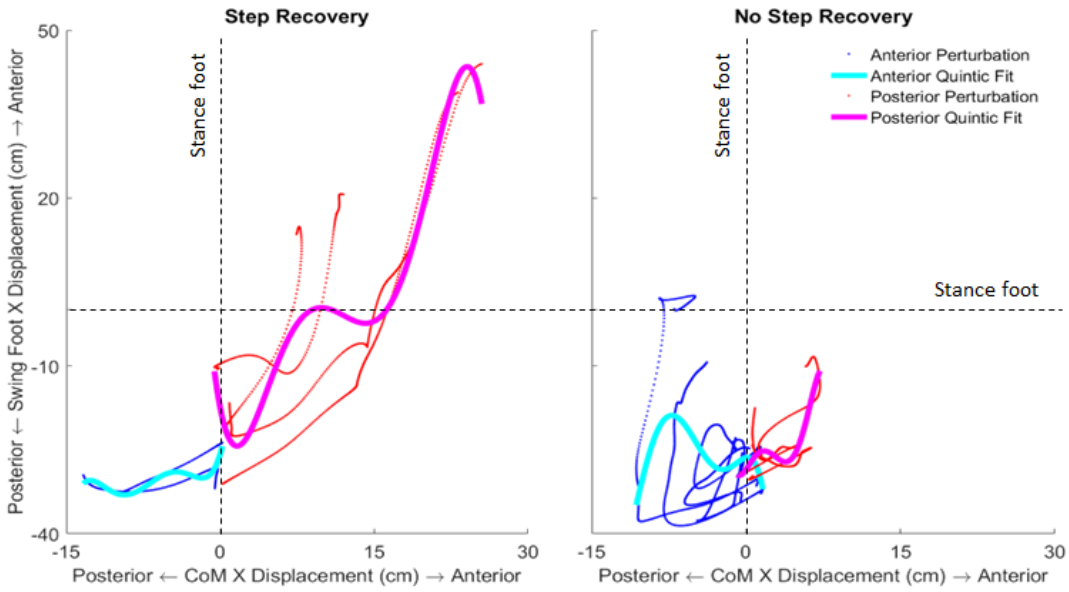

Figure 4: CoM plotted against swing foot for x-direction displacement. Data was separated by perturbation (anterior, posterior) and recovery (step, no step). Polynomial fits of order 1 to 5 were calculated for each control, perturbation, recovery, and direction.

2.1.6 Preliminary findings: ZMP based control of step response

This section was originally published by Nicolas A. Vivaldi and Jeffrey A. Reinbolt:

Vivaldi, N.A. and Reinbolt, J.A. Synthesis of subject-specific, task-level stepping response for predicting balance recovery. 26th Congress of the International Society of Biomechanics, Brisbane, Australia, July 23-27, 2017.

This section was accepted for presentation at the XXVI Congress of the International Society of Biomechanics in Brisbane, Australia in July 2017. Nicolas Vivaldi conducted the investigation and wrote the abstract with feedback from Dr. Reinbolt.

Fall related injuries motivate balance control studies focused on identifying prevention strategies for reducing the number of fall events. Experimental methods provide data about subjects' kinematic response to a loss of balance. However, simulations can offer additional insights, and may be used to make predictions about functional outcomes of various interventions. To make these predictions, simulations require accurate musculoskeletal modeling and robust control-system architecture. Several approaches already exist in biomechanics to generate accurate models on a subject-by-subject basis. Moreover, roboticists have developed control systems approaches for humanoid robots simultaneously accomplishing multiple complex tasks, including balance control [40]. Predictive subject-specific simulations of balance recovery can be generated by synthesizing approaches from both fields of study and creating surrogate models of task-level coordination from experimental data.

Related to fall prevention, roboticists use ZMP to maintain dynamic stability during inherently unstable tasks, such as stepping and gait. In human balance recovery, stepping is one of the primary reflexes used when it becomes impossible to keep the center of mass (CoM) over the

base of support (BoS) [41]. The step(s) redefine the area of the BoS in the horizontal plane to maintain control of the CoM, thereby preventing a fall.

In this study, we investigated the potential of using the ZMP approach for simulating human balance recovery during single-leg stance in response to perturbations at the BoS. Specifically, we examined support surface perturbations large enough to destabilize the subject (and model) to the point of making it impossible to recover balance without stepping. Our goal was to determine whether the ZMP approach could control the task-level motion of the model to generate a predictive, closed-loop simulation of stepping response that matches the subject's own balance recovery.

Experimental motion data was collected (female 25 yrs | 1.72 m | 68.0 kg) during perturbation from single-leg stance. An OpenSim 3D model with 17 degrees of freedom was scaled to match the subject. Trials in which a step was necessary to recover balance after perturbation (anterior | 6 cm | 40 cm/s) were identified and inverse kinematics determined model kinematics by matching the recorded marker trajectories. Body kinematics determined the body segment center of mass positions during the motion. The experimental positions of the CoM, swing foot, and torso were represented by surrogate second-order polynomial response surfaces in the anterior, vertical, and lateral directions, which defined these bodies' predicted motions. Proportional-integral-derivative (PID) controllers were used to calculate the task vectors needed to move the model by reducing errors between surrogate response surfaces and predicted body kinematics. The CoM horizontal plane position was controlled to be above the ZMP position, while vertical position followed its surrogate response surface. ZMP position was calculated from residual forces and

moments acting on the pelvis. Robotic control systems generated prioritized joint torques necessary for synthesizing the subject-specific stepping response.

The simulations resulted in a predicted stepping response to perturbation at the BoS (Figure 5a). CoM position was predicted well with the smallest RMS error (0.6 cm in the horizontal plane) among the 3 tasks. The ZMP control played a crucial role in the predicted CoM position. The largest RMS error (3.4 cm) was observed for the swing foot's vertical position, which undergoes the largest accelerations of any of the bodies during the stepping response (Figure 5b).

ZMP control with surrogate response surfaces is an effective approach for simulations predicting task-level stepping response during balance recovery. This preliminary work sets the foundation for the research described here, in that it serves as a proof of concept for merging robotics techniques with biomechanical simulations in order to replace biological feedback systems. The work described hereafter highlights the development of subject-specific, predictive simulations using this methodology.

a

b

Root Mean Square Error (cm)			
Task	***Anterior***	***Vertical***	***Lateral***
Center of mass	0.6	1.3	0.6
Swing foot	2.0	3.4	2.0
Torso	0.8	1.5	1.4

Figure 5: (a) Comparison of experimental (green) and predictive simulation (red); (b) root-mean-square (RMS) error between experiment and predictive simulation task body center of mass positions.

Chapter 3: Aim I - Synthesis of Biomimetic Stepping Response to Prevent Falls after Support Surface Perturbations

3.1 Abstract

Human balance control is a complicated process involving sensory inputs, propagation of neural signals, and musculoskeletal actuation. Because balance is a necessary part of the majority of movements that people use on a daily basis, it is essential for biomechanics researchers to fully understand the relationships between each component system that generates motion outputs. Modeling and simulation tools are highly valuable in that regard, as they can be used to calculate data that cannot be recorded in the lab setting (i.e. individual muscle forces, neuromechanical predictors, theoretical stability points, etc.). The purpose of Aim I is to develop and test a novel computational simulation platform that is capable of discerning between appropriate approaches to balance recovery given different disturbance conditions. The system will synthesize approaches from biomechanics, robotics, and control systems in order to simulate human model reactions to a loss of balance in the forward direction. The goals are 1) for the system to identify instances where limb articulation is sufficient to maintain balance, and carry out a coordinated movement to prevent falling over, and 2) for the system to detect an impending fall and step to recover balance. We compared the system's synthetic response to experimental balance data to determine whether or not the outputs are realistic.

3.2 Introduction

3.2.1 Human balance and falls

The link between biomechanics, the central nervous system, and sensory feedback requires further investigation in order to shed light on the fundamental principles of coordination that drive human movement. The majority of human movement is goal oriented, with maintaining balance chief among the tasks involved [42]. At its core, balance control is a self-preservation process

using sensory input to protect the body from harm by anticipating and preventing falls [43]. However, falls are a leading cause of both fatal (646,000) and nonfatal (37.3 million) injuries worldwide [44]. Research into individual shortcomings in balance and subsequent falls is limited due to the inherent danger of injury, especially in cohorts that include known fallers. A novel, quantitative tool set must be developed in order to expand falls research and improve functional outcomes of intervention strategies.

3.2.2 Simulations advance balance research

Simulations of human balance control and recovery may play a critical role in falls research by allowing investigators to safely assess individuals *in silico* while also identifying key relationships between the biological and mechanical processes involved that are difficult to evaluate experimentally [45]–[48]. Furthermore, simulations are capable of making predictions on a subject-specific basis that may give insight into the effects of interventions [20], [22], [37]. As a whole, simulations have proven to be effective tools for biomechanics research [49]–[53]. However, for the majority of simulations there is a gap where only the biomechanical and neuromuscular factors are characterized, not the cognitive inputs. Concepts from robotics and control systems can be used to fill the gap and improve the accuracy and quality of predictions.

3.2.3 Protective stepping response to loss of balance

Stepping is the one of the natural responses to perturbations that would otherwise cause a fall [54]–[57]. Tactile and visual feedback inform the brain and central nervous system as to the state of balance which in turn generate voluntary and involuntary control responses to regain stability [58]–[62]. Modeling the decision and execution processes involved in determining the appropriate step/no step response requires feedback and trigger systems to be included in the

simulation architecture. For this purpose, a hybrid approach to modeling from multiple fields of study would benefit system design.

3.2.4 Interdisciplinary approach to balance recovery research

The field of humanoid robotics is rapidly expanding with advanced mechanical constructs and artificial intelligence. Various systems now exist that are capable of analyzing inputs to emulate decision making and self-regulate coordination to mimic human responses [63]–[66]. Robotics concepts have started to make their way into biomechanics research with promising results [67]–[69]. However, disjointed approaches leave room for improvement of human subject simulations based on principles of robotic control. Here, we propose a novel system for simulating three-dimensional (3D) balance recovery from single leg support capable of discerning appropriate instances for taking a step based on a synthesis of prioritized task control [28], extrapolated center of mass (xCoM) stability criteria [39], and zero-moment point recovery determination [38].

3.3 Methods

3.3.1 Experimental data

We collected experimental data at 250 Hz from 2 subjects (female 25 yrs | 1.72 m | 68.0 kg; male 25 yrs | 1.79 m | 84.5 kg) standing on one foot (single-leg support) (Figure 6, left) during random support surface perturbation trials (6, 12 cm | 40 cm/s) in the posterior direction. The perturbations were introduced via the CAREN (Computer Assisted Rehabilitation Environment) system (Motekforce Link, Amsterdam, The Netherlands) which served as the support surface in each trial. Subjects were instructed to keep their arms crossed over their chest and to maintain balance (with or without stepping), and the free swing foot was lifted to a minimum of 10 cm

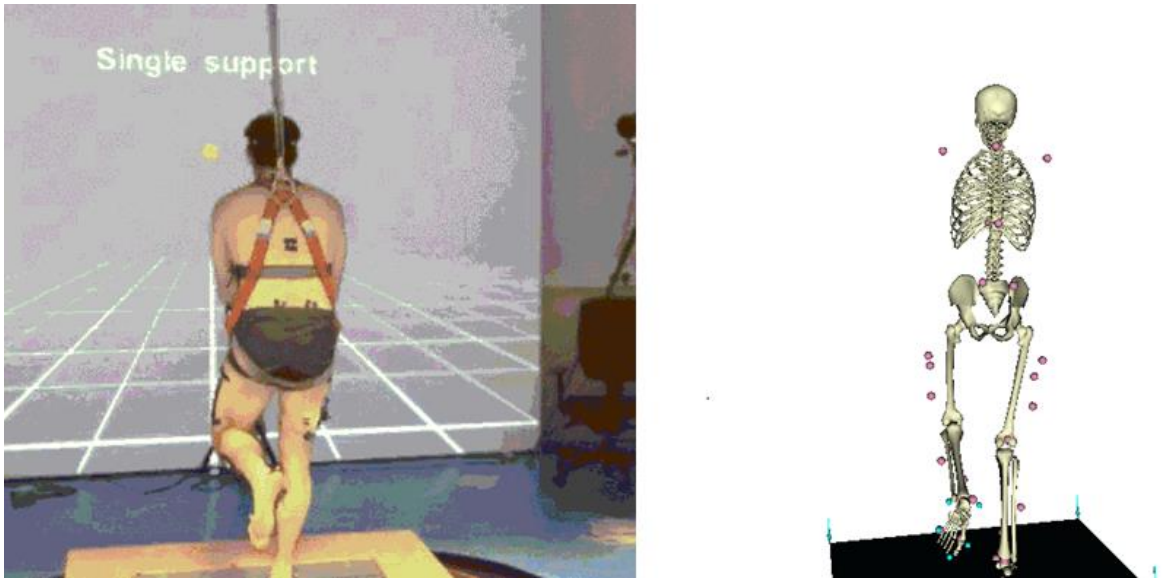

Figure 6: Experimental data collection setup (left). Subjects were instructed whether to stand on one or two legs via directions on the screen. CAREN support surface perturbation was triggered after a randomized time interval. OpenSim scaled model (right). Models were scaled to the subject's body dimensions. Inverse kinematics was carried out on marker trajectory data to determine joint angle changes through time.

above the support surface. Marker trajectory data was recorded using VICON (Oxford, UK) t40 cameras and filtered with a low-pass cutoff frequency of 6 Hz.

We used OpenSim's inverse kinematics (IK) tool in order to process the raw marker trajectory (.trc) files. Inverse kinematics minimizes the sum of the squared errors between the experimental marker locations (x_i^{exp}) and the scaled model's markers ($x_i(q)$) in the ground reference frame at each time step by calculating the joint angles (q) that align the bodies in the "best match" position. This is done iteratively according to user defined weights (w_i, ω_j) applied to each marker in order to assign differing levels of importance to the position matching, which in turn affects the calculated joint angles.

$$\min_{\mathbf{q}}\left[\sum_{i\in\text{markers}} w_i \left\|\mathbf{x}_i^{\exp}-\mathbf{x}_i(\mathbf{q})\right\|^2+\sum_{j\in\text{unprescribed coords}} \omega_j\left(q_j^{\exp}-q_j\right)^2\right]$$
$$q_j = q_j^{\exp} \text{ for all prescribed coordinates } j$$

The output of the IK routine is a motion file (.mot) that when paired with the model of the subject in OpenSim shows their movement during that trial.

With this data we used OpenSim's body kinematics (BK) analysis tool. The BK tool calculates the position and velocity of each body's center of mass, as well as the whole-body CoM. This provides data on limb coordination and establishes a measure of comparison between the experimental and simulated data sets.

3.3.2 MATLAB-OpenSim simulation framework

We expanded the platform that was developed in [29] for merging the open-source biomechanics software OpenSim [1] with the computational software MATLAB ®. This was accomplished using MATLAB's mex function, which allows users to compile C++ code in MATLAB as an s-function which then joins the long list of processes already housed in the

program's toolboxes. The resulting system laid the groundwork for closed-loop, forward dynamics simulation by consolidating biomechanical analyses, computational integration, and continuous feedback into one schematic. The loop begins with the initial states of the model, and determines the positional error between task points and their respective desired locations. The error signals are used as inputs to proportional-integral-derivative (PID) controllers that calculate the acceleration vectors necessary to move each task point to its desired location. Each acceleration vector is used by the OpenSim API in calculating the necessary joint torques to accomplish each task. Figure 7 gives a flow chart describing the process.

Forward dynamics are used to compute accelerations from the calculated joint torques.

$$\ddot{\boldsymbol{q}} = \left[\boldsymbol{M}(\boldsymbol{q})\right]^{-1}\left\{\boldsymbol{\tau} + \boldsymbol{C}(\boldsymbol{q},\dot{\boldsymbol{q}}) + \boldsymbol{G}(\boldsymbol{q}) + \boldsymbol{F}\right\}$$

Where $[M(q)]^{-1}$ [superscript -1] is the mass matrix inverse; τ are the joint torques; *C, G, and F* are Coriolis and centrifugal forces, gravitational forces, and external forces, respectively. This process applies the accelerations at each generalized coordinate (q) and the movement in each time frame is appended at the end of the motion file.

3.3.3 Zero-moment point

As its name suggests, the zero-moment point is the point on the ground about which the sum of the moments is zero about the two non-vertical, ground frame axes. Roboticists use ZMP calculation to locate the mathematically ideal tracking point for a system's center of mass during dynamic movement. Theoretically, above this point the CoM would not experience any net moments that would destabilize the system. Figure 8 shows an experimental balance recovery trial [41] with the subject's calculated ZMP location.

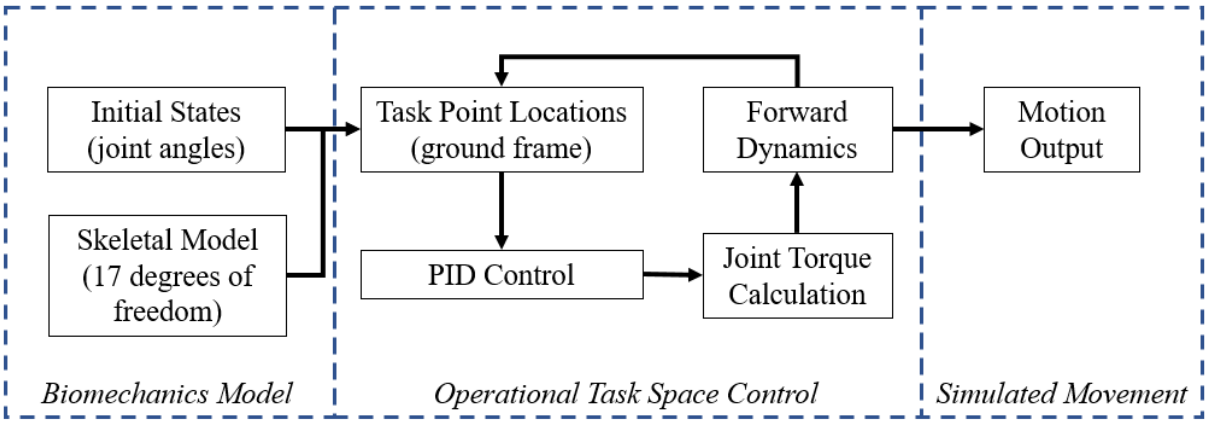

Figure 7: Flow chart of MATLAB-OpenSim platform. Beginning with a biomechanical model, the system outputs a motion file that is generated by using a closed-loop control system to minimize positional error between tasks and desired locations iteratively in time.

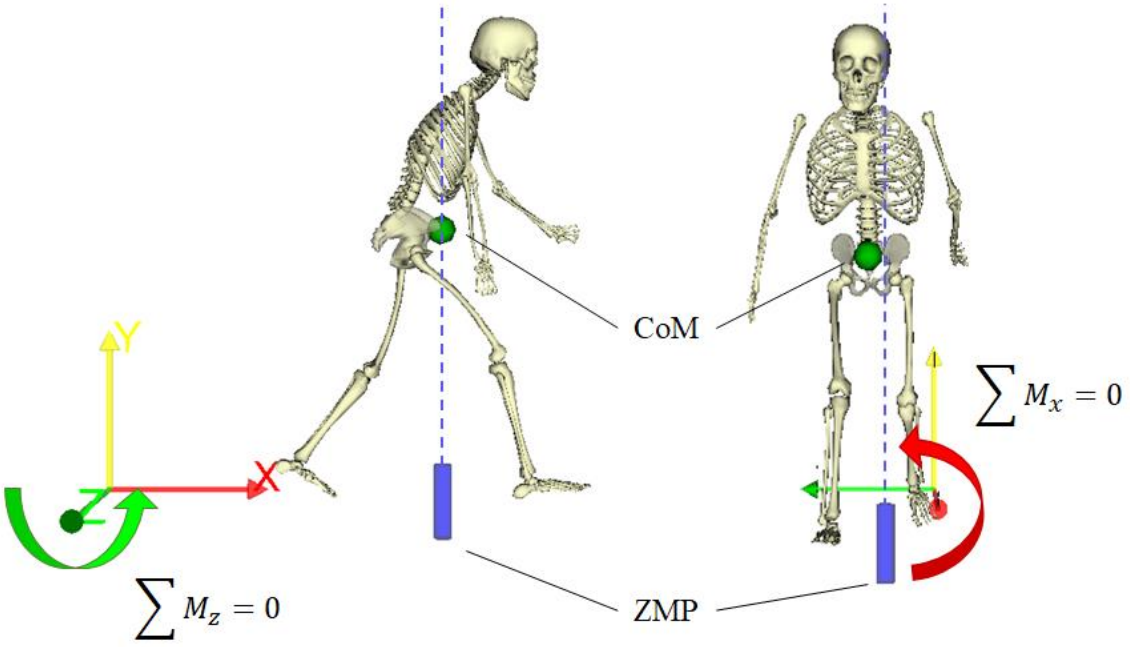

Figure 8: Side and front view of step response after forward loss of balance. Zero-moment point is displayed as a blue cylinder. The center of mass (green sphere) in human balance recovery closely follows the ZMP trajectory during stepping. ZMP is the point about which x and z moments sum to zero.

As the figure depicts, living systems also make use of ZMP for stability, although the brain interprets somatosensory feedback to generate musculoskeletal response rather than performing spatial calculations. However, the parallel exists allowing ZMP to be exploited for simulations as shown in [68], [70]. ZMP location was calculated by adding the residual moments acting on the free-floating pelvis body (M_{pelvis}) to the cross product between the residual forces acting on the pelvis (F_{pelvis}) and its location in the ground frame (r_{pelvis}), and finding the moment arms that relate the vertical force to the x and z moments [71]:

$$[M_x \quad M_y \quad M_z]_{zmp} = M_{pelvis} + r_{pelvis} \times F_{pelvis}$$

$$[F_x \quad F_y \quad F_z]_{zmp} = F_{pelvis}$$

$$zmp_x = M_z/F_y$$

$$zmp_x = -M_x/F_y$$

3.3.4 Prioritized task control

Previous work [15] has shown the efficacy of adapting robotic prioritized task control for use in simulations of human subjects. The benefit of this approach is that complicated whole-body goals, such as balance control/recovery, can be decomposed into component tasks, which can then be assigned rank relative to each other. This technique has been thoroughly explored for use with simulations of humanoid robots [28], and can be adapted for *in silico* musculoskeletal simulations of human subjects. Here, we identified three tasks for balance control and subsequent recovery after sufficiently large perturbations in priority order: (1) center of mass, (2) stepping foot, and (3) posture. Figure 9 shows the task points (green markers) as defined on the single support model. As previously stated, each task is assigned a rank relative to the others; Table 2 describes the hierarchy, as well as the task definition for each point. Proportional-Integral-Derivative (PID)

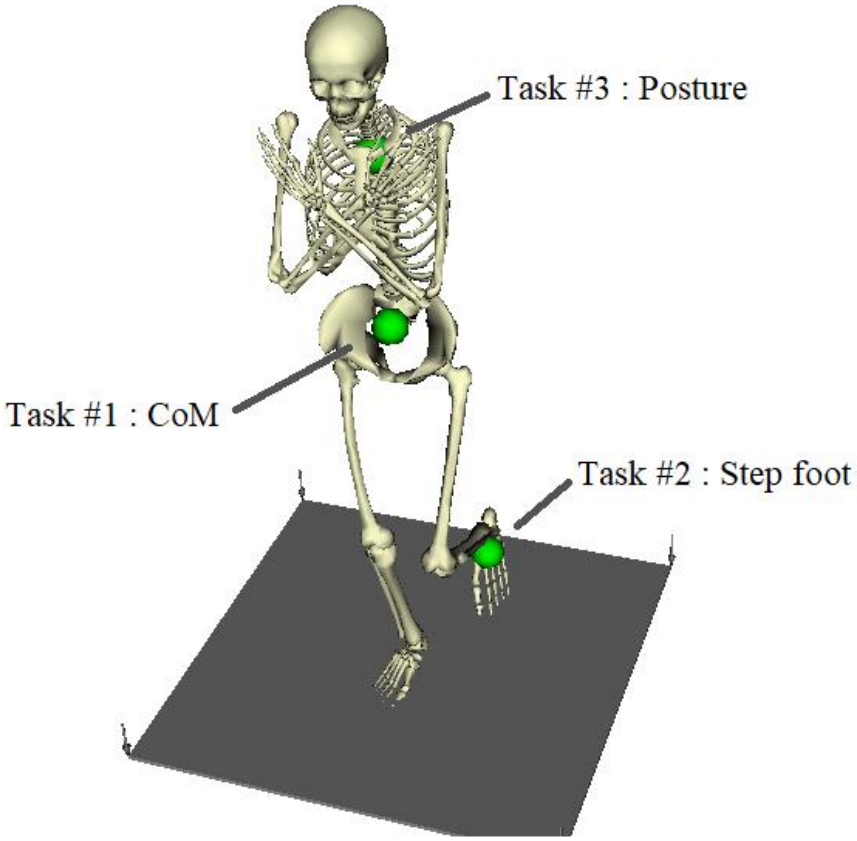

Figure 9: Task point definitions across the single-support model. Each task is fixed within its respective body's frame (e.g. Task #2 remains at the same position on the left foot relative to its frame of reference).

Table 2: Task prioritization hierarchy and definitions of behavior during balance recovery simulations. Locations are displayed in Figure 9, above.

Priority	***Name***	***Location***	***Description***
1	CoM	Whole-body CoM	Stay above the ZMP
2	Step foot	Left calcaneus CoM	Step to recover balance (if necessary)
3	Posture	C7 Vertebrae	Stay above the CoM

controllers calculate the acceleration vector necessary to minimize the error between each task point and its desired output. Within this framework, the joint torques necessary to accomplish each task, without letting lower priority tasks interfere with tasks above are calculated for each time step of a forward dynamics simulation following the process described in [15], [28]:

$$\Lambda_s = J_s[M(q)]^{-1} J_s^T \tag{6}$$

Λ [lambda], the support (*s*) operational space (mass/inertia) matrix, is formulated from the Jacobian matrix of the support body (in this case the right foot), J_s [subscript s], and the inverse of the system mass matrix, *M(q)*. It is used in Equation 7 to calculate the dynamically consistent generalized inverse of the support Jacobian, which is needed to find the support null space (N_s [subscript s], Equation 8) that is necessary for limiting movements to a feasible space.

$$\overline{J_s} = [M(q)]^{-1} J_s^T \Lambda_s \tag{7}$$

$$N_s = I - (\overline{J_s} J_s) \tag{8}$$

In Equation 9, we calculate the constrained projection (*) of the inverse inertia matrix, ϕ [phi], where *S* is a selection matrix identifying which joints, *q*, are available to generate torques for driving movement.

$$\phi^* = S_q N_s [M(q)]^{-1} [S_q N_s]^T \tag{9}$$

Equation 10 gives the formula for the generalized inverse of $S_q N_s$ [subscript q][subscript s], which is used to implement velocity constraints as well as to project each task Jacobian into the support-consistent space (Equation 11).

$$\overline{S_q N_s} = [M(q)]^{-1} [S_q N_s]^T \phi_*^{-1} \tag{10}$$

Equations 11 – 15 describe the process of calculating joint torques for accomplishing task 1, limited by the support space and system inertia. J_1* [subscript 1], the support-consistent reduced

Jacobian described previously, is calculated using J_1 [subscript 1], the station Jacobian at task point 1.

$$J_1^* = J_1\overline{S_q N_s} \tag{11}$$

For each task, Λ* [lambda] is the dynamically consistent generalized inverse of the task station Jacobian.

$$\Lambda_1^* = J_1^* \phi^* [J_1^{*T}]^{-1} \tag{12}$$

Compensating terms must be included in the calculation in order to account for additional forces that affect the body's movement. μ* [mu] is the compensating term for Coriolis and centrifugal forces, formulated using *b*, the vector of inertial forces across the body multiplied the full system Jacobian.

$$\mu_1^* = \Lambda_1^* J_1 [M(q)]^{-1} N_s^T b \tag{13}$$

*p** is the gravity compensation term where *g* is the gravitational vector [0 -9.81 0].

$$p_1^* = \Lambda_1^* J_1 [M(q)]^{-1} N_s^T g \tag{14}$$

Finally, the torque vector for accomplishing task 1, Γ_1 [gamma][subscript 1], is computed using the results of the above equations, and the acceleration vector output by the task 1 PID controller, a_{ref} [subscript ref].

$$\Gamma_1 = J_1^{*T}(\Lambda_1^* a_{ref} + \mu_1^* + p_1^*) = J_1^{*T} F_1 \tag{15}$$

Subsequent tasks must be limited to the prioritization hierarchy so as not to interfere with higher tasks. To do this we limit the support-consistent reduced Jacobian used in Equation 15 by imposing the null space of preceding tasks. As an example, the formulation of the task 2 support-consistent reduced Jacobian is given in Equations 16 – 18.

$$\overline{J_1^*} = \phi^* J_1^{*T} \Lambda_1^* \tag{16}$$

$$N_1^* = I - (\overline{J_1^*} J_1^*) \tag{17}$$

$$J_{2|1}^* = J_2^* N_1^* \tag{18}$$

Calculations from Equations 12 – 15 are then repeated using $J_{2|1}$* [subscript 2|1]. The full process is again repeated until the torque vectors from each task are calculated then summed to give the whole-body torque vector for coordinated movement (Equation 19).

$$\Gamma = \Gamma_1 + \Gamma_{2|1} + \Gamma_{3|2,1} \tag{19}$$

3.3.5 Biomimetic decision making

Task 2 described in Table 2 defines the motion of the step foot with the condition to only step if necessary. Humans do not always require a step to recover balance, and for simulations to be accurate a trigger is needed to model the decision making and execution process that differentiates balance control (postural adjustments and limb movement) from balance recovery (stepping). We used extrapolated center of mass (xCoM) as this trigger:

$$xCoM = x + \dot{x}\sqrt{l/g} \tag{20}$$

Where x is the current position of the CoM and l and g are the leg length and gravity term, respectively. This is based off the inverse pendulum model described in [39]. When perturbed, the projection of the model's xCoM on the ground translates forward. In the event that the xCoM remains inside the base of support, task 2 is defined as "no task" so that the foot can be manipulated to compensate for CoM inertia. When the xCoM leaves the base of support, it becomes impossible to recover balance based on the limited torque output of each joint. Therefore, in this case task 2 is defined as stepping to the point of maximum forward displacement of the xCoM from the CoM.

3.3.6 Simulation

Generic step response was simulated using the MATLAB-OpenSim platform with the prioritized task control and biomimetic decision making described above. The simulated model was perturbed using the same 6 and 12 cm posterior perturbations that subjects experienced in the experimental data collection trials. 5 contact points were modeled by Hunt-Crossley Force spheres placed at the toe, midfoot, and heel of the (right) support foot. This simulated frictional forces between the right calcaneus and the model's translatable support platform to perturb its stance. Each simulation was compared from quiet standing before perturbation to the time frame prior to contact between the step foot and ground.

3.4 Results

3.4.1 Response to 6 cm perturbation

The 6 cm perturbation did not provide sufficient disturbance to force the xCoM outside of the base of support. Of the three experimental trials that also had a 6 cm perturbation, one trial (subject 2, trial 31) did not produce a step response. Figures 10 – 12 compare the CoM task point trajectories plotted against time normalized to percentages of the movement. Each vector component (X, Y, or Z) is the displacement in that direction between the task point and the support foot. Figures 35-40 describing step foot and posture trajectories can be found in the Appendix A1.

3.4.2 Response to 12 cm perturbation

Due to the movement of the xCoM relative to the base of support, the generic response met the criteria for engaging task 2 as a step. Based on movement patterns, the generic response matched most closely with subject 1, trial 46. Figures 13 – 15 compare the CoM task point

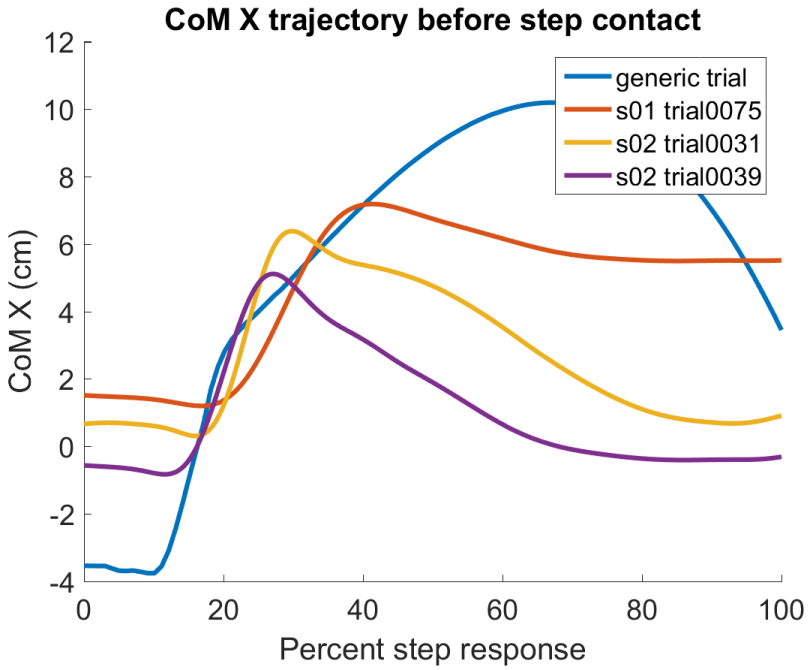

Figure 10: Plot of center of mass x-direction displacement from the support foot after 6 cm perturbation.

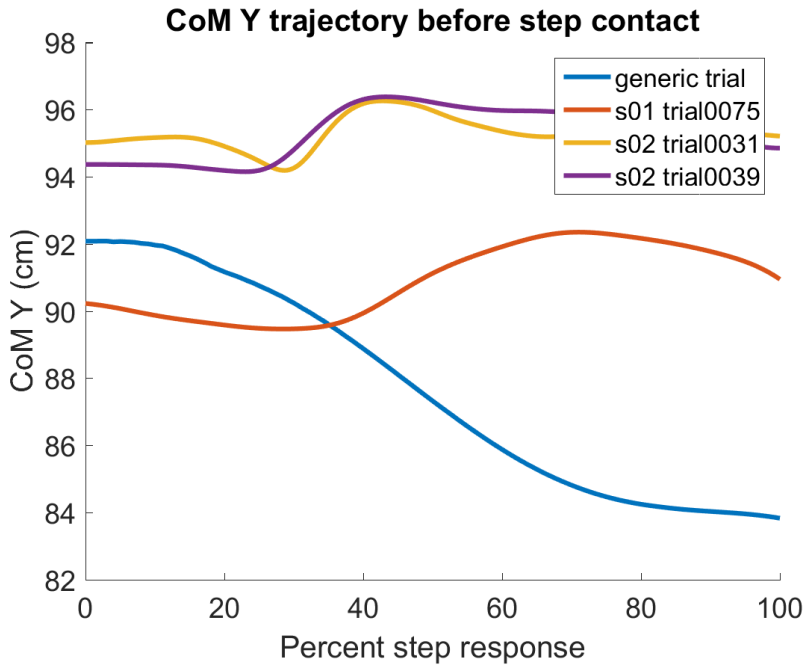

Figure 11: Plot of center of mass y-direction displacement from the support foot after 6 cm perturbation.

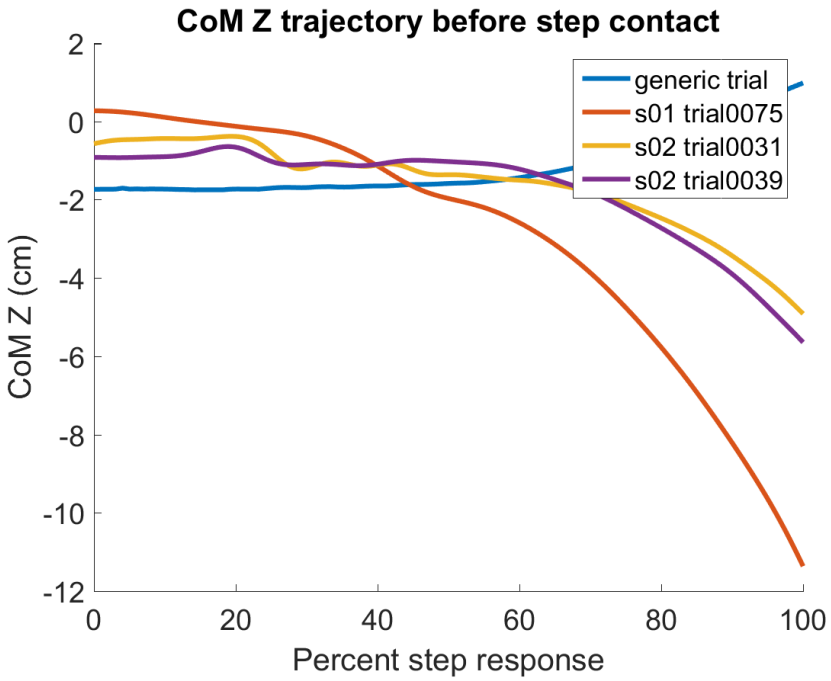

Figure 12: Plot of center of mass z-direction displacement from the support foot after 6 cm perturbation.

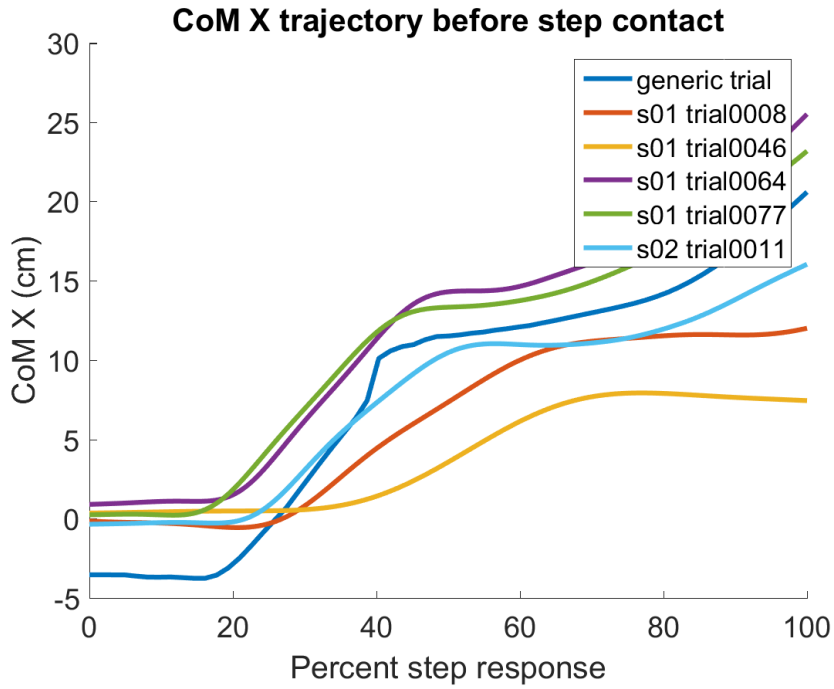

Figure 13: Plot of center of mass x-direction displacement from the support foot after 12 cm perturbation.

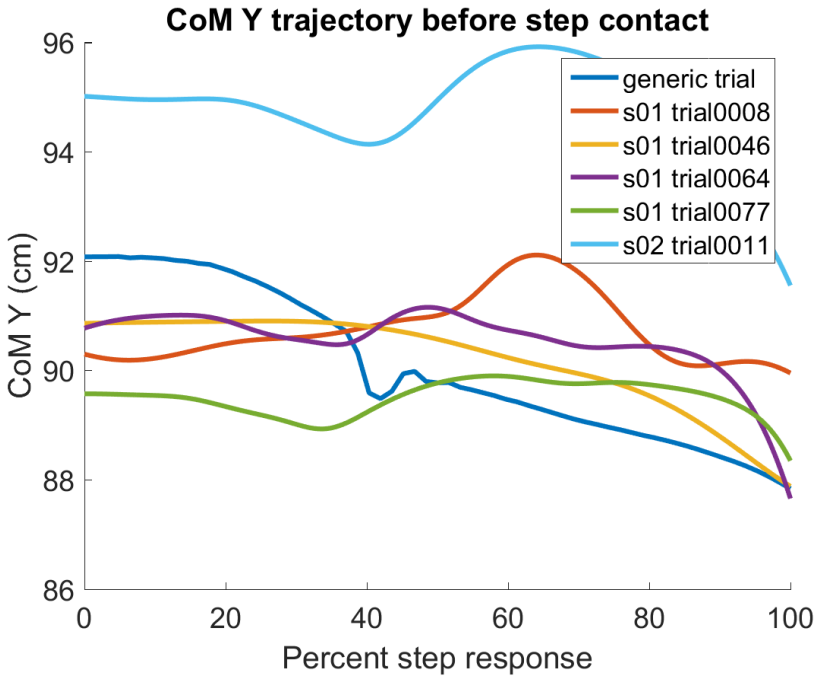

Figure 14: Plot of center of mass y-direction displacement from the support foot after 12 cm perturbation.

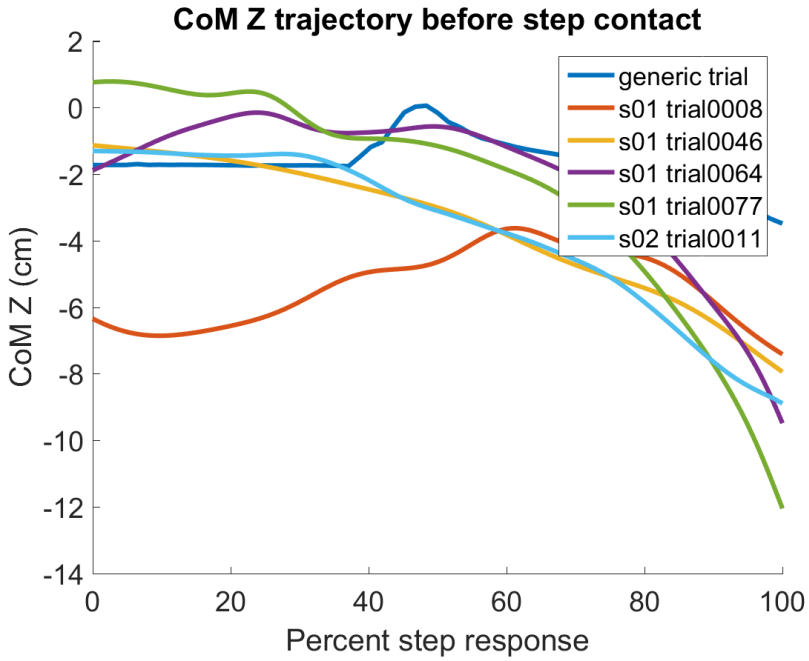

Figure 15: Plot of center of mass z-direction displacement from the support foot after 12 cm perturbation.

trajectories plotted against time normalized to percentages of the movement. Figures 41-46 describing step foot and posture trajectories can be found in Appendix A2.

3.5 Discussion

The purpose of Aim I was two-fold: to design a prioritized task based controller capable of differentiating between instances of stepping and not stepping using principles of humanoid robotics, and to compare the synthesized motion output to experimental data. With regard to the first goal Aim I succeeded. When exposed to a 6 cm perturbation the controller was capable of generating a coordinated response that prevented it from losing balance. On the other hand, when a 12 cm perturbation was introduced, the system successfully recognized an impending loss of balance due to the movement of the xCoM. At that time, the task definition of priority 2 changed and a step was initiated in order to biomimetically expand the base of support in order to stabilize the CoM. In both cases, the zero-moment point served as the CoM tracking task which provided sufficient agreement with CoM trajectories observed in experimental data.

Biological systems are noisy, and as such no two trials will be exactly the same, even in the same subject. This is shown in the variation between trials for both subjects 1 and 2 in the task point trajectory plots. One limitation of this system is that due to the intensive calculations used to determine response, the output will remain consistent for a given input (i.e. multiple simulations using 6 cm perturbation will yield the same no step coordination output, as would a 12 cm perturbation input produce the same step output). However, it is useful to identify concepts such as ZMP and xCoM that can be used in a cross-disciplinary fashion in order to replace biological feedback that is not present *in silico*. Moving forward, these techniques will be refined to make this platform more clinically relevant.

By comparing task point trajectories, it can be shown that the generic controller produces movement patterns that are consistent to what we have observed experimentally. This is particularly clear when comparing the generic response to 6 cm perturbation with subject 2's trial 31 (Figure 16). The coordination patterns are not identical, but he platform decision making framework and calculated movement pattern agree with the balance response displayed experimentally. Similarly, the step response to a 12 cm perturbation compares favorably with subject 1's trial 46 (Figure 17). Although there is variation in the human responses that is not present in the simulations, both generic outputs are well within the range of our observations. Simulating generic responses is a crucial milestone to generating subject-specific simulations because it provides a basis from which the artificial intelligence can be molded to match a unique individual. Without the ability of the controller to emulate decision making on its own, we would be unable to support the arguments supporting predictive simulations presented in Chapter 5. The controller can be improved further by optimizing PID gains in order to produce the desired responses. Purposefully including latency, or adding noise to the task signals, could be one method of modeling abnormal movements in unhealthy subjects.

In Chapters 4 and 5, we will explore techniques for improving these simulations in order to expand the scope of their impact. The generic responses generated here in Aim I will serve as a baseline for the following studies. New experimental and computational tools will be merged with the designed system in order to alter the model's parameters for the purpose of 1) making the simulated response for a particular trial subject-specific, and 2) generalizing the model based on multiple trials to generate predictions of movements.

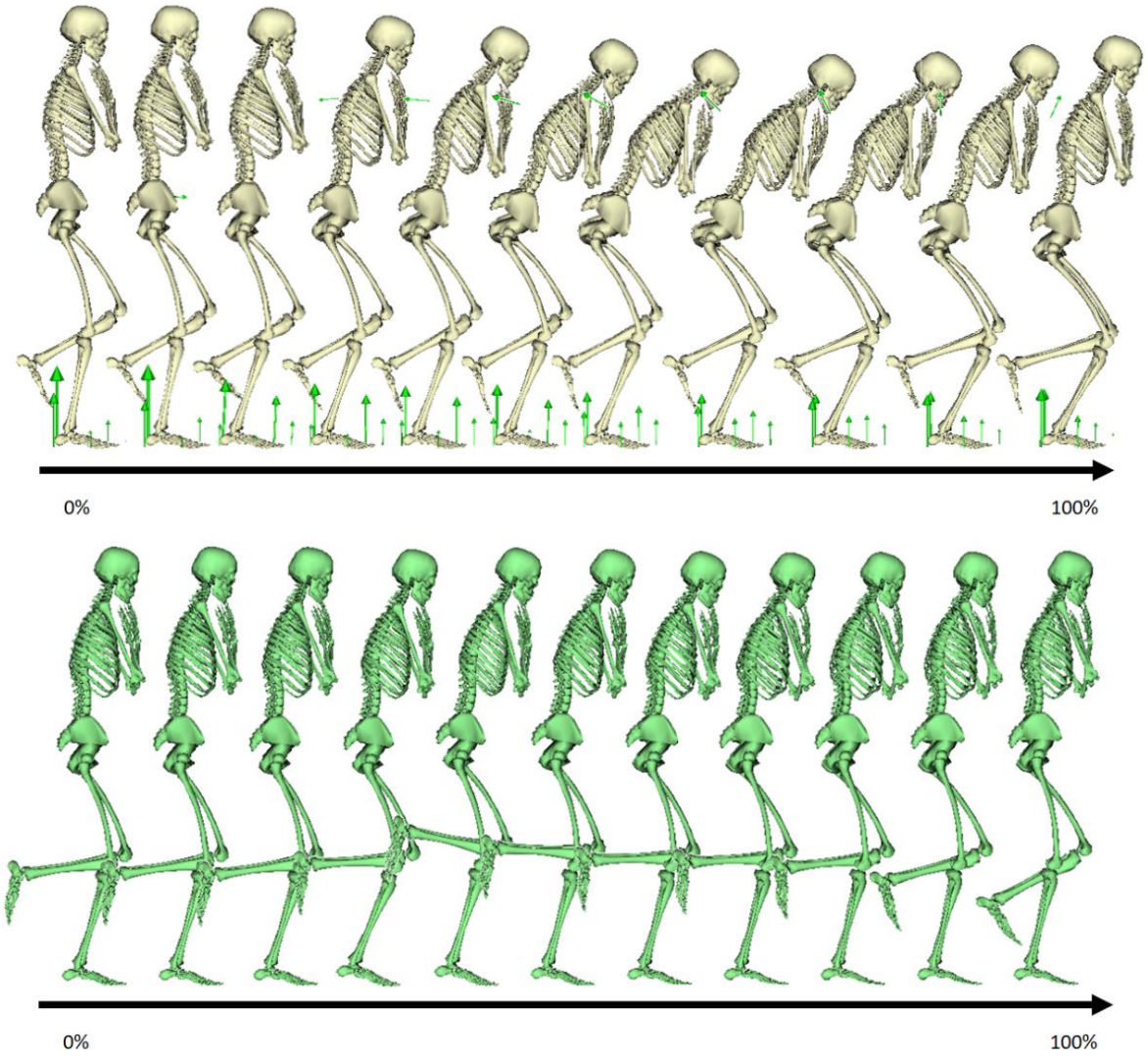

Figure 16: Time lapse showing 0 - 100% of response movement. (Above) Generic prioritized task, biomimetic decision, forward dynamics simulated response after 6 cm posterior perturbation. (Below) Subject 2, trial 31 response.

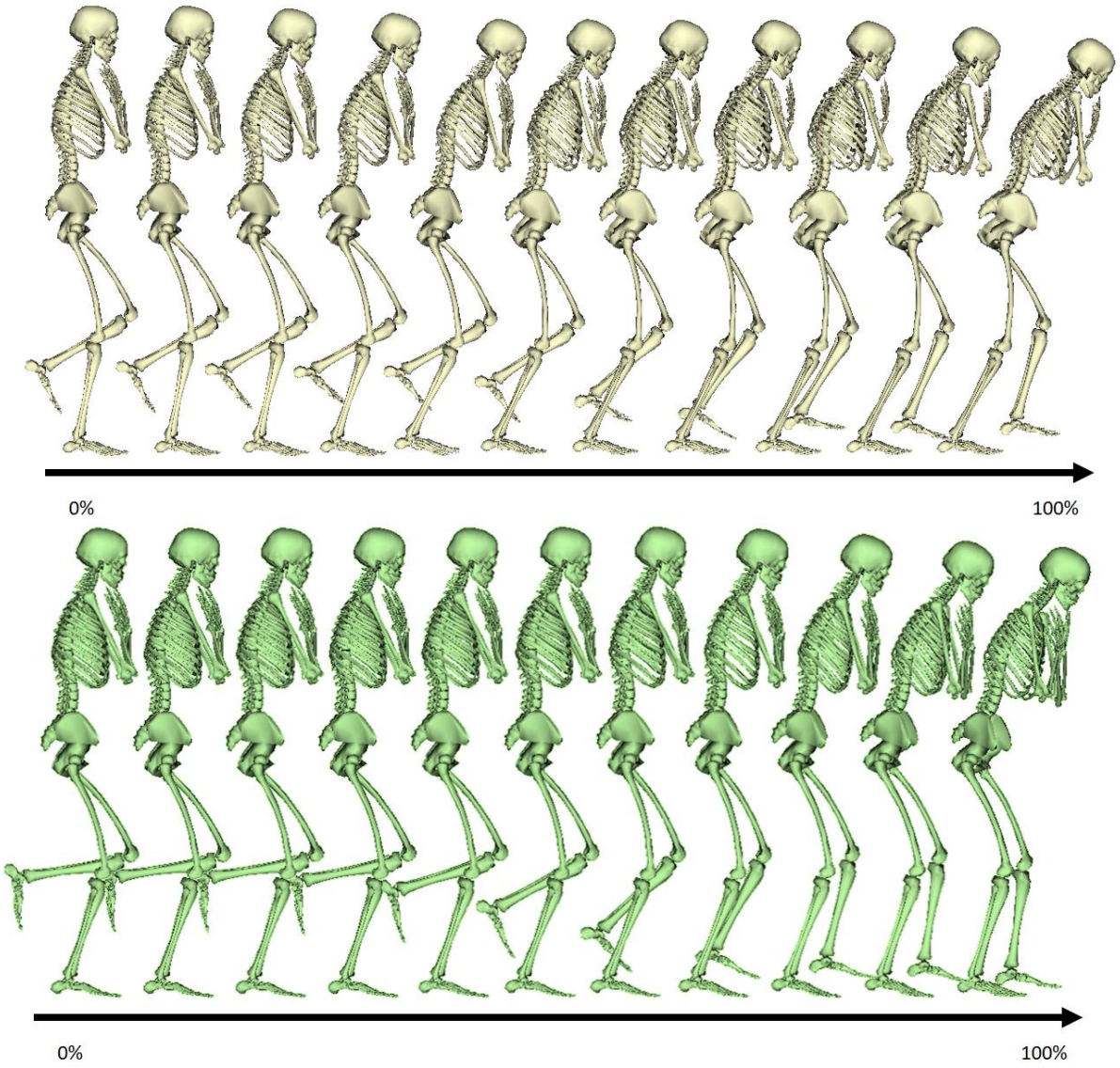

Figure 17: Time lapse showing 0 - 100% of response movement. (Above) Generic forward dynamics simulated response after 12 cm posterior perturbation. (Below) Subject 1, trial 46 response.

Chapter 4: Aim II - Development of Neuromechanical Models and Evaluation of Differences Between Single and Multiple Steppers

4.1 Abstract

Advances in biomechanical modeling and simulation have significantly improved research and functional outcomes of human movement studies. However, biomechanics research remains generalized by population (e.g. athletes, elderly, impaired) and subject-specific models have not been widely adopted. Advantages of subject-specific models include capturing unique cause-and-effect relationships for individuals that would otherwise be overlooked within populations. Here, we present a novel method for generating subject-specific models of human movement that can be produced rapidly and can accurately represent any level of physical fitness. We use these models to compare differences in task coordination between three cohorts of different balance recovery ability.

4.2 Introduction

4.2.1 Balance control and protective stepping

Balance control is a fundamental task that requires limb and postural adjustments in response to somatosensory, visual, and vestibular feedback [72], [73]. Under normal circumstances, healthy individuals are able to regulate balance by coordinating limb articulation [74], [75]. However, after a sufficiently large perturbation the brain's recognition of an imminent fall triggers a protective step which expands the base of support to enclose the projection of the body's center of mass (CoM) on the ground [76]–[78]. For some, multiple steps may be necessary in order to decelerate the CoM enough to recover balance, which in turn reduces the overall chance of successfully recovering [79]–[81]. Differences between single and multiple steppers' coordination strategies and neuromechanics should be evaluated in addition to physical fitness, in order to determine whether or not correctable shortcomings exist. These concepts are difficult to

investigate experimentally, but their principles may be uncovered through complementary modeling and simulation [82], [83].

4.2.2 Task-based movement

Coordinated whole-body movements can be broken down into component tasks. Humans do not consciously think about individual task definitions, but they drive movement nonetheless (i.e. stay balanced, do not get hurt, grab object, etc.) [84]–[86]. Task separation in operational space control is a widely used concept for generating movements in robotic systems [87]–[89], but the concepts can be adapted for evaluating human subjects for clinical purposes. In particular, by separating out the component tasks of a step balance recovery (CoM control, step trajectory, and posture) we can compare single and multiple steppers to identify specific differences in their response strategies. The purpose of Aim II is to develop subject-specific surrogate models of single and multiple steppers task-space response to forward loss of balance, and to identify differences in balance recovery strategy.

4.3 Methods

4.3.1 Experimental data

We used experimental data collected at 200 Hz from 15 subjects standing with feet shoulder width apart, tilted forward via cable in parallel with the floor until 20% of body weight was recorded by a series-connected load cell [35]. Subjects were then released and instructed to take a single step, though some needed to take multiple steps in order to prevent a fall. 36 degree of freedom models were scaled to each subject in OpenSim by iteratively changing a scale factor in order to minimize the positional error between marker locations on the subject using a static standing trial and on the model *in silico*. Inverse kinematics was used to calculate joint angles at

each time step from the marker trajectory recordings. Body kinematics was used to find component bodies' center of mass and velocities. We calculated the ZMP using pelvis residual forces and moments taken from inverse dynamics and body kinematics.

4.3.2 Task space surrogate response surfaces

For this study we were interested in comparing step response between the three cohorts present in the experimental data set: older multiple steppers (OMS), older single steppers (OSS), and younger single steppers (YSS). As such, three tasks were defined for the purpose of developing a model of the balance coordination: the center of mass tracking the zero-moment point, the stepping foot movement, and posture orientation. Previous work has shown the benefits of modeling individual tasks as they relate to each other [33], [34], [70]. This was done here by defining vectors between the CoM and the ZMP, stepping foot, and posture as shown in Figure 18, using the same task point definitions described in Table 2.

Surrogate response surfaces are modeling tools used to define the operational space that a task occupies. Response surfaces are powerful tools because they are subject-specific and represent the subject's actual movement during a given trial thereby incorporating all neural control including reflexes and proprioception. The surrogate models are formulated by decomposing the task vectors, V1, V2, and V3 into component x, y and z parts. Each vector shares CoM as its origin point. One of the benefits of using this type of model is that parameter definitions are flexible to the point that any task could be selected as the origin relating vectors. However, for this investigation we selected CoM due to its status as primary (rank 1) task in our prioritization hierarchy in prior and future simulations. Stabilizing the CoM over ZMP is the primary task, so V2 and V3 response surface models are calculated as 3D quadratic fits of the x, y, and z

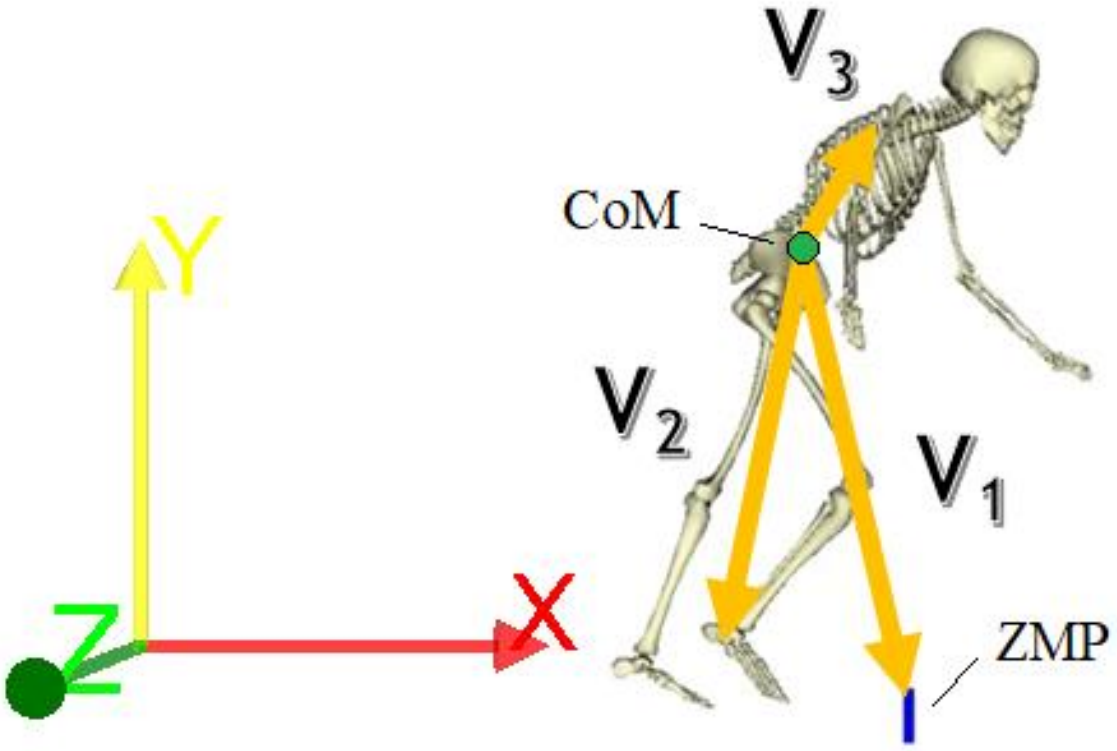

Figure 18: Definition of task vectors for step trials. Task 1 defines vector V1 between whole-body center of mass and zero-moment point. Task 2 defines vector between whole-body center of mass and the center of mass of the step foot body (calcaneus). Task 3 defines vector between whole-body center of mass and the posture (C7 vertebrae).

displacements as a function of the x and z displacement of the CoM from the ZMP. The formulation is as follows:

$$A = \begin{bmatrix} 1 & V1_{x_0} & V1_{z_0} & V1_{x_0}^2 & V1_{x_0}V1_{z_0} & V1_{z_0}^2 \\ 1 & V1_{x_1} & V1_{z_1} & V1_{x_1}^2 & V1_{x_1}V1_{z_1} & V1_{z_1}^2 \\ 1 & V1_{x_2} & V1_{z_2} & V1_{x_2}^2 & V1_{x_2}V1_{z_2} & V1_{z_2}^2 \\ \vdots & \vdots & \vdots & \vdots & \vdots & \\ 1 & V1_{x_n} & V1_{z_n} & V1_{x_n}^2 & V1_{x_n}V1_{z_n} & V1_{z_n}^2 \end{bmatrix}$$

Where A is a matrix representing the system of linear equations that defines a quadratic equation with the x and z components of task vector V1 as inputs, and each row of A is a time frame of the movement.

$$x = Ab \tag{21}$$

The standard formulation for a system of linear equations, *A*, where the output, *x*, is dependent on a vector of coefficients, *b*. Coefficients for each component of V2 and V3 are calculated by substituting the vector component into Equation 21 for *x* and solving for *b*. Using the x component of V2 as an example:

$$V2_x = Ab_{2_x} \tag{22}$$

$$V2_x = \begin{bmatrix} 1 & V1_{x_0} & V1_{z_0} & V1_{x_0}^2 & V1_{x_0}V1_{z_0} & V1_{z_0}^2 \\ 1 & V1_{x_1} & V1_{z_1} & V1_{x_1}^2 & V1_{x_1}V1_{z_1} & V1_{z_1}^2 \\ 1 & V1_{x_2} & V1_{z_2} & V1_{x_2}^2 & V1_{x_2}V1_{z_2} & V1_{z_2}^2 \\ \vdots & \vdots & \vdots & \vdots & \vdots & \\ 1 & V1_{x_n} & V1_{z_n} & V1_{x_n}^2 & V1_{x_n}V1_{z_n} & V1_{z_n}^2 \end{bmatrix} \begin{bmatrix} b_{2_{x1}} \\ b_{2_{x2}} \\ b_{2_{x3}} \\ b_{2_{x4}} \\ b_{2_{x5}} \\ b_{2_{x6}} \end{bmatrix}$$

The *b* vector of coefficients defines a surface representation of the x-direction space occupied by the body of V2, the step foot, during the balance recovery motion. This is done for x, y, and z of both V2 and V3 in order to have a mathematical picture of the subject's exact response. The maximum and minimum x and z component of the composite V1 including all subjects' data was

used to define vectors X and Z, equally distributed vectors encompassing the task spaces of all trials. X and Z provide inputs to the surface function by creating a mesh grid. The equation used to plot the surfaces for visual representation is given in Equation 23.

$$S2_x = b_{2_{x1}} + b_{2_{x2}}X + b_{2_{x3}}Z + b_{2_{x4}}X^2 + b_{2_{x5}}XZ + b_{2_{x6}}Z^2 \qquad (23)$$

Where $S2_x$ [subscript x] is the surrogate response surface for the x component of task vector 2. The coefficients define the response space and the surfaces are plotted for the same corresponding X and Z displacements for consistency in comparison.

4.4 Results

4.4.1 Traditional biomechanical measures of balance recovery

Tables 3 and 4 summarize the data of each subject's balance recovery trial as standard measures used in biomechanics research. Researchers are typically interested in step length, forward lean angle, and center of mass height as they each contribute to the overall braking forces produced when the step foot comes in contact with the ground, as well as the forward momentum changes at that time that determine stability.

4.4.2 Surrogate response surface models

Figures 19-21 and Figures 22-24 display the surrogate models of step foot response and posture response to CoM-ZMP displacement, respectively. Each plot represents data taken from all subjects belonging to a single cohort. These surrogate models define the operational space that is required by each subject in each cohort in responding to loss of balance. For x and z-direction displacement of CoM from ZMP, that is error between center of mass location and the stability point defined by the vector normal to the ground originating at the zero-moment point, each

Table 3: Table reporting traditional measures of the biomechanics of forward loss of balance: step length, forward lean, and center of mass height. Step length is reported both as a distance from both the ZMP and the plant foot. Forward lean angle is measured from the vertical y-axis (Fig. 18) to the posture task point using the subject's CoM as the origin point of rotation.

COHORT	*SUBJECT*	*STEP LENGTH FROM ZMP (CM)*	*STEP LENGTH FROM PLANT FOOT (CM)*	*FORWARD LEAN ANGLE (DEG)*	*COM HEIGHT (CM)*
OMS	1	15.8	61.4	23.8	98.0
	2	18.7	56.3	11.0	100.6
	3	17.4	51.9	10.8	89.9
	4	2.7	49.1	22.7	95.5
	5	9.1	41.6	7.0	89.7
OSS	1	21.5	59.7	2.5	86.3
	2	29.8	74.8	11.4	96.9
	3	38.4	87.2	4.7	94.4
	4	27.9	60.8	6.5	85.9
	5	34.3	78.8	5.3	92.9
YSS	1	32.5	79.1	5.5	92.3
	2	30.5	76.1	4.6	92.3
	3	43.5	74.3	4.9	93.9
	4	18.0	55.9	6.1	102.3
	5	19.8	67.8	14.7	104.9

Table 4: Mean and standard deviation for biomechanical measures of balance recovery of each cohort displayed in Table 3.

COHORT	*STEP LENGTH FROM ZMP (CM)*	*STEP LENGTH FROM PLANT FOOT (CM)*	*FORWARD LEAN ANGLE (DEG)*	*COM HEIGHT (CM)*
OMS	12.7 ± 6.0	52.1 ± 6.7	15.1 ± 6.8	94.7 ± 4.3
OSS	30.4 ± 5.7	72.3 ± 10.6	6.1 ± 3.0	91.3 ± 4.4
YSS	28.9 ± 9.3	70.6 ± 8.2	7.2 ± 3.8	97.1 ± 5.4

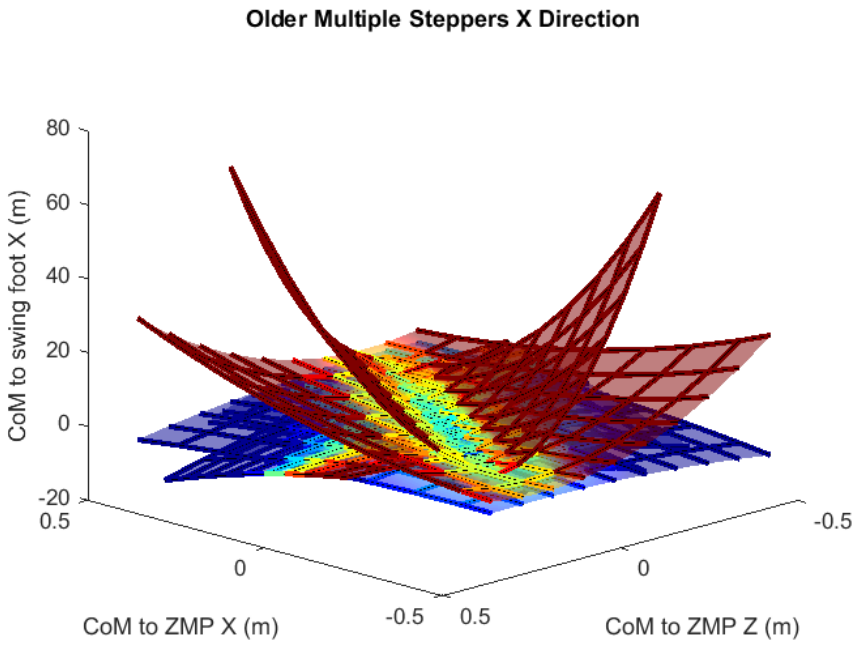

Figure 19: Surrogate response surface models of step foot x direction task space from OMS cohort trials.

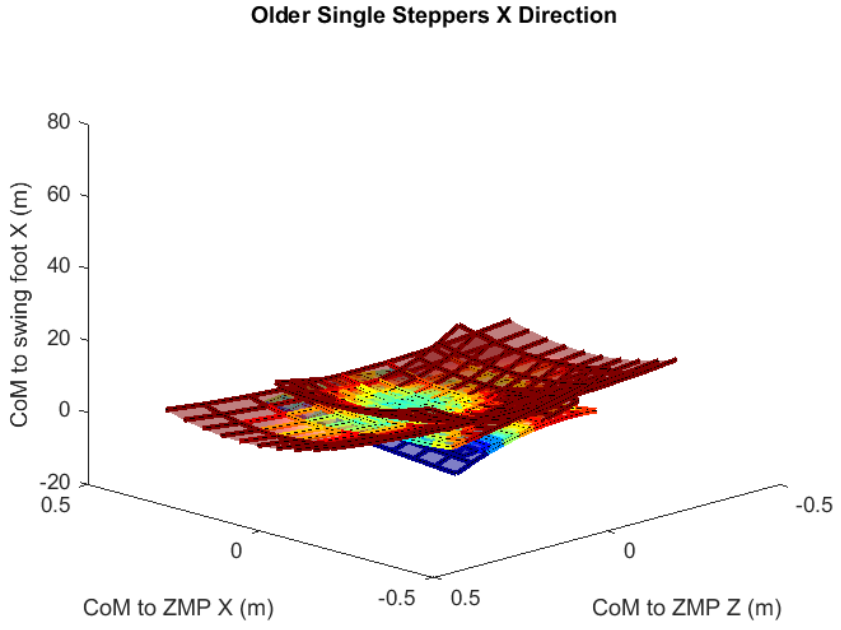

Figure 20: Surrogate response surface models of step foot x direction task space from OSS cohort trials.

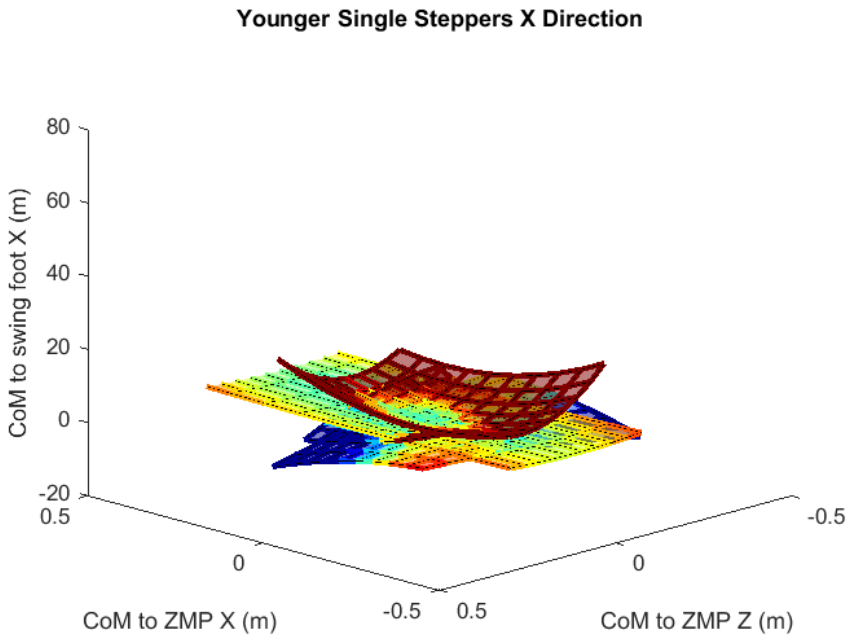

Figure 21: Surrogate response surface models of step foot x direction task space from YSS cohort trials.

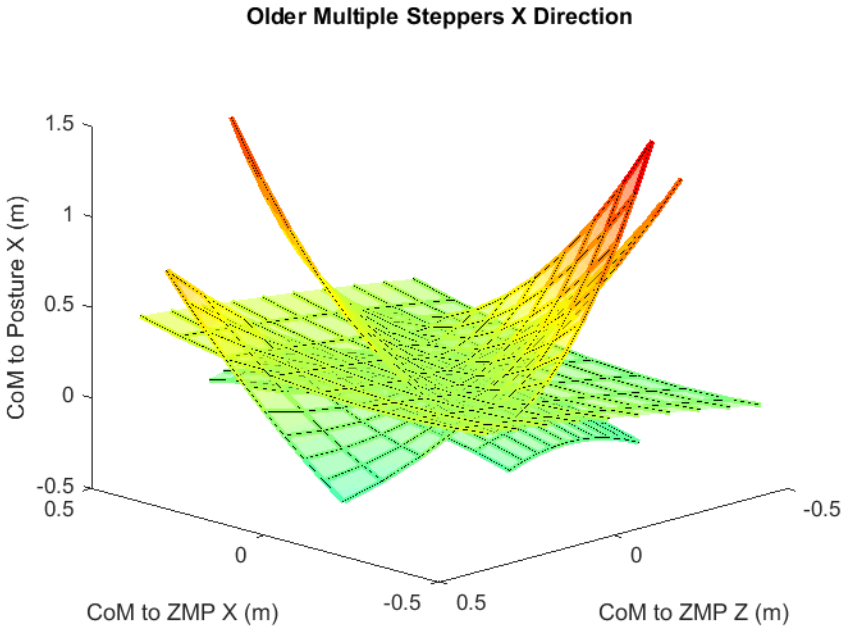

Figure 22: Surrogate response surface models of posture x direction task space from OMS cohort trials.

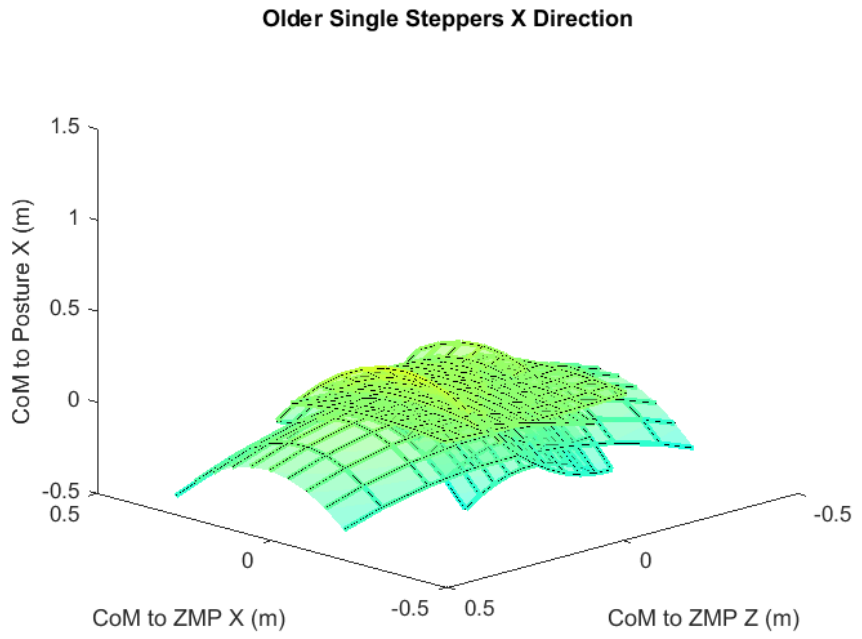

Figure 23: Surrogate response surface models of posture x direction task space from OSS cohort trials.

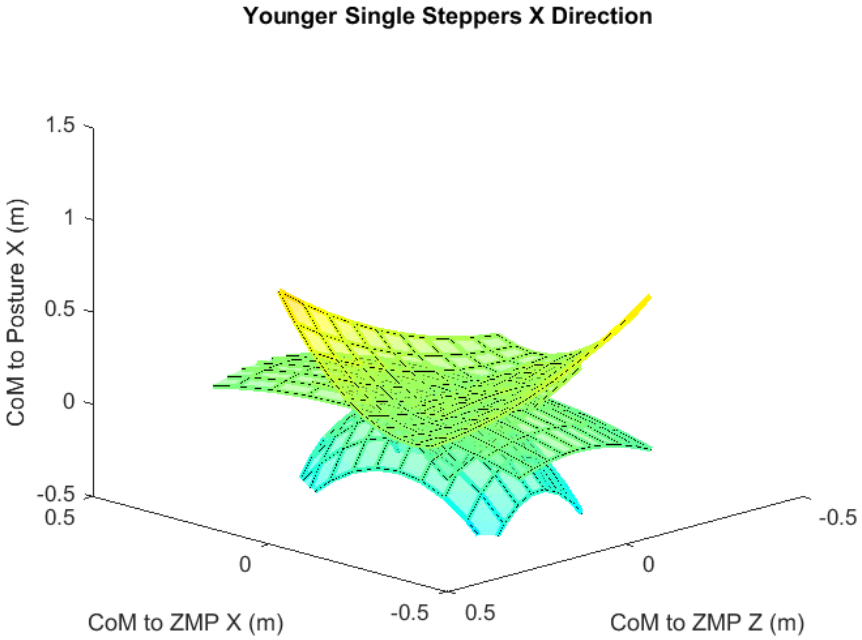

Figure 24: Surrogate response surface models of posture x direction task space from YSS cohort trials.

surrogate model extrapolates the subject-specific position of task points for step and posture, relative to the primary task point, CoM.

4.5 Discussion

4.5.1 Instability projections of surrogate models

Figures 19-24 depict the surrogate response surface models for the three cohorts' step and posture x-direction responses to forward loss of balance after cable release (Figures 47-52 in Appendix B1 give the y-direction responses; Figures 53-58 in Appendix B2 give the z-direction responses). In the case of both tasks, the older multiple stepper cohort surrogates occupy significantly more operational space than the older or younger single stepper groups, which are fairly similar. The curvature of the OMS surrogate surfaces and the greater space occupied indicates that for the same range of displacements of the center of mass from the zero-moment point, in the x and z-directions, OMS display significantly more variability in step foot trajectory and posture orientation. The steeper gradients visualized by the response surfaces correspond to greater degrees of instability for those subjects. Using the surrogate models, task point trajectories can be extrapolated past the observed range of motion, defining stable regions.

4.5.2 Biomechanically consistent differences between cohorts

Tables 3 and 4 report biomechanical measures associated with balance and falls research that are prevalent in clinical studies. As reported, the OMS cohort takes shorter steps than the single stepper groups. When related to the ZMP location the steps are approximately half as long as the others'. This task coordination, coupled with nearly double the amount of forward lean, produces a net moment about the step foot that cannot be overcome and results in additional steps. Similarly, fundamental balance mechanics shows that lowering the center of mass during recovery

improves stability due to the enhanced ability to generate lateral ground reaction forces [90]–[92]. The more unstable cohort, OMS, had on average 5 cm higher CoM at the completion of the first step.

4.5.3 Surrogate models in biomechanics simulations

Surrogate response models are powerful tools for improving simulations because they represent observed responses in the lab setting. The influence of sensory input, such as visual interpretation or joint pain, cannot be dissociated from the surrogate model, and are therefore integrated into the model fit. Previous work has shown that prioritized task-based simulations of subject-specific responses can be modeled using surrogate response surface models as the tracking objective for controllers determining spatial error between the task vectors [33], [70], [93]. However, in all previous studies a single surrogate from a single trial response was used for each simulation. Replicating subject trial data is an important milestone for this research, but the end goal is to make subject-specific predictions. The surrogate response surface method employed here will be further developed in Chapter 5 in order to model a subject's complete neuromechanical coordination for the purpose of simulating predictive responses to external perturbations.

Chapter 5: Aim III - Evaluation of the Predictive Accuracy of Subject-Specific Simulations of Whole-Body, Step Recovery Strategies to Prevent Falls

5.1 Abstract

The relationship between sensory feedback, neurological interpretation, and mechanical output in human subjects is not fully understood. However, in order to uncover principles of movements in healthy and impaired subjects, it is necessary to model each aspect of the biological systems that contribute to motion development. The complicated transformations between perception and execution are difficult to model by existing means, so novel tools are necessary in order to enhance simulation research. Here, we present a novel approach to modeling subject-specific neuromechanical coordination over multiple trials, in order to complete models of complete feasible operational space given particular initial states and inputs. We show that surrogate models of balance recovery response can be used to make predictive simulations that accurately reflect the same decision making and movement coordination displayed by the subject in the experimental lab setting.

5.2 Introduction

5.2.1 Factors impacting human balance

Human movement is an intricate mechanical output that is the result of several distinct biological processes working synergistically [94]–[96]. Despite the importance of each phase, few tools exist in biomechanics research that are capable of modeling and simulating the complete path from signal to movement with feedback. It is becoming increasingly important to represent external factors associated with changes in motion due to the significant impact they can have, specifically when designing interventions for movement disorders [97]. More than half of the United States' population is affected by some type of musculoskeletal disease, which results in approximately $882 billion in treatment costs and lost wages [2]. The prevalence of movement

disorders, and its forecasted growth due to the aging population, necessitates improved evaluation techniques that can be tailored to individual subjects for making recommendations in the clinical setting.

5.2.2 Simulation of dynamically changing tasks

Predictive simulations in biomechanical studies have improved in recent years due to novel modeling techniques for replicating the characteristics of human movement [20], [98], [99]. Estimates of various fundamental activities, including gait and balance recovery, have been developed by minimizing an objective function under some set of constraints [10], [20], [21], [37], and have yielded promising results. While these simulations are able to accurately generate movement patterns that compare well to observed experimental data, they do not typically account for somatosensory or proprioceptive feedback, such as joint pain or fear of falling, that would normally influence a subject's voluntary and involuntary processes for selecting movements [100], [101]. External stimuli that may negatively influence the optimal solution, are unaccounted for in such cases. Furthermore, research into motor control has shown that muscle redundancy generates a large set of coordination patterns for producing any given movement, with the optimized motion pattern included [102], [103]. At its core, human movement is a series of tasks designed and executed in order to accomplish some goal with intermediate aims, e.g. stand and walk from point A to point B; move quickly but do not get hurt, with sensory inputs and a desire to protect the body directly influencing real-time decision making [104]–[106]. Goal dependent voluntary changes in coordination and the inherent noise of biological systems makes it unlikely that neuromechanical outputs target some optimal performance in situations where an immediate response is more important than an efficient one.

Research suggests that rather than minimizing effort, humans minimize spatial error between the control point and its goal [107]. This concept is supported by research showing subjects' coordination patterns as being dependent on initial conditions and target articulation position, as well as changes in sensory inputs [108]–[111]. Previous research has implemented this theory in generating subject-specific simulations of balance recovery [34], [93]. Novel modeling techniques are therefore necessary in order to fill this gap and generate true subject-specific simulations that reflect the complete neuromechanical input and output processes of motion.

Here, we present a novel method of simulating subject-specific neuromechanical coordination using compound surrogate response models. The proposed method is tested using balance recovery data collected after forward and backward support surface perturbation during single support in human subjects. This technique synthesizes the prioritized task-control with decision making strategies described in Chapter 3 with the surrogate response models introduced in Chapter 4.

5.3 Methods

5.3.1 Experimental balance recovery data

Balance recovery data was collected by recording marker trajectories with a Vicon Camera system at 250 Hz with one subject (female 25 yrs | 1.72 m | 68.0 kg) standing on one foot (Figure 6, left) during random support surface perturbation trials (6, 12 cm | 40 cm/s) in the anterior and posterior directions. There was no prior training, and the subject was not aware of the magnitude or direction of the perturbation in advance. The perturbations were introduced via the CAREN system. Subjects were instructed to keep their arms crossed over their chest and to maintain balance (with or without stepping), and the free swing/step foot was lifted to a minimum of 10 cm above

the support surface prior to introduction of the perturbation. Marker trajectory data was filtered with a low-pass cutoff frequency of 6 Hz. Of 96 trials from which data was collected, 10 trials involved strictly anterior and posterior perturbations (no translation in the z-direction). These trials were used to develop the compound surrogate model for the subject.

5.3.2 Compound surrogate response model

The surrogate response surface approach described in Chapter 4 was improved to define multiple trials in order to complete the model of a specific subject's neuromechanics. The technique used is modeled after K-Fold Cross Validation. A conceptual diagram of K-fold Cross Validation is shown in Figure 25.

In this system, the trials are made up of the body kinematics data that is used to generate individual surrogate response surfaces. Ten trials met the criteria for inclusion, so a 10-Fold Cross Validation was performed. Each training set consisted of 9 trials, while the 10^{th} trial was withheld for testing. The testing input used was the perturbation associated with the withheld trial (posterior or anterior, 6 or 12 cm). The data compiled from the nine trials in the training set was used to define task vectors between the whole-body center of mass and three task points. Figure 26 describes the set up.

Both center of mass location and posture were fit with quadratic response surfaces using x and z-direction displacement from the plant foot as inputs. For the complete formulation see 4.3.2. Following results reported in [68] the step foot trajectory was fit with a quintic polynomial. The quintic fit more accurately represented the plateau effect of maintaining the step foot at 10 cm above the ground during single support, and stepping when perturbed past the bounds of the base of support.

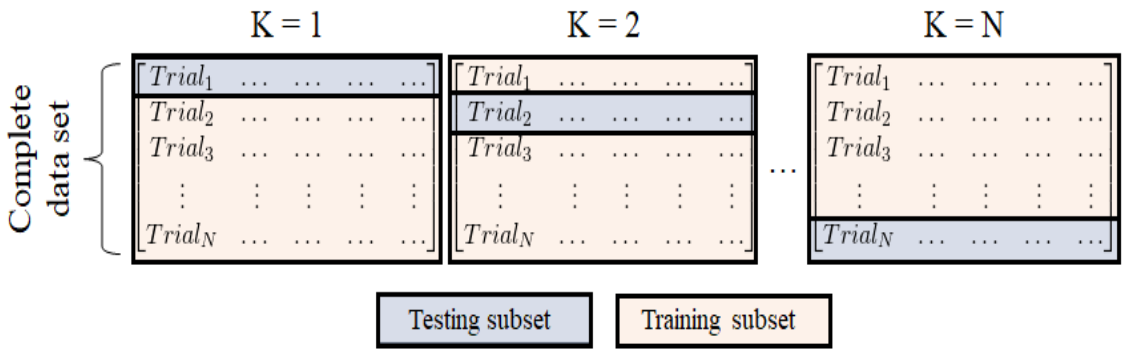

Figure 25: Depiction of K-Fold Cross Validation. In each iteration (K) a subset consisting of one trial is withheld from the modeling process (testing subset). The remaining N – 1 trials are used to build the model and train the system (training subset). The system is tested using the inputs that originally generated the test set. The output is compared to the test set in order to determine how well the model predicts the subject's response. The power behind this technique is that each trial is guaranteed use in both testing and training.

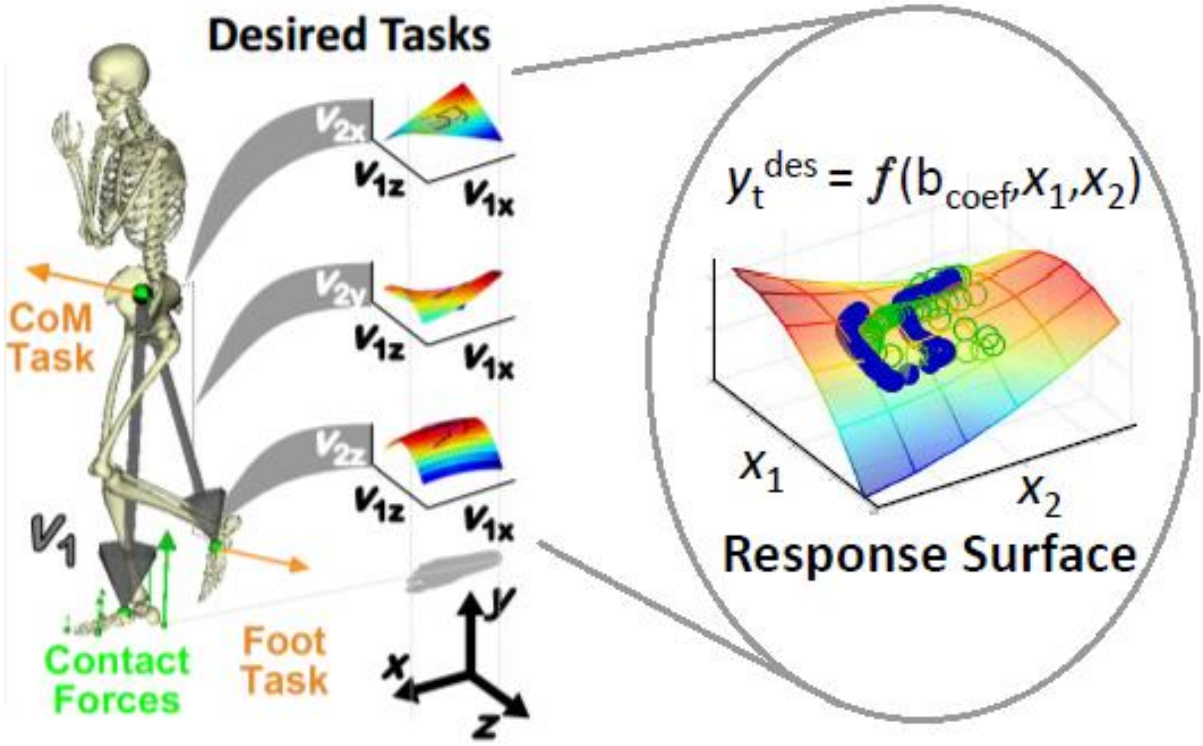

Figure 26: Definition and formulation of surrogate response surface. Task vectors were defined between CoM and plant foot (V1), CoM and step foot (V2) and CoM and posture (V3). Quadratic surfaces were used to model CoM and posture movement while a quintic fit was applied to the step foot.

5.3.3 Prioritized task simulation of compound surrogate models of neuromechanics

Aim III is the culmination of work from Aims I and II. Here we synthesize the improved, compound surrogate response surface models for representing a specific subject's neuromechanical balance recovery coordination ability in 3D space with the robust control system architecture, biomimetic decision making, and prioritized task-based simulation. Figure 27 describes the flow of data through the system. Each trial from the 10-trial data set is used once as a testing set and compared to the simulated prediction. For comparison, following procedures used in previous studies of biomechanical stepping response, for comparison of the simulation to the experimental testing set, the time frame of both motions was limited to before the perturbation to the instant before contact was made between the step foot and the ground.

5.4 Results

The test sets and the corresponding predicted responses were compared qualitatively to determine whether the correct directional response was generated, and numerically to determine percent error between prediction and experiment. Figure 28 shows the end frame of a predicted movement (blue) and the experimental data used as the test set (green) for Trial 64 from the data set. Figures 29-31 display the corresponding task point trajectories for the center of mass, step foot, and posture as percentages of the total movement response. Finally, Table 5 displays the percent error of the predicted response's x, y and z components for each task. The plots for the remaining trial data can be found in Appendix C, Figures 59-82.

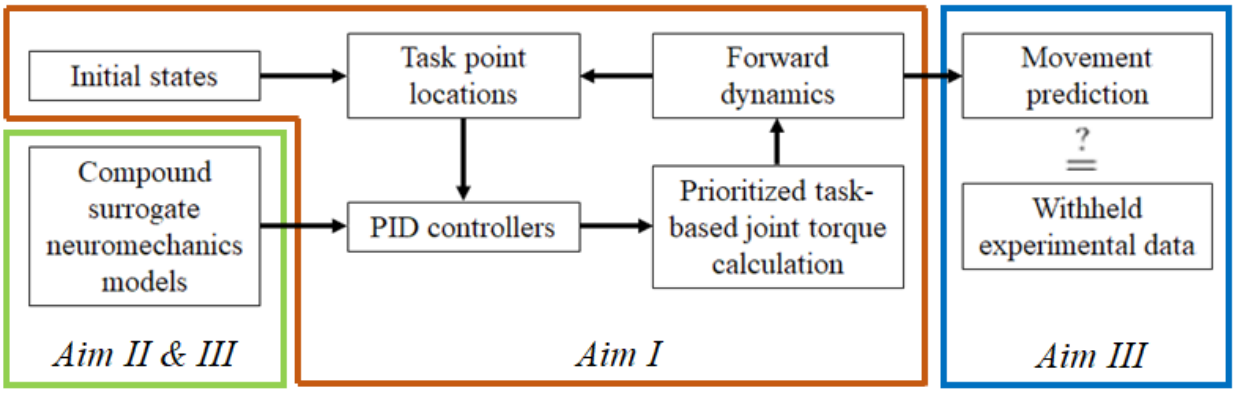

Figure 27: Flow diagram describing system process. Initial states inform original task locations. Errors between task locations and compound surrogate models drive PID calculation of acceleration vector to move task points to desired positions by prioritized task calculation. Output movement prediction is compared to the testing subset movement.

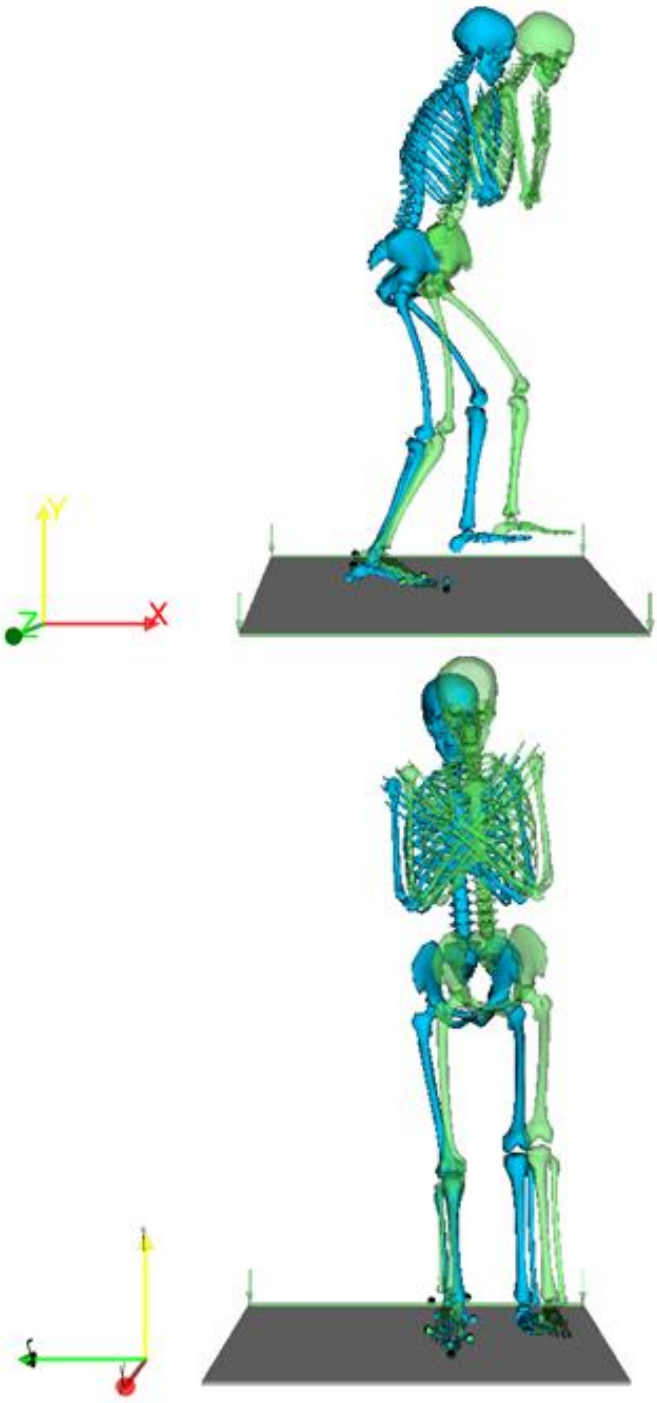

Figure 28: Depiction of the lateral (top) and front (bottom) view of the predicted response (blue) to the 12 cm perturbation experienced by the subject in Trial 0064 and their experimental response (green). The predicted response was generated using the compound surrogate response surface of the other nine trials in the training set, while the experimental response was withheld in the testing set.

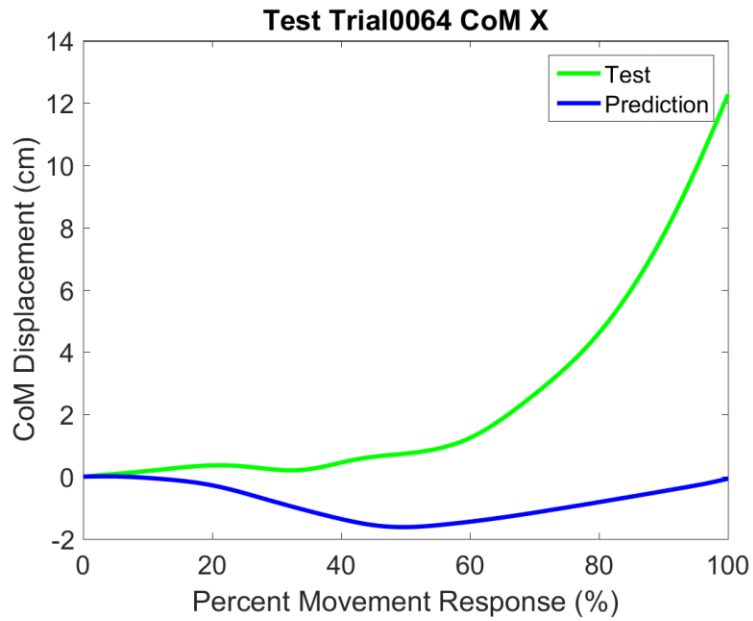

Figure 29: Displacement of center of mass in the x-direction from its initial position. Test line (green) represents experimental data collected from the subject during Trial 0064. Prediction line (blue) represents the system response to the same perturbation input.

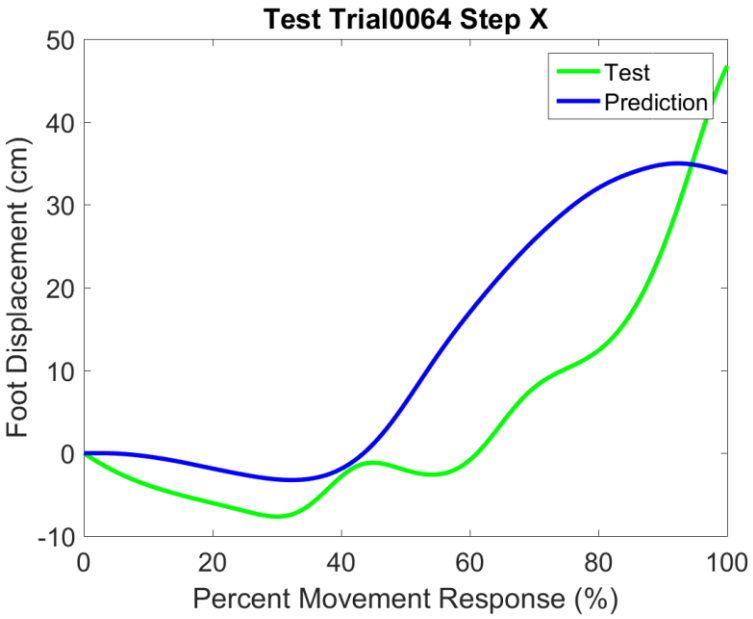

Figure 30: Displacement of step foot in the x-direction from its initial position. Test line (green) represents experimental data collected from the subject during Trial 0064. Prediction line (blue) represents the system response to the same perturbation input.

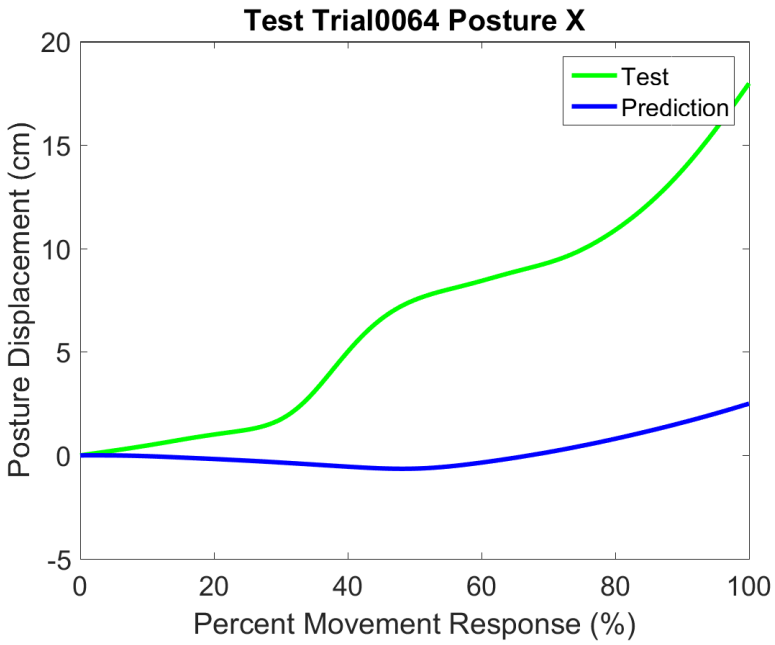

Figure 31: Displacement of posture in the x-direction from its initial position. Test line (green) represents experimental data collected from the subject during Trial 0064. Prediction line (blue) represents the system response to the same perturbation input.

Table 5: Table listing percent error values for each component of the three predicted task points located in the ground frame compared against the experimental data. Trial 64, displayed in Figures 28-31 above, was withheld from task point location mean calculation (bottom row) in order to remove outlier percentage error values. Mean error for all tasks in a single trial is diplayed in the right column.

TASK POINT LOCATION PERCENT ERROR										
	Center of Mass			Step Foot			Posture			
TRIAL	X	Y	Z	X	Y	Z	X	Y	Z	**TRIAL MEAN**
0010	-4.52	1.50	-5.84	-11.97	1.00	-61.30	-5.64	0.36	-2.41	-9.87
0018	-1.12	2.12	-6.76	-5.18	6.90	-64.57	-8.14	0.76	-2.37	-8.71
0063	-0.33	1.35	-6.61	-7.71	13.31	-37.98	-6.29	0.29	-8.10	-5.79
0075	-0.33	0.50	-6.90	-10.42	12.89	-9.01	-3.21	1.59	-15.48	-3.37
0077	-54.76	0.20	-13.61	-20.39	81.69	-6.14	-93.98	1.21	-23.37	-14.35
0085	-10.31	0.99	-2.36	-4.14	8.01	-24.62	-1.56	1.85	-22.38	-6.06
0064	-70.60	0.76	-7.87	-1173.7	9.43	-6.49	-118.1	0.66	-10.62	-152.9
TASK MEAN	-11.89	1.11	-7.01	-9.97	20.63	-33.94	-19.80	1.01	-12.35	

5.5 Discussion

5.5.1 Overview of results

Despite positional errors exceeding 10 cm in some trials, the predicted responses based off compound surrogate response surface representations of the subject's neuromechanical response to varying perturbation directions and magnitudes showed good agreement with the coordination patterns displayed in the lab setting. No individual prediction exceeded a mean absolute percent error of 15% (not including Trial 0064). Using just nine trials per training set resulted in average absolute percent error below 35% for each directional component of the coordinated task responses.

It should be noted that due to the step foot x-direction percent error of Trial 0064, it was withheld from the mean calculations. However, as displayed in Figures 28-31 the Trial 0064 prediction mimicked the experimentally observed motion, despite lagging behind and generating larger percent error values as compared to other trials. Figures 32-34 display the x-direction task response predictions from Trial 0064 in relation to the standard deviation about the mean for the subset of posterior perturbations. Despite the lag and large percent error, the predicted movement response remains within one standard deviation of the mean for center of mass and posture tasks, and two standard deviations for step. In Trial 0008 the subject started from an unstable configuration, creating a no solution singularity in the Jacobian matrix calculations. For this reason, Trial 0008 was not tested, although the response data was used for training the surrogate models. Trials 0046 and 0072 were used for both testing and training, however, the predicted responses did not produce steps. This gives the system an overall misclassification error percentage of 22%. The remaining trial data given in the Appendix C provides supporting evidence of this

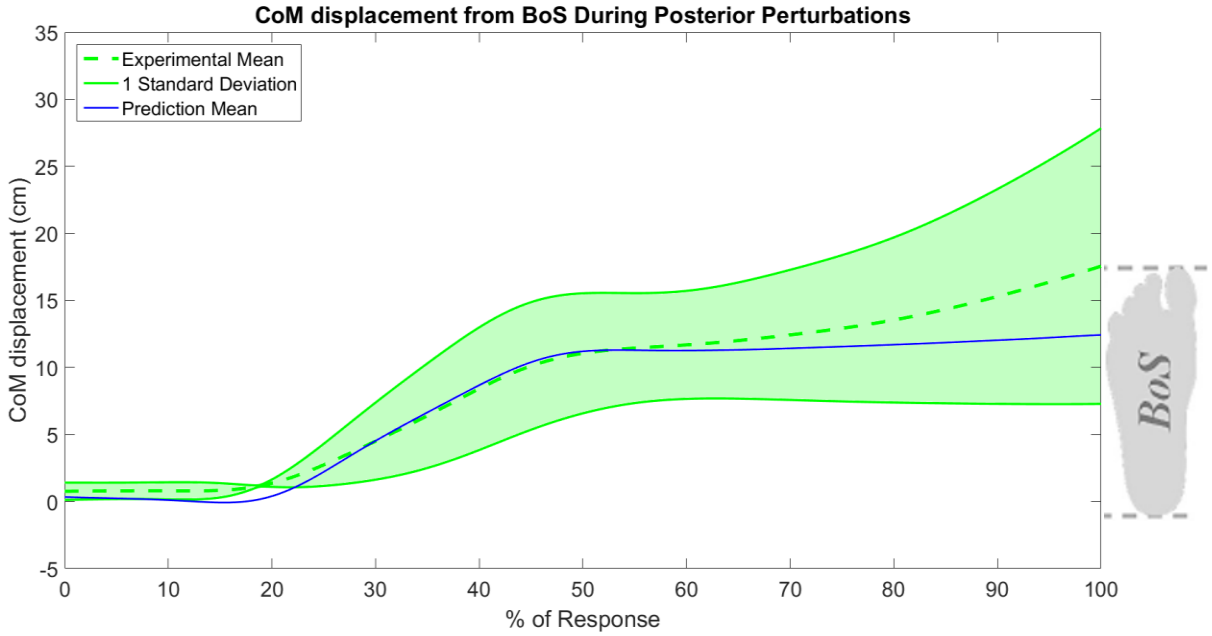

Figure 32: Predicted (Trial 0064) center of mass movement (blue) in the x-direction as a percentage of step response. Shaded (green) region represents one standard deviation about the mean experimental center of mass trajectory for all posterior perturbation trials. Both predicted and experimental trajectories are reported as displacements from the base of support (right, plant foot).

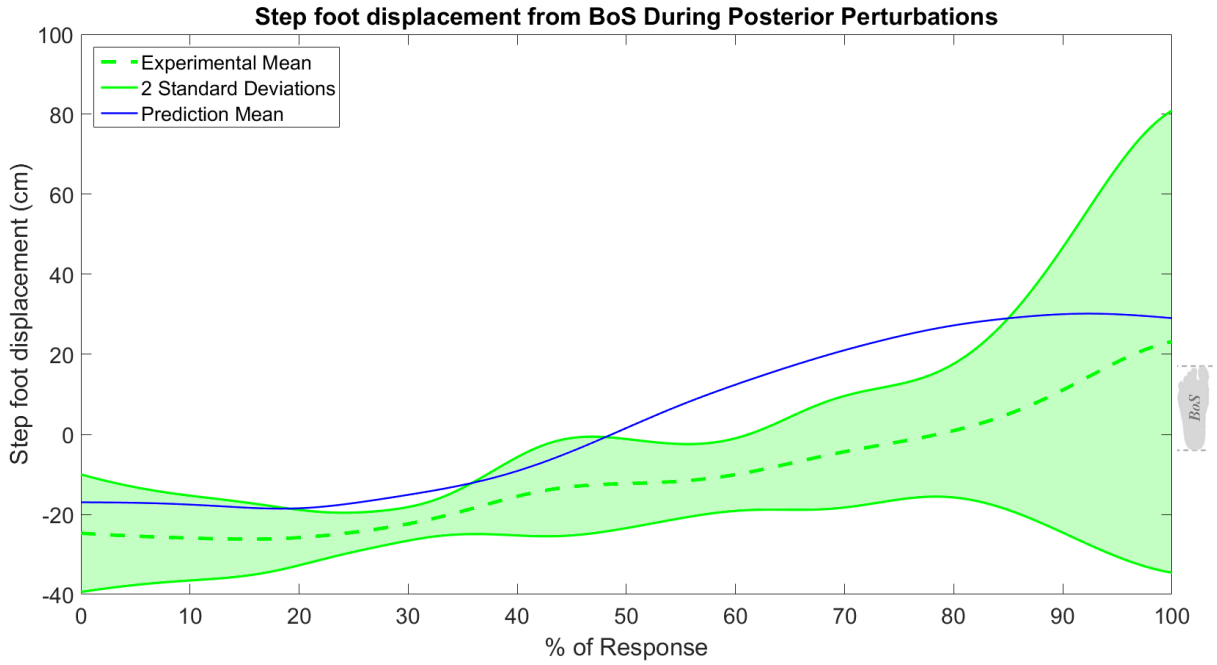

Figure 33: Predicted (Trial 0064) step foot movement (blue) in the x-direction as a percentage of step response. Shaded (green) region represents two standard deviations about the mean experimental step foot trajectory for all posterior perturbation trials. Both predicted and experimental trajectories are reported as displacements from the base of support (right, plant foot).

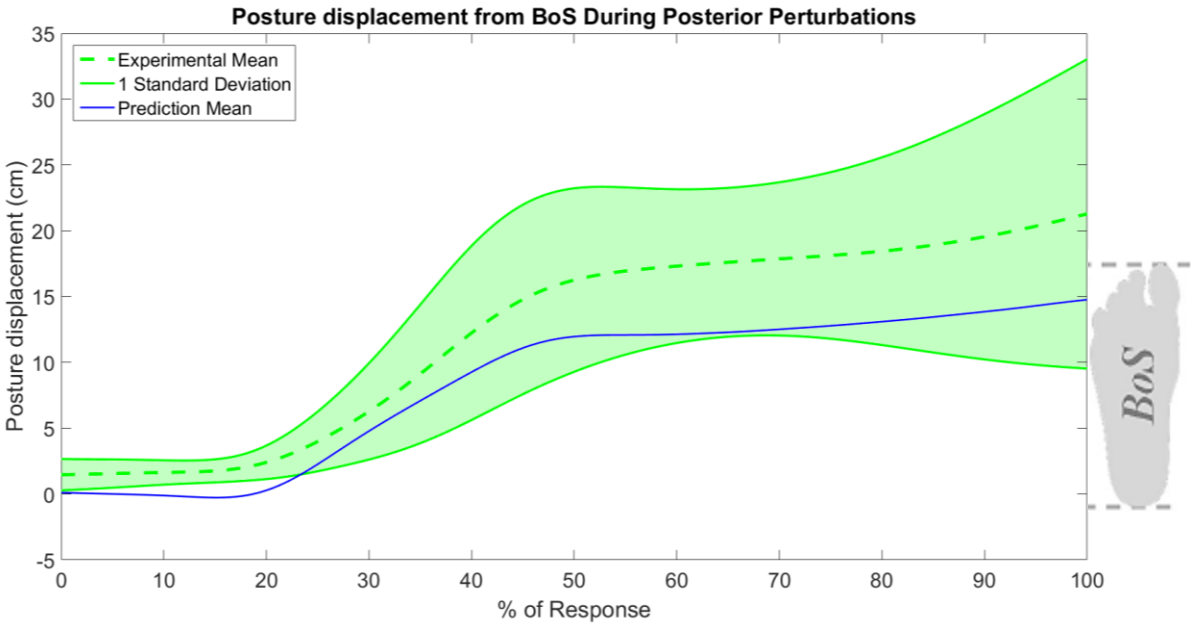

Figure 34: Predicted (Trial 0064) posture movement (blue) in the x-direction as a percentage of step response. Shaded (green) region represents one standard deviation about the mean experimental posture trajectory for all posterior perturbation trials. Both predicted and experimental trajectories are reported as displacements from the base of support (right, plant foot).

platform's ability to discern the correct response to an input anterior or posterior perturbation, and the coordinate body movements so as to match the strategy that would be employed by the same subject *in vivo*.

5.5.2 Controller performance

The platform itself may be improved in order to generate more accurate predictions. The separate proportional, integral, and derivative gains of each tasks' controller may be optimized in order to maximize agreement between simulations and experimental data. Furthermore, gain optimization in the control system architecture may reduce lag time resulting in delayed responses compared to experimental observations (as shown in Figure 28). Further research into subject-specific optimal control will be required for future iterations of this system and research aims investigated.

5.5.3 Challenges and recommendations

Only anterior and posterior perturbations were considered for this study. Due to limited z-direction displacement of the center of mass, the z surrogate models generate limited change in task positioning as there is significantly more data points in each compound surrogate corresponding to little or no z-direction movement. The z surrogates should improve with the inclusion of lateral, medial, and diagonal perturbation data, which would better define the operational space relationship between each task. Increasing the data set would likely also improve tracking accuracy overall between all tasks and directions.

Stepping research as it pertains to falls places a premium on the first step taken, due to significantly higher risk of falling as multiple steps are used. For this reason, biomechanists and clinical researchers typically focus analysis efforts on the time span from perturbation to step

contact. Similarly, we limited our analysis of both the predicted movements and the experimentally collected data to the time from perturbation to before first contact between the step foot (heel or toe) and the platform body. The simulation does not recognize double support, and does not include routines for weight acceptance and transfer that follow touch down. Future work will bridge this gap in order to predict multiple step placements and address parallel studies' aims in gait and other double support movements.

Chapter 6: Conclusion

In the work presented here, we developed a control systems approach for replacing biological feedback mechanisms with computational information modeled after humanoid robotics. In Aim I, as well as in preliminary research, we demonstrated to the efficacy of a synthesized approach, merging these techniques for planning movement strategy with prioritized task execution, at generating expected responses for human balance recovery simulations. Utilizing the described control scheme and three tasks, the platform was able to respond appropriately to small and large perturbation inputs and remain balanced.

Clinically, subject-specific treatment and rehabilitation strategies are becoming more prevalent. In order to improve functional outcomes, it is necessary to develop new computational toolsets for generating complementary simulations. These simulations may play a crucial role in patient care in the near future, as they are easily manipulated to uncover biomechanical and neurological relationships that are not made apparent through traditional data collection and observation. This places a heavy burden on simulators, as the models must be both accurate and comprehensive. That is, full representations of signal-to-movement output pathways must be developed rapidly and reliably.

In Aim II, we demonstrated the power of surrogate response surface models in meeting this need for balance recovery research. The surrogate model represents actual movements recorded *in vivo*, therefore it encompasses all decision making and execution processes involved in producing the complex multifaceted response. This is particularly important for balance recovery and falls research, as identifying different data relationships may lead to new approaches in training strategies for improving stability in at-risk groups, such as the older multiple stepper cohort evaluated here. Furthermore, exploring concepts from multiple fields of study and providing

interdisciplinary innovations is of great benefit. This work sought not only to develop novel evaluation methods for falls research, but also to promote cross disciplinary research by demonstrating the unique products of studies that approach biomechanical systems from multiple angles.

The novel platform developed in Aim III is the first of its kind for predicting subject-specific response to destabilization by modeling that subject's chosen neuromechanical coordination as recorded in the lab setting. While the predictions are not perfect, recommendations for improving accuracy include optimization of controller gains and expansion of the training data set. This work used a simplified model of balance recovery which included only three subtasks: center of mass control, step foot response, and posture alignment. However, the operational space task-prioritization described in Aim I is limitless in the number of tasks that can be represented and coordinated. Future versions of the system may improve upon the results given here by defining additional tasks at the knee and hip in order to track a larger array of task point trajectories. Likewise, only the step response task was altered over the course of any given simulation trial in order to change the task definition from balance control (via limb articulation) to balance recovery (e.g. taking a forward or backwards step). The prioritization hierarchy is flexible in that any task definition can be made higher priority than any other task. To take this concept a step further, future work will need to explore dynamically changing the prioritization hierarchy during simulated response in order to determine its effect on movement output.

The system concept developed and validated in Aim III is a first step towards comprehensive predictive simulation of specific subjects. While on a trial-to-trial basis the accuracy of the system's prediction was always above 80%, the minimum accuracy across testing

sets dropped off into the 60% range. Recommendations for improving the system response have been discussed above, and it is reasonable to expect predictive accuracies consistently above 90% before making clinically relevant claims. For comparison, the United States Food and Drug Administration assigns a “High Quality” level of evidence rating for Phase III drug and medical device testing where success rates are >80% at follow-up in at least two double-blinded studies [112], [113]. However, the performance of the system as described here contributes to the argument that simulation in research, rehabilitation, and clinical practices shows significant promise for expanding and improving.

The platform described here is novel technology for making subject-specific predictive simulations. Despite the focus of this dissertation being on applications to balance recovery research, there are no limits on task-based prioritization in terms of number of tasks defined, and compound surrogate response modeling can be applied to any set of task vector definitions. This means that although balance recovery was studied here, any movement goal (e.g. gait, sit-to-stand, throwing, jumping, etc.) can be modeled and simulated so long as subtasks can be appropriately defined and controlled. For these reasons this work may have far reaching applications in other areas of human movement science and research. Furthermore, this modeling technique can be used for any subject, healthy or impaired, greatly expanding the range of application and significance of the predictions. The inherent flexibility in choice of tasks and control strategies will allow this system to be used for a number of investigations across fields in the future.

Future work involving this platform will address double-support contact between both feet and the ground, as this changes the support Jacobian which is the basis for the prioritized task simulations. Double-support is also a fundamental part of other movement goals, and will need to

be included in order to generate predictive simulations of other activities. Optimizing controller gains and the prioritization hierarchy will also contribute to more accurate representations of subjects. The end goal for this system is to fine tune it as a comprehensive representation of an impaired subject's neuromechanics. Changes can then be made to the surrogate models, controllers, priorities, or the musculoskeletal model itself that reflect rehabilitation techniques used clinically. Based on its ability to predict subject-specific movement coordination, the platform would simulate and predict what changes would occur due to the intervention. In this way clinicians may evaluate personalized care routines prior to implementation, thereby identifying the best strategies ahead of time and improving functional outcomes. Future work will continue towards this goal and eventually test this platform against clinical data to determine how well it is able to predict success rates for a wide range of musculoskeletal disease and movement disorder treatments.

References

[1] S. L. Delp *et al.*, "OpenSim: Open source to create and analyze dynamic simulations of movement," *IEEE Trans. Biomed. Eng.*, vol. 54, no. 11, pp. 1940–1950, 2007.
[2] "United States Bone and Joint Initiative: The Burden of Musculoskeletal Diseases in the United States (BMUS)," *United States Bone and Joint Initiative*, 2014. [Online]. Available: http://www.boneandjointburden.org.
[3] R. D. R. Komistek, D. a. D. D. A. Dennis, and M. Mahfouz, "In vivo fluoroscopic analysis of the normal human knee," *Clin. Orthop. Relat. Res.*, vol. 410, no. 410, pp. 69–81, 2003.
[4] J.-J. Wu, "Clinical application of vicon system to evaluate the gait pattern after toe-to-thumb reconstruction," *J. Biomech.*, vol. 20, no. 9, p. 910, 1987.
[5] J. Schmid, a. Sandholm, and F. Chung, "Musculoskeletal simulation model generation from MRI data sets and motion capture data," *Recent Adv. 3D Physiol. Hum.*, pp. 3–20, 2009.
[6] J. Gall, C. Stoll, E. De Aguiar, C. Theobalt, B. Rosenhahn, and H. P. Seidel, "Motion capture using joint skeleton tracking and surface estimation," in *2009 IEEE Computer Society Conference on Computer Vision and Pattern Recognition Workshops, CVPR Workshops 2009*, 2009, pp. 1746–1753.
[7] C. J. De Luca, "The use of surface electromyography in biomechanics," in *Journal of Applied Biomechanics*, 1997, vol. 13, no. 2, pp. 135–163.
[8] R. Kram, T. M. Griffin, J. Maxwell Donelan, and Y. Hui Chang, "Force treadmill for measuring vertical and horizontal ground reaction forces," *J. Appl. Physiol.*, vol. 7, no. 9, pp. 764–769, 1998.
[9] Z. P. Luo, L. J. Berglund, and K. N. An, "Validation of F-Scan pressure sensor system: a technical note.," *J. Rehabil. Res. Dev.*, vol. 35, no. 2, pp. 186–191, 1998.
[10] L.-F. Lee and B. R. Umberger, "Generating optimal control simulations of musculoskeletal movement using OpenSim and MATLAB," *PeerJ*, vol. 4, p. e1638, 2016.
[11] K. D. Morgan, "Dynamic Simulations and Data Mining of Single- Leg Jump Landing: Implications for Anterior Cruciate Ligament Injury Prevention," *PhD diss., Univ. Tennessee*, 2014.
[12] D. Fleming-Farrell, K. Michailidis, A. Karantanas, N. Roberts, and E. F. Kranioti, "Virtual assessment of perimortem and postmortem blunt force cranial trauma," *Forensic Sci. Int.*, vol. 229, no. 1–3, 2013.
[13] N. A. Vavalle, D. P. Moreno, A. C. Rhyne, J. D. Stitzel, and F. S. Gayzik, "Lateral impact validation of a geometrically accurate full body finite element model for blunt injury prediction," *Ann. Biomed. Eng.*, vol. 41, no. 3, pp. 497–512, 2013.
[14] A. J. Golman, K. A. Danelson, L. E. Miller, and J. D. Stitzel, "Injury prediction in a side impact crash using human body model simulation," *Accid. Anal. Prev.*, vol. 64, pp. 1–8, 2014.
[15] M. Mansouri Boroujeni, "Dynamic Simulation and Neuromuscular Control of Movement: Applications for Predictive Simulations of Balance Recovery," 2015.
[16] W. Wach and J. Unarski, "Fall from height in a stairwell - mechanics and simulation analysis," *Forensic Sci. Int.*, vol. 244, pp. 136–151, 2014.
[17] D. G. Thelen and F. C. Anderson, "Using computed muscle control to generate forward dynamic simulations of human walking from experimental data," *J. Biomech.*, vol. 39, no. 6, pp. 1107–1115, 2006.
[18] M. G. Pandy, "Computer modeling and simulation of human movement," *Annu. Rev.*

Biomed. Eng., vol. 3, no. 1, pp. 245–273, 2001.
[19] J. S. Higginson, F. E. Zajac, R. R. Neptune, S. A. Kautz, and S. L. Delp, "Muscle contributions to support during gait in an individual with post-stroke hemiparesis," *J. Biomech.*, vol. 39, no. 10, pp. 1769–1777, 2006.
[20] T. W. Dorn, J. M. Wang, J. L. Hicks, and S. L. Delp, "Predictive simulation generates human adaptations during loaded and inclined walking," *PLoS One*, vol. 10, no. 4, 2015.
[21] B. J. Fregly, J. A. Reinbolt, K. L. Rooney, K. H. Mitchell, and T. L. Chmielewski, "Design of patient-specific gait modifications for knee osteoarthritis rhabilitation," *IEEE Trans. Biomed. Eng.*, vol. 54, no. 9, pp. 1687–1695, 2007.
[22] M. Mansouri, A. E. Clark, A. Seth, and J. A. Reinbolt, "Rectus femoris transfer surgery affects balance recovery in children with cerebral palsy: A computer simulation study," *Gait Posture*, vol. 43, pp. 24–30, 2016.
[23] O. Khatib, "Inertial Properties in Robotic Manipulation: An Object-Level Framework," *Int. J. Rob. Res.*, vol. 14, no. 1, pp. 19–36, 1995.
[24] O. Khatib, E. Demircan, V. De Sapio, L. Sentis, T. Besier, and S. Delp, "Robotics-based synthesis of human motion," *J. Physiol. Paris*, vol. 103, no. 3–5, pp. 211–219, 2009.
[25] B. Dariush, G. Bin Hammam, and D. Orin, "Constrained resolved acceleration control for humanoids," in *IEEE/RSJ 2010 International Conference on Intelligent Robots and Systems, IROS 2010 - Conference Proceedings*, 2010, pp. 710–717.
[26] O. Khatib, "A unified approach for motion and force control of robot manipulators: The operational space formulation," *IEEE J. Robot. Autom.*, vol. 3, no. 1, pp. 43–53, 1987.
[27] L. Sentis and O. Khatib, "Control of free-floating humanoid robots through task prioritization," in *Proceedings - IEEE International Conference on Robotics and Automation*, 2005, vol. 2005, pp. 1718–1723.
[28] L. Sentis, "Synthesis And Control of Whole-body Behaviors in Humanoid Systems," 2007.
[29] M. Mansouri and J. A. Reinbolt, "A platform for dynamic simulation and control of movement based on OpenSim and MATLAB," *J. Biomech.*, vol. 45, no. 8, pp. 1517–1521, 2012.
[30] M. Mansouri, V. De Sapio, and J. A. Reinbolt, "Prioritized Task-Based Control of Movement with Supporting Contacts Using OpenSim and Matlab," in *XV International Symposium on Computer Simulation in Biomechanics*, 2015, pp. 2–3.
[31] M. Mansouri Boroujeni, C. J. Donnelly, M. Robinson, J. Vanrenterghem, and J. A. Reinbolt, "Synthesis of Subject-Specific Task-Level Motions for Predictive Simulations of Balance Recovery," in *American Society of Biomechanics 39th Annual Meeting*, 2015, pp. 47–50.
[32] J. A. Reinbolt, "Task-Level Simulation of Subject-Specific Movement Using Opensim," in *XXV Congress of the International Society of Biomechanics*, 2015.
[33] J. A. Reinbolt, N. Vivaldi, and M. B. Mansouri, "Subject-specific Surrogate Models of Task-level Human Movement," in *Biomechanics and Neural Control of Movement*, 2016.
[34] M. B. Mansouri, N. A. Vivaldi, C. J. Donnelly, M. A. Robinson, J. Vanrenterghem, and J. A. Reinbolt, "Synthesis of Subject-Specific Human Balance Responses using a Task-Level Neuromuscular Control Platform," *IEEE Trans. Neural Syst. Rehabil. Eng.*, vol. PP, no. 99, p. 1, 2018.
[35] D. F. Graham, C. P. Carty, D. G. Lloyd, and R. S. Barrett, "Biomechanical predictors of maximal balance recovery performance amongst community-dwelling older adults," *Exp.*

Gerontol., vol. 66, pp. 39–46, 2015.
[36] M. Afschrift, F. De Groote, S. Verschueren, and I. Jonkers, "Increased sensory noise and not muscle weakness explains changes in non-stepping postural responses following stance perturbations in healthy elderly," *Gait Posture*, vol. 59, pp. 122–127, 2018.
[37] Z. Aftab, T. Robert, and P. B. Wieber, "Balance recovery prediction with multiple strategies for standing humans," *PLoS One*, vol. 11, no. 3, 2016.
[38] M. Vukobratović and B. Borovac, "Zero-Moment Point — Thirty Five Years of Its Life," *Int. J. Humanoid Robot.*, vol. 1, no. 1, pp. 157–173, 2004.
[39] A. L. Hof, "The 'extrapolated center of mass' concept suggests a simple control of balance in walking," *Hum. Mov. Sci.*, vol. 27, no. 1, pp. 112–125, 2008.
[40] L. Sentis, J. Park, and O. Khatib, "Compliant control of multicontact and center-of-mass behaviors in humanoid robots," *IEEE Trans. Robot.*, vol. 26, no. 3, pp. 483–501, 2010.
[41] C. P. Carty *et al.*, "Reactive stepping behaviour in response to forward loss of balance predicts future falls in community-dwelling older adults," *Age Ageing*, vol. 44, no. 1, pp. 109–115, 2015.
[42] A. L. Hof, M. G. J. Gazendam, and W. E. Sinke, "The condition for dynamic stability," *J. Biomech.*, vol. 38, no. 1, pp. 1–8, 2005.
[43] B. E. Maki and W. E. McIlroy, "The role of limb movements in maintaining upright stance: The 'change- in-support' strategy," *Physical Therapy*, vol. 77, no. 5. pp. 488–507, 1997.
[44] World Health Organization, "Falls: fact sheet," *World Health Organization*, 2018. [Online]. Available: http://www.who.int/mediacentre/factsheets/fs344/en/.
[45] K. Iqbal and Y. C. Pai, "Predicted region of stability for balance recovery: Motion at the knee joint can improve termination of forward movement," *J. Biomech.*, vol. 33, no. 12, pp. 1619–1627, 2000.
[46] L. R. Humphrey and H. Hemami, "A computational human model for exploring the role of the feet in balance," *J. Biomech.*, vol. 43, no. 16, pp. 3199–3206, 2010.
[47] C. S. Versteeg, L. H. Ting, and J. L. Allen, "Hip and ankle responses for reactive balance emerge from varying priorities to reduce effort and kinematic excursion: A simulation study," *J. Biomech.*, vol. 49, no. 14, pp. 3230–3237, 2016.
[48] K. D. Morgan, C. J. Donnelly, and J. A. Reinbolt, "Elevated gastrocnemius forces compensate for decreased hamstrings forces during the weight-acceptance phase of single-leg jump landing: Implications for anterior cruciate ligament injury risk," *J. Biomech.*, vol. 47, no. 13, pp. 3295–3302, 2014.
[49] C. L. Vaughan, "Computer simulation of human motion in sports biomechanics.," *Exerc. Sport Sci. Rev.*, vol. 12, pp. 373–416, 1984.
[50] Y. Bei and B. J. Fregly, "Multibody dynamic simulation of knee contact mechanics," *Med. Eng. Phys.*, vol. 26, no. 9 SPEC.ISS., pp. 777–789, 2004.
[51] R. R. Neptune, C. P. McGowan, and S. A. Kautz, "Forward dynamics simulations provide insight into muscle mechanical work during human locomotion," *Exerc Sport Sci Rev*, vol. 37, no. 4. pp. 203–210, 2009.
[52] F. E. Donaldson, J. C. Coburn, and K. L. Siegel, "Total hip arthroplasty head-neck contact mechanics: A stochastic investigation of key parameters," *J. Biomech.*, vol. 47, no. 7, pp. 1634–1641, 2014.
[53] P. B. Shull, Y. Huang, T. Schlotman, and J. A. Reinbolt, "Muscle force modification

strategies are not consistent for gait retraining to reduce the knee adduction moment in individuals with knee osteoarthritis," *J. Biomech.*, vol. 48, no. 12, pp. 3163–3169, 2015.
[54] P. Y. Lee, K. Gadareh, and A. M. Bronstein, "Forward-backward postural protective stepping responses in young and elderly adults," *Hum. Mov. Sci.*, vol. 34, no. 1, pp. 137–146, 2014.
[55] C. Miller Buffinton, E. M. Buffinton, K. A. Bieryla, and J. E. Pratt, "Biomechanics of Step Initiation After Balance Recovery With Implications for Humanoid Robot Locomotion.," *J. Biomech. Eng.*, vol. 138, no. 3, p. 31001, 2016.
[56] L. Rocchi, L. Chiari, M. Mancini, P. Carlson-Kuhta, A. Gross, and F. B. Horak, "Step initiation in Parkinson's disease: Influence of initial stance conditions," *Neurosci. Lett.*, vol. 406, no. 1–2, pp. 128–132, 2006.
[57] M. W. Rogers, M. E. Johnson, K. M. Martinez, M.-L. Mille, and L. D. Hedman, "Step Training Improves the Speed of Voluntary Step Initiation in Aging," *Journals Gerontol. Ser. A Biol. Sci. Med. Sci.*, vol. 58, no. 1, pp. M46–M51, 2003.
[58] R. A. Speers, A. D. Kuo, and F. B. Horak, "Contributions of altered sensation and feedback responses to changes in coordination of postural control due to aging," *Gait Posture*, vol. 16, no. 1, pp. 20–30, 2002.
[59] D. B. Elliot, A. Vale, D. Whitaker, and J. G. Buckley, "Does my step look big in this? A visual illusion leads to safer stepping behaviour," *PLoS One*, vol. 4, no. 2, 2009.
[60] D. L. Sturnieks, J. Menant, J. Vanrenterghem, K. Delbaere, R. C. Fitzpatrick, and S. R. Lord, "Sensorimotor and neuropsychological correlates of force perturbations that induce stepping in older adults," *Gait Posture*, vol. 36, no. 3, pp. 356–360, 2012.
[61] D. L. Sturnieks *et al.*, "Force-Controlled Balance Perturbations Associated with Falls in Older People: A Prospective Cohort Study," *PLoS One*, vol. 8, no. 8, 2013.
[62] T. P. Huryn, B. L. Luu, H. F. M. Van Der Loos, J. S. Blouin, and E. A. Croft, "Investigating human balance using a robotic motion platform," in *Proceedings - IEEE International Conference on Robotics and Automation*, 2010, pp. 5090–5095.
[63] J. Pratt, J. Carff, S. Drakunov, and A. Goswami, "Capture point: A step toward humanoid push recovery," in *Proceedings of the 2006 6th IEEE-RAS International Conference on Humanoid Robots, HUMANOIDS*, 2006, pp. 200–207.
[64] A. Elhasairi and A. Pechev, "Humanoid Robot Balance Control Using the Spherical Inverted Pendulum Mode," *Front. Robot. AI*, vol. 2, no. October, pp. 1–13, 2015.
[65] B. Stephens, "Integral control of humanoid balance," in *IEEE International Conference on Intelligent Robots and Systems*, 2007, pp. 4020–4027.
[66] H. Hauser, G. Neumann, A. J. Ijspeert, and W. Maass, "Biologically inspired kinematic synergies enable linear balance control of a humanoid robot," *Biol. Cybern.*, vol. 104, no. 4–5, pp. 235–249, 2011.
[67] Z. Aftab, T. Robert, and P. B. Wieber, "Predicting multiple step placements for human balance recovery tasks," *J. Biomech.*, vol. 45, no. 16, pp. 2804–2809, 2012.
[68] N. A. Vivaldi and J. A. Reinbolt, "Identifying novel strategies for controlling step response during balance recovery simulations," in *8th World Congress of Biomechanics*, 2018.
[69] N. A. Vivaldi, J. A. Reinbolt, and R. S. Barrett, "Using zero-moment point to predict single versus multiple step recovery from forward loss of balance," in *8th World Congress of Biomechanics*, 2018.

[70] N. A. Vivaldi and J. A. Reinbolt, “Synthesis of subject-specific, task-level stepping response for predicting balance recovery,” in *XXVI Congress of the International Society of Biomechanics*, 2017.
[71] Y. Xiang, J. S. Arora, S. Rahmatalla, and K. Abdel-Malek, “Optimization-based dynamic human walking prediction: One step formulation,” *Int. J. Numer. Methods Eng.*, vol. 79, no. 6, pp. 667–695, 2009.
[72] M. S. Redfern, L. Yardley, and A. M. Bronstein, “Visual influences on balance,” *J. Anxiety Disord.*, vol. 15, no. 1–2, pp. 81–94, 2001.
[73] J. H. van Dieën, M. van Leeuwen, and G. S. Faber, “Learning to balance on one leg: motor strategy and sensory weighting,” *J. Neurophysiol.*, vol. 114, no. 5, pp. 2967–2982, 2015.
[74] D. S. Marigold, “Role of the Unperturbed Limb and Arms in the Reactive Recovery Response to an Unexpected Slip During Locomotion,” *J. Neurophysiol.*, vol. 89, no. 4, pp. 1727–1737, 2002.
[75] M. Pijnappels, I. Kingma, D. Wezenberg, G. Reurink, and J. H. Van Dieën, “Armed against falls: The contribution of arm movements to balance recovery after tripping,” *Exp. Brain Res.*, vol. 201, no. 4, pp. 689–699, 2010.
[76] W. E. McIlroy and B. E. Maki, “The control of lateral stability during rapid stepping reactions evoked by antero-posterior perturbation: Does anticipatory control play a role?,” *Gait Posture*, vol. 9, no. 3, pp. 190–198, 1999.
[77] A. L. Hof, “The equations of motion for a standing human reveal three mechanisms for balance,” *J. Biomech.*, vol. 40, no. 2, pp. 451–457, 2007.
[78] M. W. Rogers, L. D. Hedman, M. E. Johnson, K. M. Martinez, and M. L. Mille, “Triggering of protective stepping for the control of human balance: Age and contextual dependence,” *Cogn. Brain Res.*, vol. 16, no. 2, pp. 192–198, 2003.
[79] M. L. Mille, M. Johnson-Hilliard, K. M. Martinez, Y. Zhang, B. J. Edwards, and M. W. Rogers, “One step, two steps, three steps more... directional vulnerability to falls in community-dwelling older people,” *Journals Gerontol. - Ser. A Biol. Sci. Med. Sci.*, vol. 68, no. 12 A, pp. 1540–1548, 2013.
[80] M. Fujimoto, W. N. Bair, and M. W. Rogers, “Single and multiple step balance recovery responses can be different at first step lift-off following lateral waist-pull perturbations in older adults,” *J. Biomech.*, vol. 55, pp. 41–47, 2017.
[81] C. P. Carty, N. J. Cronin, G. A. Lichtwark, P. M. Mills, and R. S. Barrett, “Mechanisms of adaptation from a multiple to a single step recovery strategy following repeated exposure to forward loss of balance in older adults,” *PLoS One*, vol. 7, no. 3, 2012.
[82] C. P. Carty, R. S. Barrett, N. J. Cronin, G. A. Lichtwark, P. M. Mills, and L. Ferrucci, “Lower limb muscle weakness predicts use of a multiple-versus single-step strategy to recover from forward loss of balance in older adults,” *Journals Gerontol. - Ser. A Biol. Sci. Med. Sci.*, vol. 67, no. 11, pp. 1246–1252, 2012.
[83] N. J. Cronin, R. S. Barrett, G. Lichtwark, P. M. Mills, and C. P. Carty, “Decreased lower limb muscle recruitment contributes to the inability of older adults to recover with a single step following a forward loss of balance,” *J. Electromyogr. Kinesiol.*, vol. 23, no. 5, pp. 1139–1144, 2013.
[84] L. R. Bent, B. J. McFadyen, and J. T. Inglis, “Vestibular contributions during human locomotor tasks,” *Exercise and Sport Sciences Reviews*, vol. 33, no. 3. pp. 107–113, 2005.

[85] I. Renshaw and K. Davids, “Nested task constraints shape continuous perception-action coupling control during human locomotor pointing,” *Neuroscience Letters*, vol. 369, no. 2. pp. 93–98, 2004.
[86] A. Sawers, V. E. Kelly, D. Kartin, and M. E. Hahn, “Gradual training reduces the challenge to lateral balance control during practice and subsequent performance of a novel locomotor task,” *Gait Posture*, vol. 38, no. 4, pp. 907–911, 2013.
[87] M. Hutter, H. Sommer, C. Gehring, M. Hoepflinger, M. Bloesch, and R. Siegwart, “Quadrupedal locomotion using hierarchical operational space control,” *Int. J. Rob. Res.*, vol. 33, no. 8, pp. 1047–1062, 2014.
[88] S. Alatartsev, S. Stellmacher, and F. Ortmeier, “Robotic Task Sequencing Problem: A Survey,” *J. Intell. Robot. Syst. Theory Appl.*, vol. 80, no. 2, pp. 279–298, 2015.
[89] S. Hak, N. Mansard, O. Stasse, and J. P. Laumond, “Reverse control for humanoid robot task recognition,” *IEEE Trans. Syst. Man, Cybern. Part B Cybern.*, vol. 42, no. 6, pp. 1524–1537, 2012.
[90] T. Koolen, M. Posa, and R. Tedrake, “Balance control using center of mass height variation: Limitations imposed by unilateral contact,” in *IEEE-RAS International Conference on Humanoid Robots*, 2016, pp. 8–15.
[91] C. W. L. Almeida, C. H. M. Castro, P. G. Pedreira, R. E. Heymann, and V. L. Szejnfeld, “Percentage height of center of mass is associated with the risk of falls among elderly women: A case-control study.,” *Gait Posture*, vol. 34, no. 2, pp. 208–12, 2011.
[92] D. Bazylev, A. Kremlev, A. Margun, and K. Zimenko, “Control system of biped robot balancing on board,” in *2014 19th International Conference on Methods and Models in Automation and Robotics, MMAR 2014*, 2014, pp. 794–799.
[93] N. A. Vivaldi and J. A. Reinbolt, “Using zero-moment point to synthesize subject-specific, task-level predictions of balance recovery with stepping,” in *XVI International Symposium on Computer Simulation in Biomechanics*, 2017.
[94] R. S. Hinman, K. L. Bennell, B. R. Metcalf, and K. M. Crossley, “Balance impairments in individuals with symptomatic knee osteoarthritis: A comparison with matched controls using clinical tests,” *Rheumatology*, vol. 41, no. 12, pp. 1388–1394, 2002.
[95] K. P. Westlake and E. G. Culham, “Sensory-Specific Balance Training in Older Adults: Effect on Proprioceptive Reintegration and Cognitive Demands,” *Phys. Ther.*, vol. 87, no. 10, pp. 1274–1283, 2007.
[96] T. Wojtara, F. Alnajjar, S. Shimoda, and H. Kimura, “Muscle synergy stability and human balance maintenance,” *J. Neuroeng. Rehabil.*, vol. 11, no. 1, 2014.
[97] N. Patel, J. Jankovic, and M. Hallett, “Sensory aspects of movement disorders,” *The Lancet Neurology*, vol. 13, no. 1. pp. 100–112, 2014.
[98] J. A. Nichols, M. S. Bednar, and W. M. Murray, “Surgical Simulations Based on Limited Quantitative Data: Understanding How Musculoskeletal Models Can Be Used to Predict Moment Arms and Guide Experimental Design,” *PLoS One*, vol. 11, no. 6, 2016.
[99] N. Mehrabi, R. Sharif Razavian, B. Ghannadi, and J. McPhee, “Predictive Simulation of Reaching Moving Targets Using Nonlinear Model Predictive Control,” *Front. Comput. Neurosci.*, vol. 10, 2017.
[100] J. Verghese, A. LeValley, C. B. Hall, M. J. Katz, A. F. Ambrose, and R. B. Lipton, “Epidemiology of gait disorders in community-residing older adults,” *J. Am. Geriatr. Soc.*,

vol. 54, no. 2, pp. 255–261, 2006.
[101] J. Babič, E. Oztop, and M. Kawato, "Human motor adaptation in whole body motion," *Sci. Rep.*, vol. 6, no. 1, p. 32868, 2016.
[102] M. H. Sohn, J. L. McKay, and L. H. Ting, "Defining feasible bounds on muscle activation in a redundant biomechanical task: Practical implications of redundancy," *J. Biomech.*, vol. 46, no. 7, pp. 1363–1368, 2013.
[103] C. S. Simpson, M. H. Sohn, J. L. Allen, and L. H. Ting, "Feasible muscle activation ranges based on inverse dynamics analyses of human walking," *J. Biomech.*, vol. 48, no. 12, pp. 2990–2997, 2015.
[104] A. L. Wong, A. M. Haith, and J. W. Krakauer, "Motor Planning," *Neurosci.*, vol. 21, no. 4, pp. 385–398, 2015.
[105] W. Pirker and R. Katzenschlager, "Gait disorders in adults and the elderly: A clinical guide," *Wiener Klinische Wochenschrift*, vol. 129, no. 3–4. pp. 81–95, 2017.
[106] P. M. Bays and D. M. Wolpert, "Computational principles of sensorimotor control that minimize uncertainty and variability," *Journal of Physiology*, vol. 578, no. 2. pp. 387–396, 2007.
[107] C. M. Harris and D. M. Wolpert, "Signal-dependent noise determines motor planning," *Nature*, vol. 394, no. 6695, pp. 780–784, 1998.
[108] R. Ranganathan, A. Adewuyi, and F. A. Mussa-Ivaldi, "Learning to be Lazy: Exploiting Redundancy in a Novel Task to Minimize Movement-Related Effort," *J. Neurosci.*, vol. 33, no. 7, pp. 2754–2760, 2013.
[109] F. R. Sarlegna and P. K. Mutha, "The influence of visual target information on the online control of movements," *Vision Res.*, vol. 110, no. PB, pp. 144–154, 2015.
[110] N. W. Willigenburg, I. Kingma, and J. H. Van Dieën, "Center of pressure trajectories, trunk kinematics and trunk muscle activation during unstable sitting in low back pain patients," *Gait Posture*, vol. 38, no. 4, pp. 625–630, 2013.
[111] M. W. Shrader, L. F. Draganich, L. A. Pottenger, and G. A. Piotrowski, "Effects of Knee Pain Relief in Osteoarthritis on Gait and Stair-Stepping," *Clin. Orthop. Relat. Res.*, vol. 421, pp. 188–193, 2004.
[112] G. A. Van Norman, "Drugs, Devices, and the FDA: Part 1: An Overview of Approval Processes for Drugs," *JACC Basic to Transl. Sci.*, vol. 1, no. 3, pp. 170–179, 2016.
[113] G. A. Van Norman, "Drugs, Devices, and the FDA: Part 2," *JACC Basic to Transl. Sci.*, vol. 1, no. 4, pp. 277–287, 2016.

Appendix

Appendix A

A1: Response to 6 cm perturbation

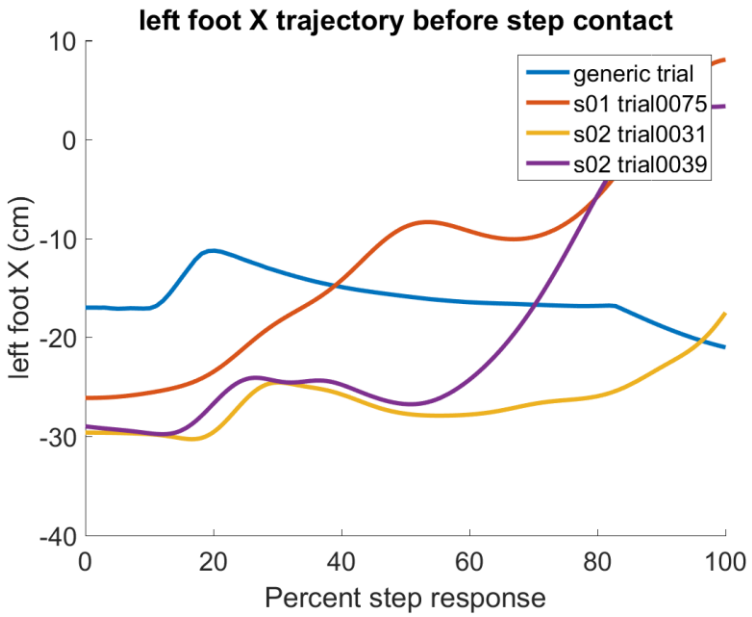

Figure 35: Plot of step foot x-direction displacement from the support foot (6 cm perturbation).

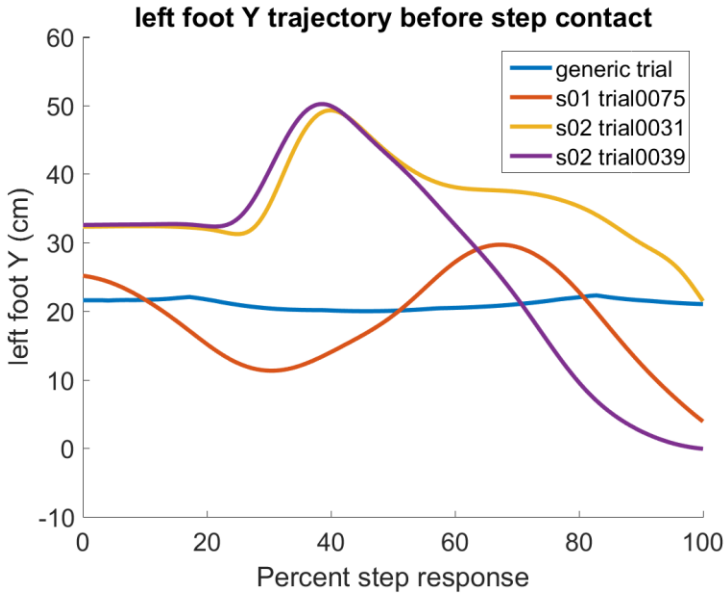

Figure 36: Plot of step foot y-direction displacement from the support foot (6 cm perturbation).

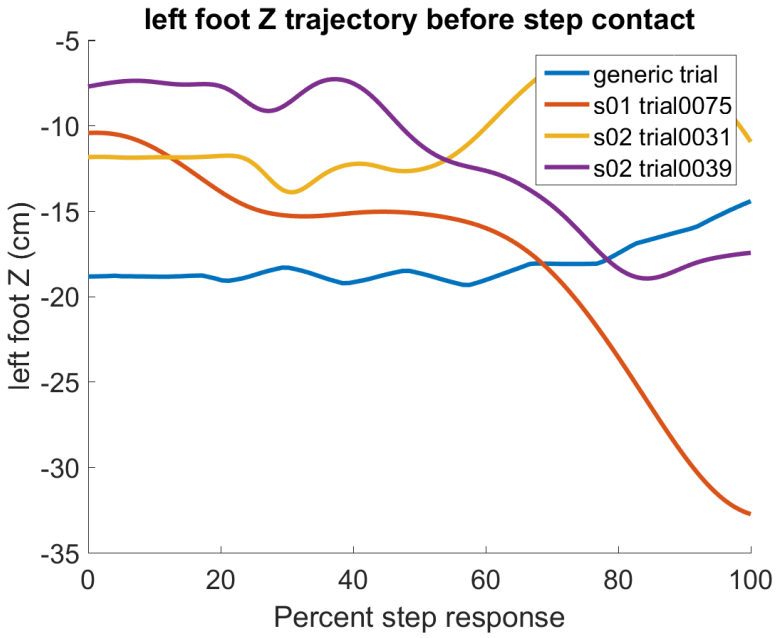

Figure 37: Plot of step foot z-direction displacement from the support foot (6 cm perturbation).

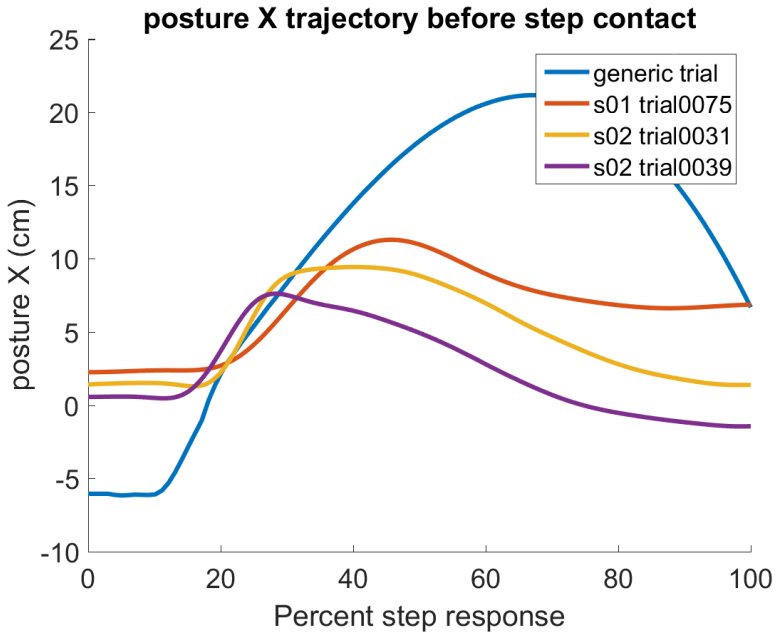

Figure 38: Plot of posture x-direction displacement from the support foot (6 cm perturbation).

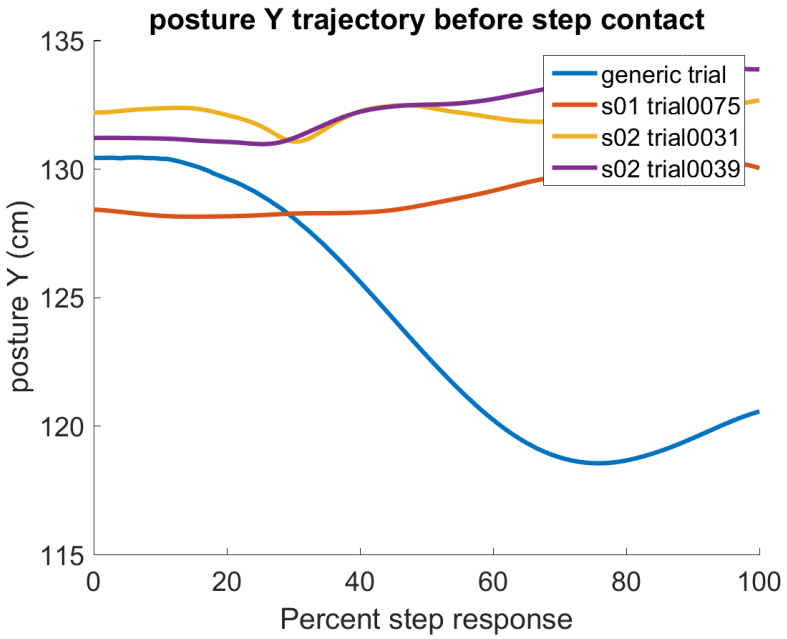

Figure 39: Plot of posture y-direction displacement from the support foot (6 cm perturbation).

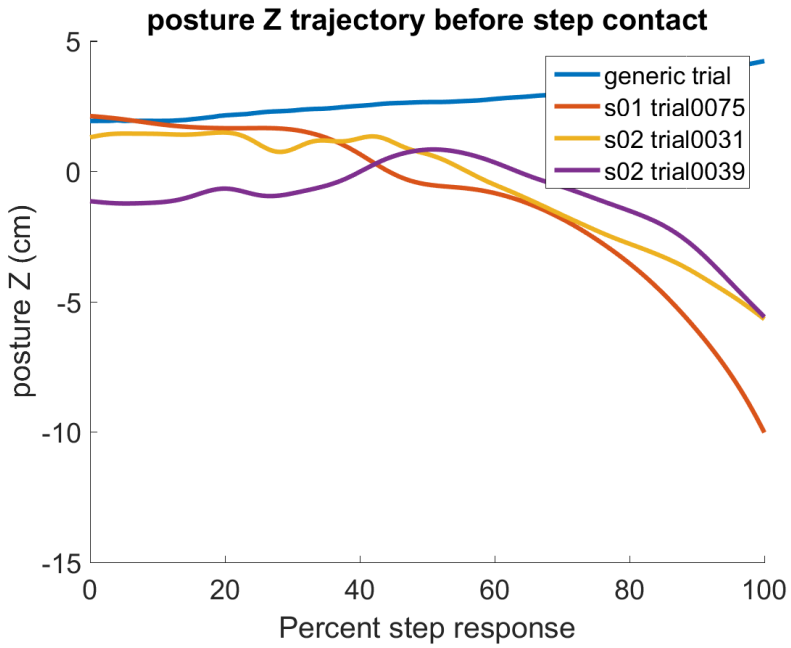

Figure 40: Plot of posture z-direction displacement from the support foot (6 cm perturbation).

A2: Response to 12 cm perturbation

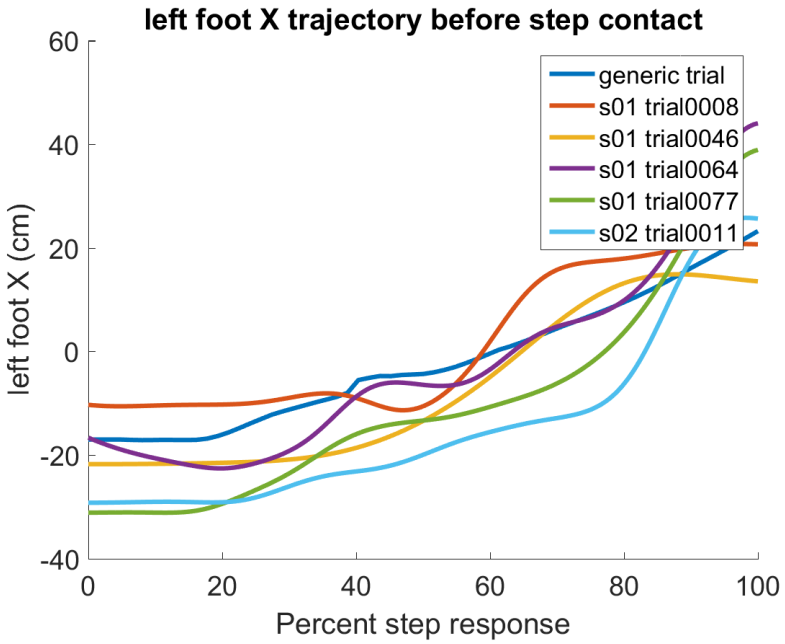

Figure 41: Plot of step foot x-direction displacement from the support foot (12 cm perturbation).

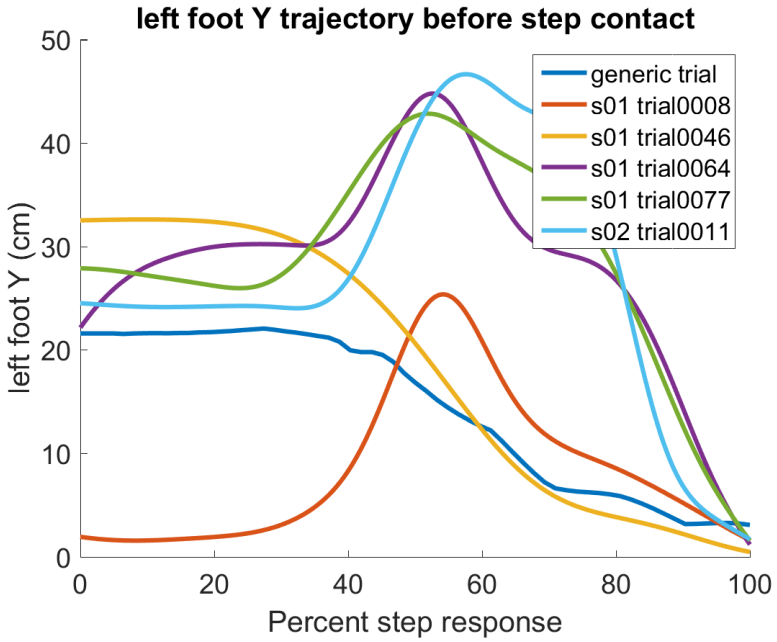

Figure 42: Plot of step foot y-direction displacement from the support foot (12 cm perturbation).

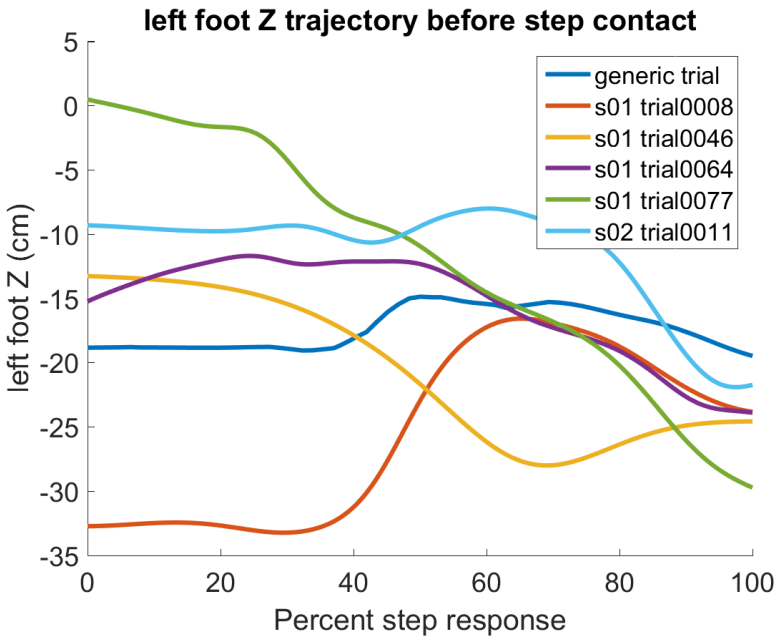

Figure 43: Plot of step foot z-direction displacement from the support foot (12 cm perturbation).

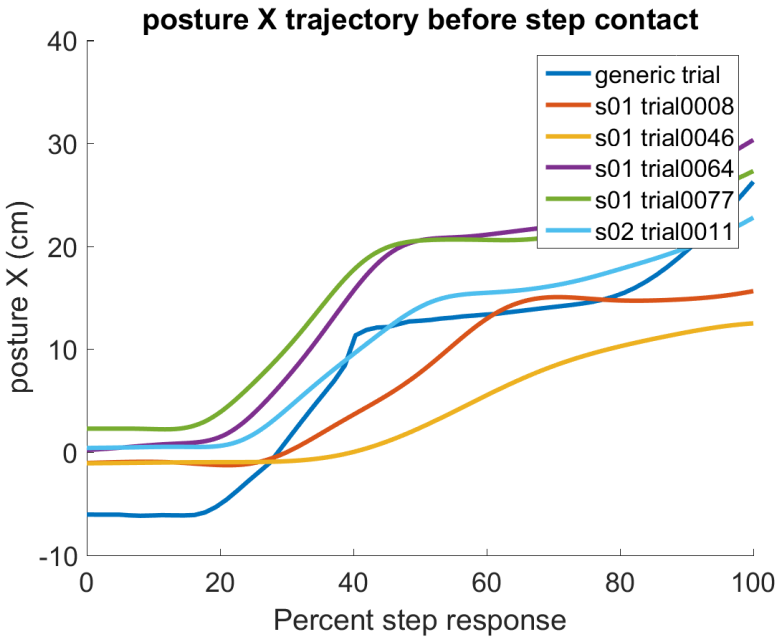

Figure 44: Plot of posture x-direction displacement from the support foot (12 cm perturbation).

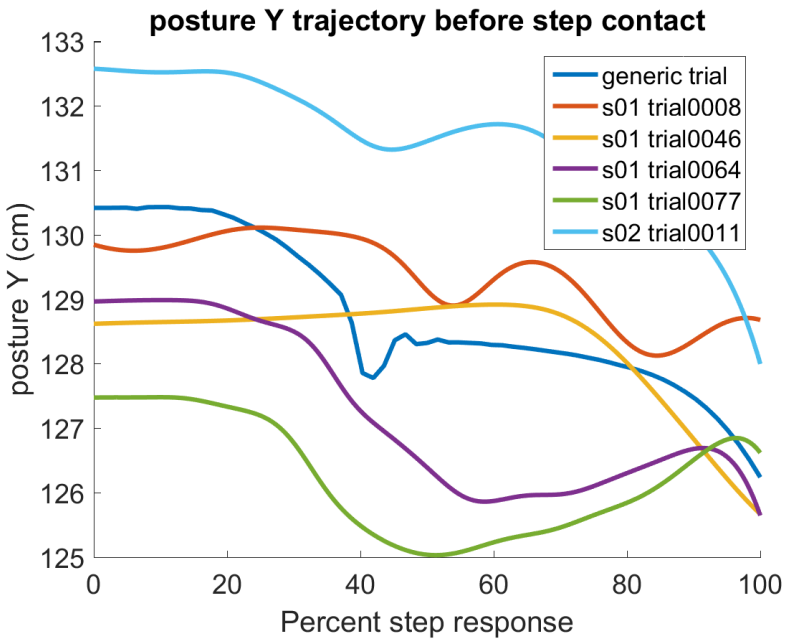

Figure 45: Plot of posture y-direction displacement from the support foot (12 cm perturbation).

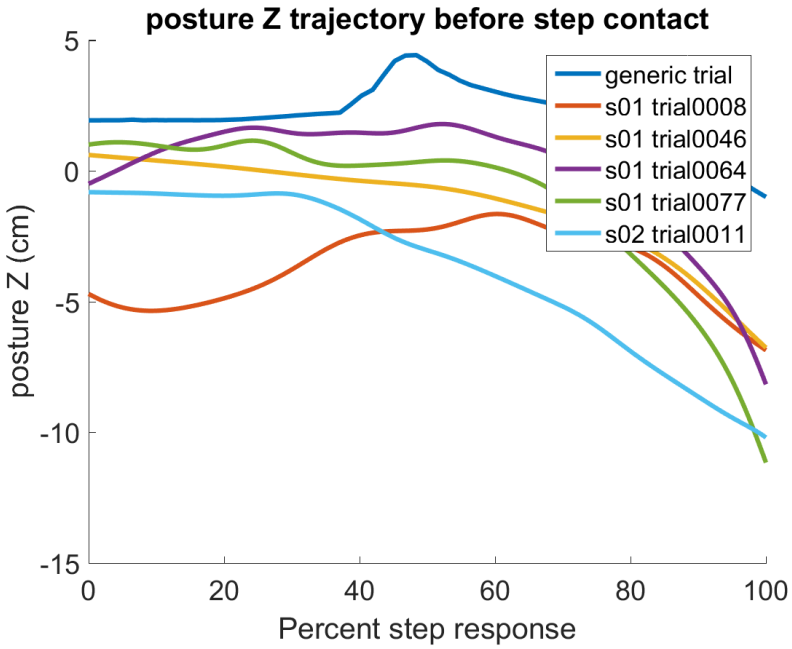

Figure 46: Plot of posture z-direction displacement from the support foot (12 cm perturbation).

Appendix B

B1: Surrogate response surfaces for step foot y and z components

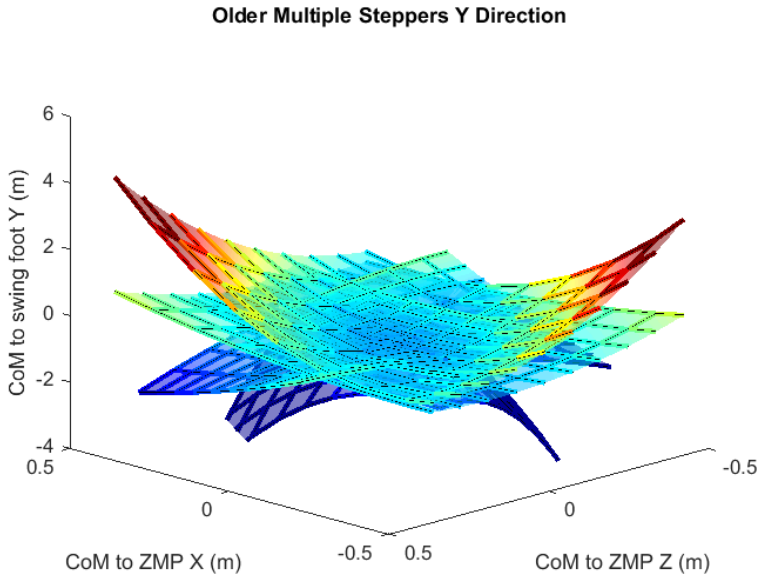

Figure 47: Surrogate response surface models of step foot y-direction task space from OMS cohort trials.

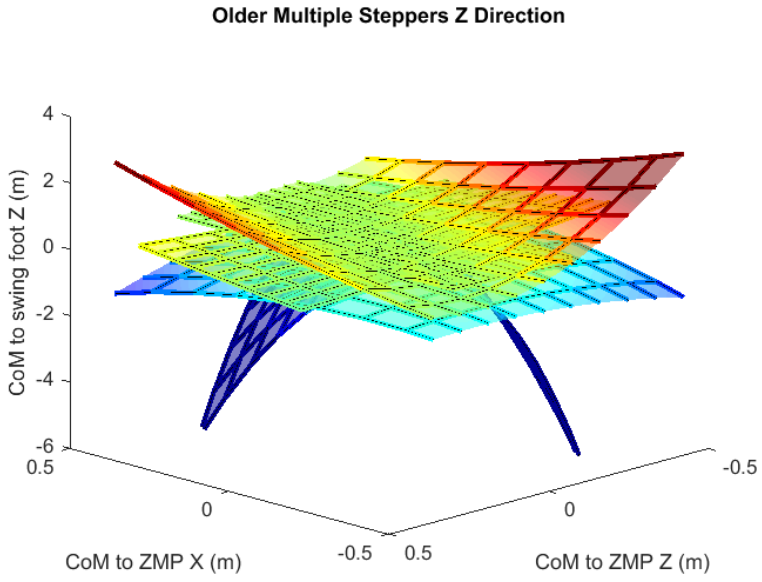

Figure 48: Surrogate response surface models of step foot z-direction task space from OMS cohort trials.

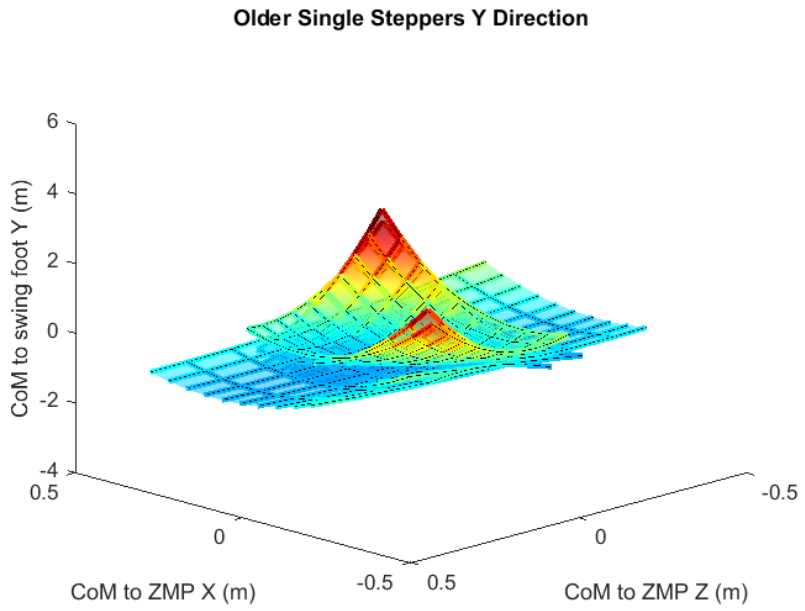

Figure 49: Surrogate response surface models of step foot y-direction task space from OSS cohort trials.

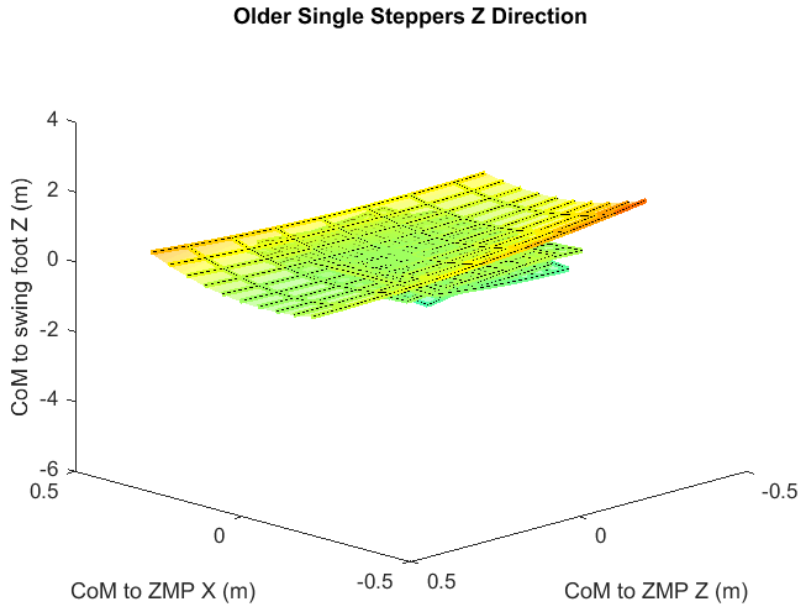

Figure 50: Surrogate response surface models of step foot z-direction task space from OSS cohort trials.

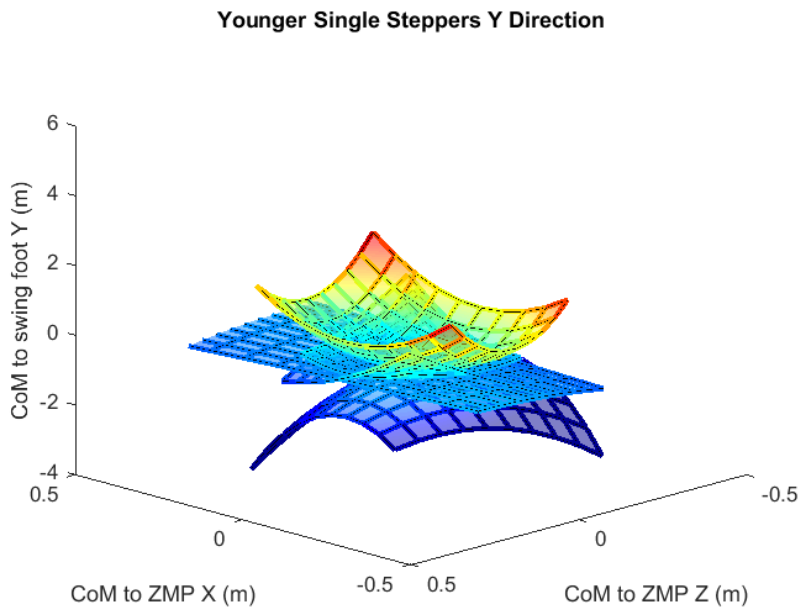

Figure 51: Surrogate response surface models of step foot y-direction task space from YSS cohort trials.

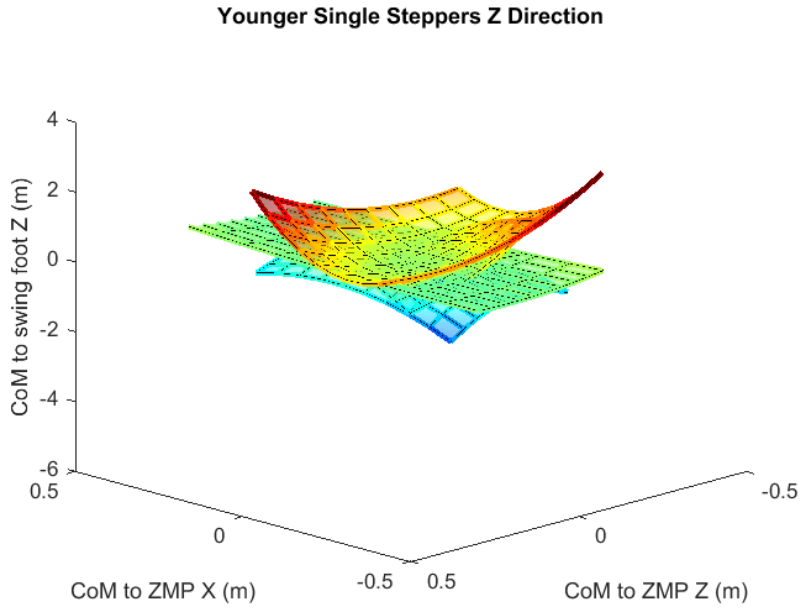

Figure 52: Surrogate response surface models of step foot z-direction task space from YSS cohort trials.

B2: Surrogate response surfaces for posture y and z components

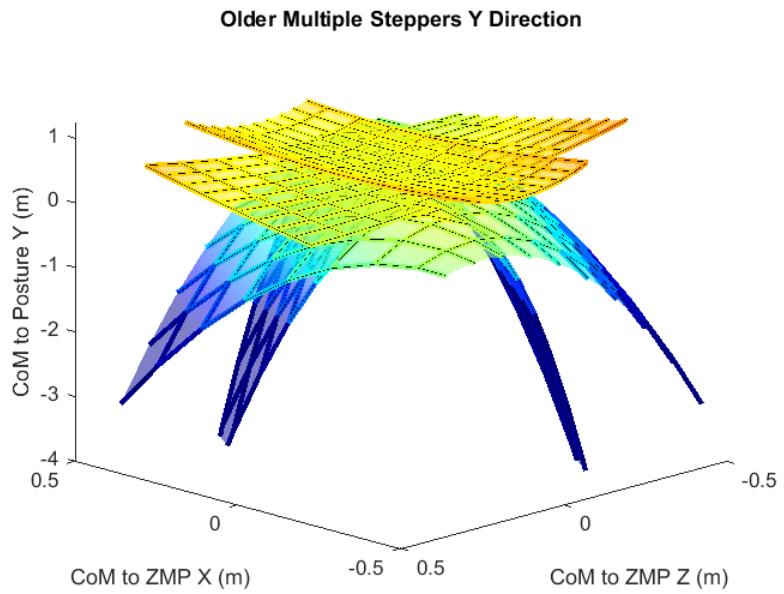

Figure 53: Surrogate response surface models of posture y-direction task space from OMS cohort trials.

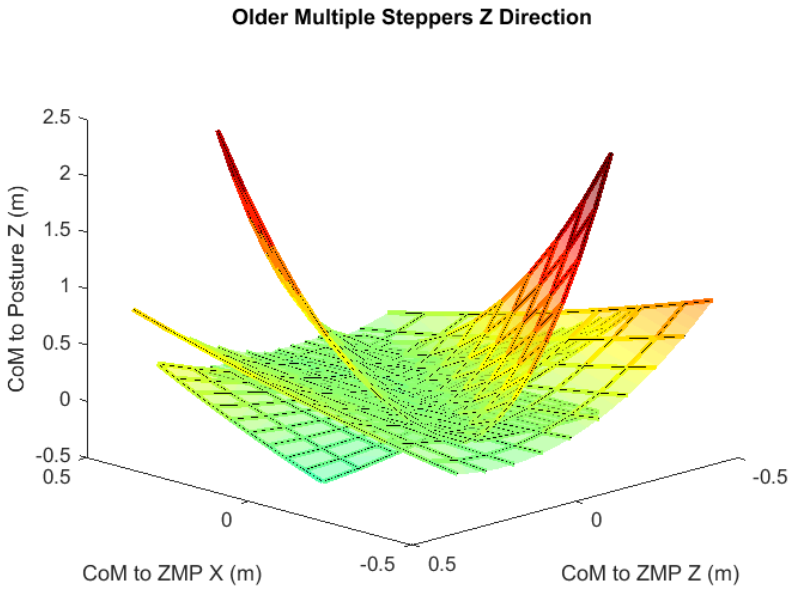

Figure 54: Surrogate response surface models of posture z-direction task space from OMS cohort trials.

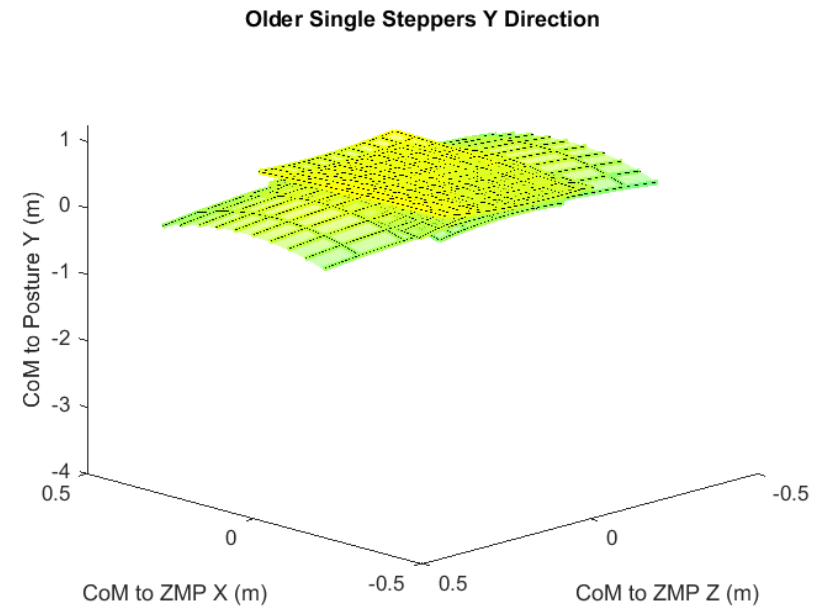

Figure 55: Surrogate response surface models of posture y-direction task space from OSS cohort trials.

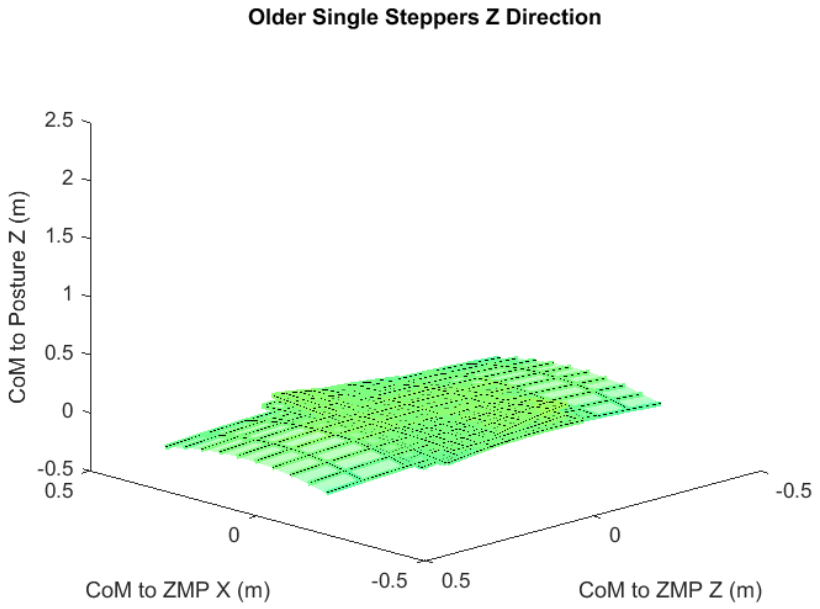

Figure 56: Surrogate response surface models of posture z-direction task space from OSS cohort trials.

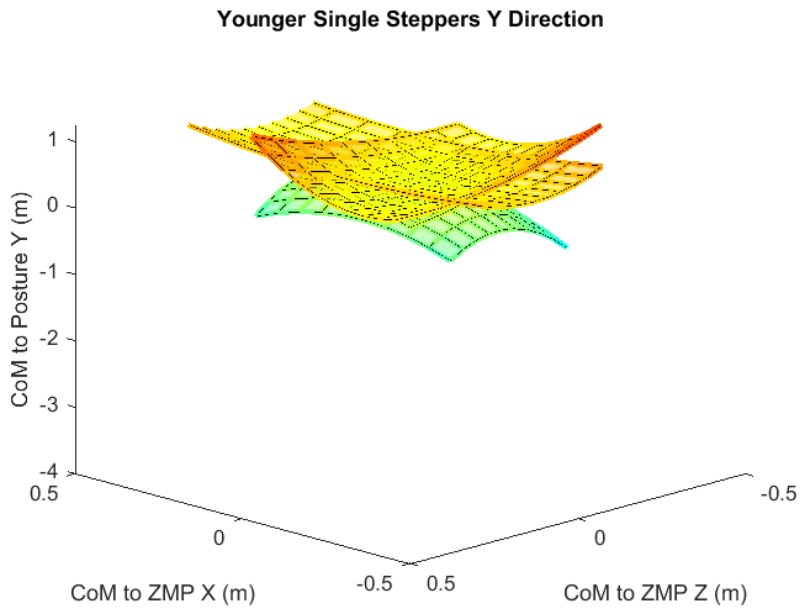

Figure 57: Surrogate response surface models of posture y-direction task space from YSS cohort trials.

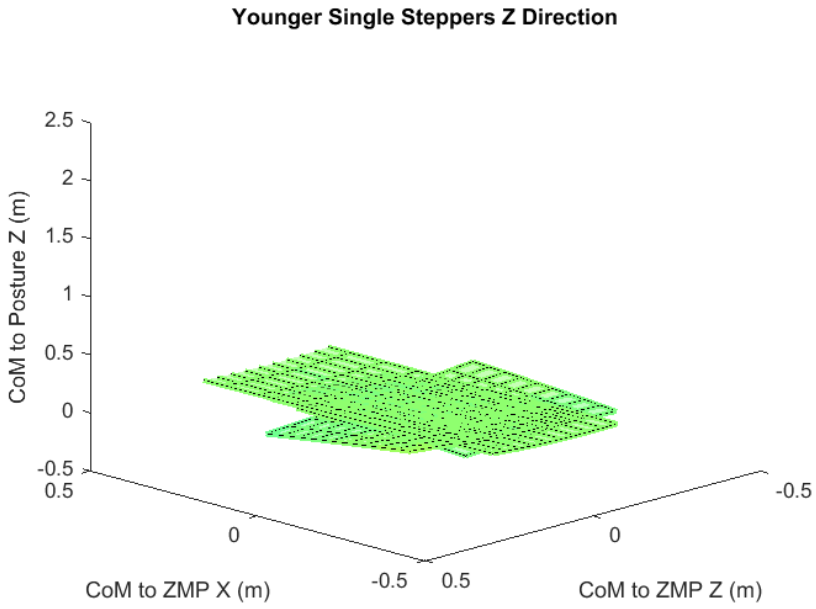

Figure 58: Surrogate response surface models of posture z-direction task space from YSS cohort trials.

Appendix C

C1: Trial 0010

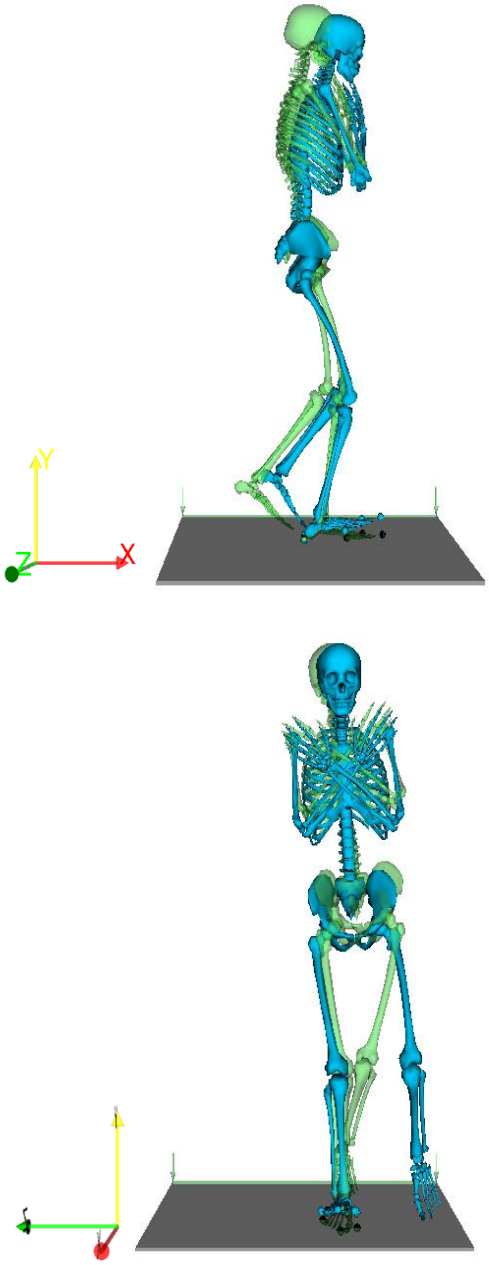

Figure 59: Depiction of the lateral (top) and front (bottom) view of the predicted response (blue) to the 6 cm anterior perturbation experienced by the subject in Trial 0010 and their experimental response (green).

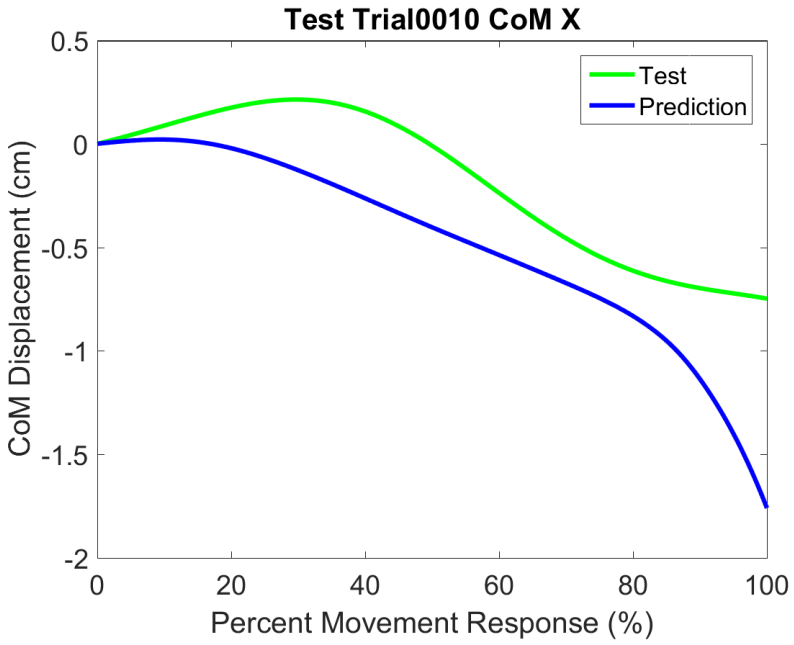

Figure 60: Displacement of center of mass in the x-direction from its initial position. Test line (green) represents experimental data collected from the subject during Trial 0010. Prediction line (blue) represents the system response to the same perturbation input.

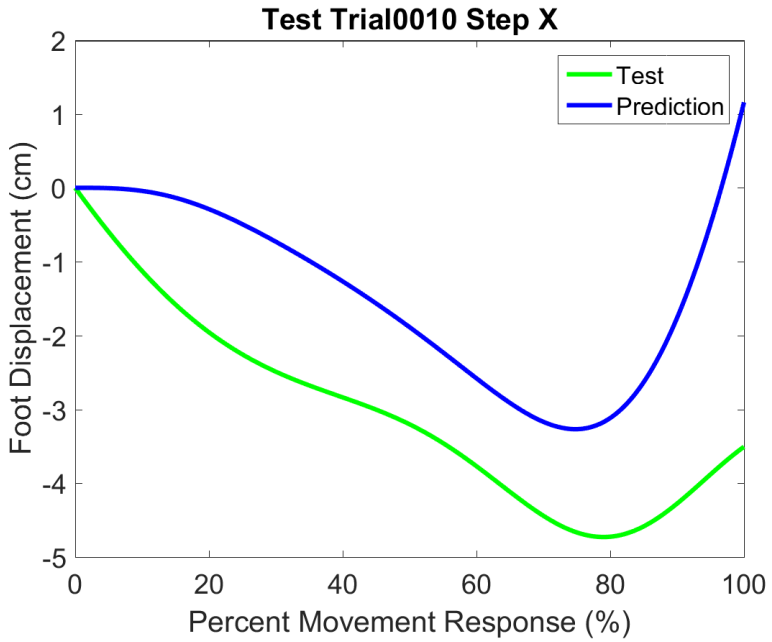

Figure 61: Displacement of step foot in the x-direction from its initial position. Test line (green) represents experimental data collected from the subject during Trial 0010. Prediction line (blue) represents the system response to the same perturbation input.

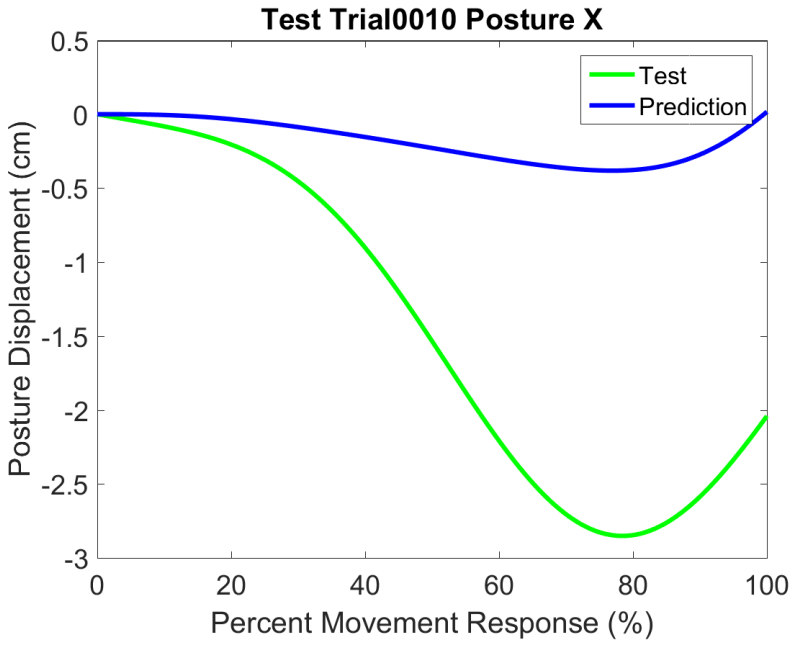

Figure 62: Displacement of posture in the x-direction from its initial position. Test line (green) represents experimental data collected from the subject during Trial 0010. Prediction line (blue) represents the system response to the same perturbation input.

C2: Trial 0018

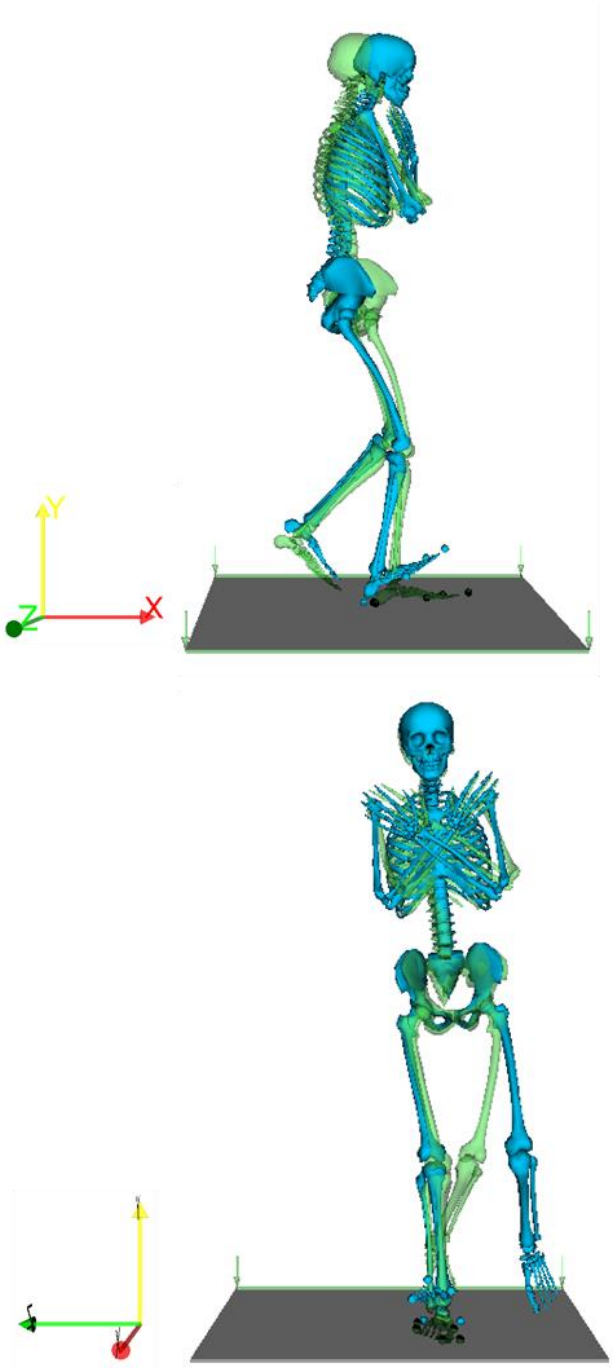

Figure 63: Depiction of the lateral (top) and front (bottom) view of the predicted response (blue) to the 12 cm anterior perturbation experienced by the subject in Trial 0018 and their experimental response (green).

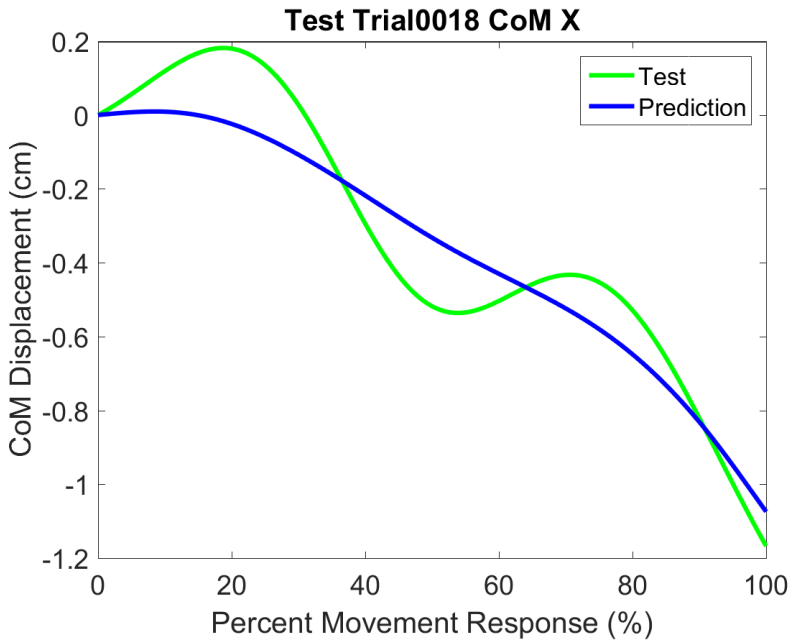

Figure 64: Displacement of center of mass in the x-direction from its initial position. Test line (green) represents experimental data collected from the subject during Trial 0018. Prediction line (blue) represents the system response to the same perturbation input.

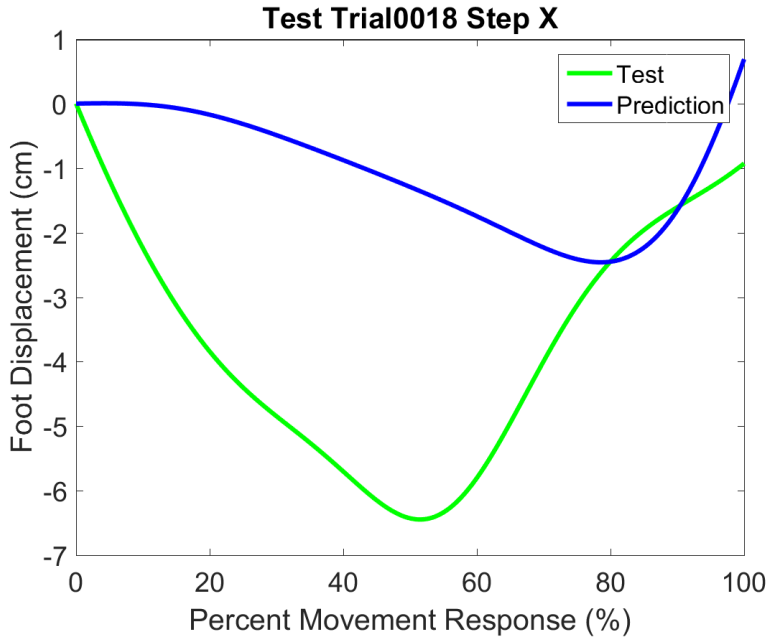

Figure 65: Displacement of step foot in the x-direction from its initial position. Test line (green) represents experimental data collected from the subject during Trial 0018. Prediction line (blue) represents the system response to the same perturbation input.

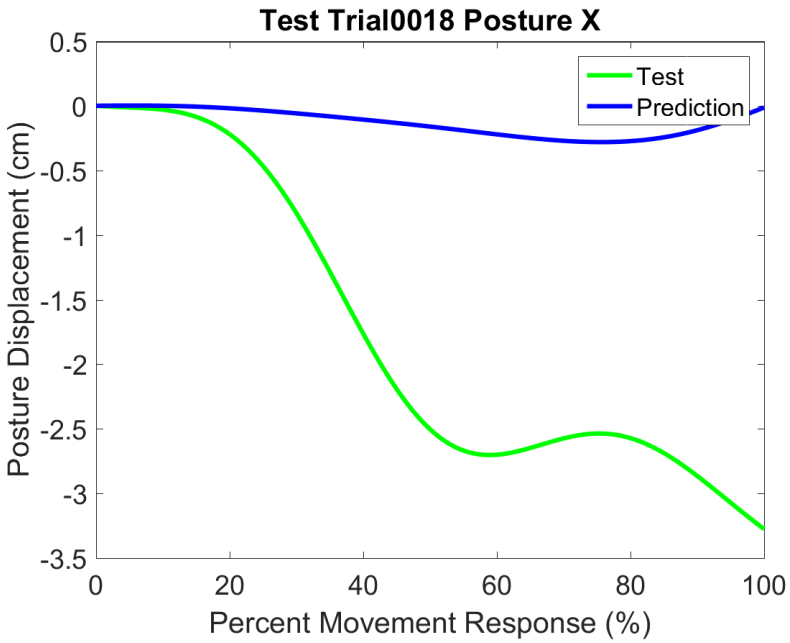

Figure 66: Displacement of posture in the x-direction from its initial position. Test line (green) represents experimental data collected from the subject during Trial 0018. Prediction line (blue) represents the system response to the same perturbation input.

C3: Trial 0063

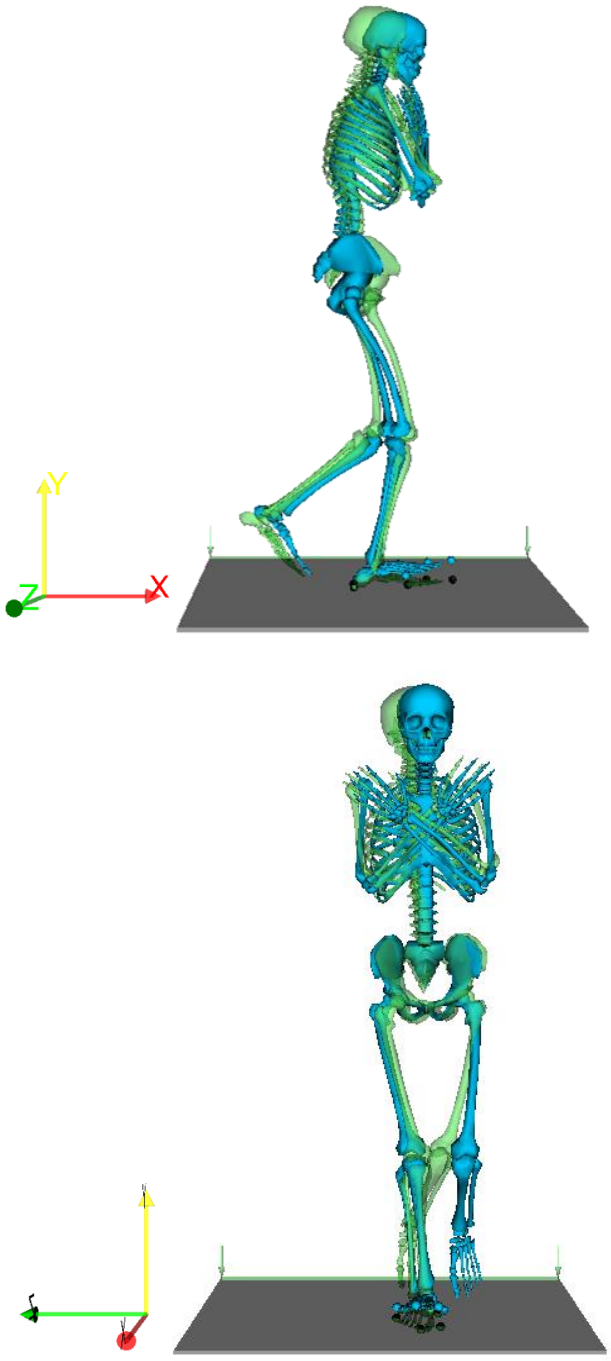

Figure 67: Depiction of the lateral (top) and front (bottom) view of the predicted response (blue) to the 6 cm anterior perturbation experienced by the subject in Trial 0063 and their experimental response (green).

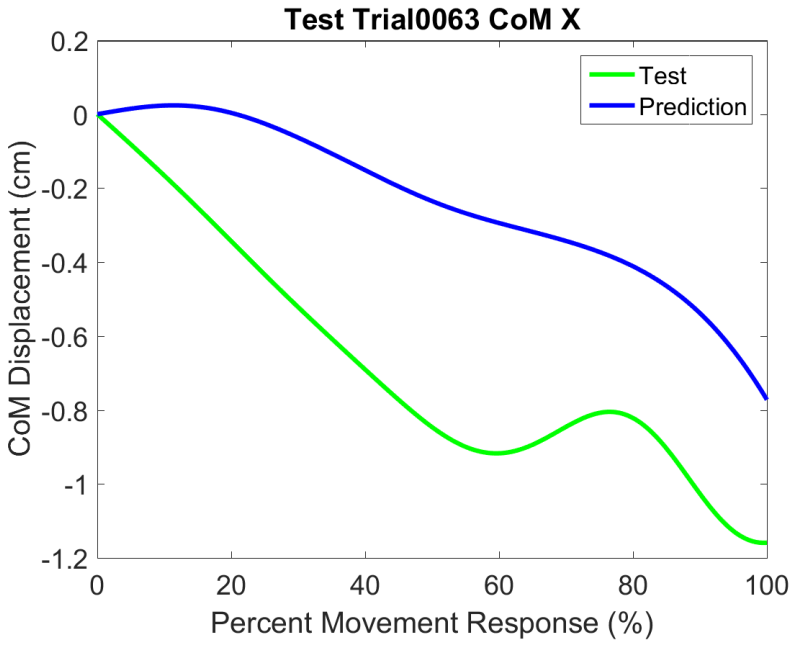

Figure 68: Displacement of center of mass in the x-direction from its initial position. Test line (green) represents experimental data collected from the subject during Trial 0063. Prediction line (blue) represents the system response to the same perturbation input.

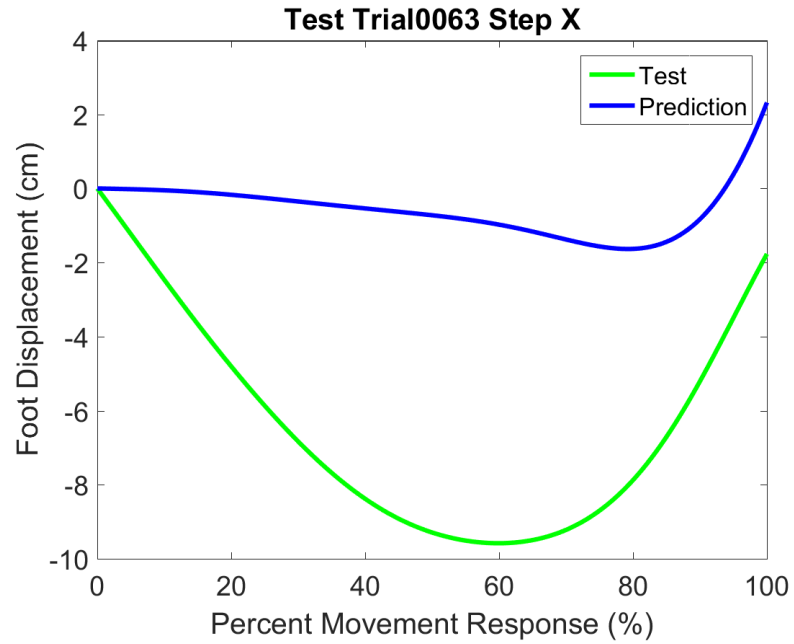

Figure 69: Displacement of step foot in the x-direction from its initial position. Test line (green) represents experimental data collected from the subject during Trial 0063. Prediction line (blue) represents the system response to the same perturbation input.

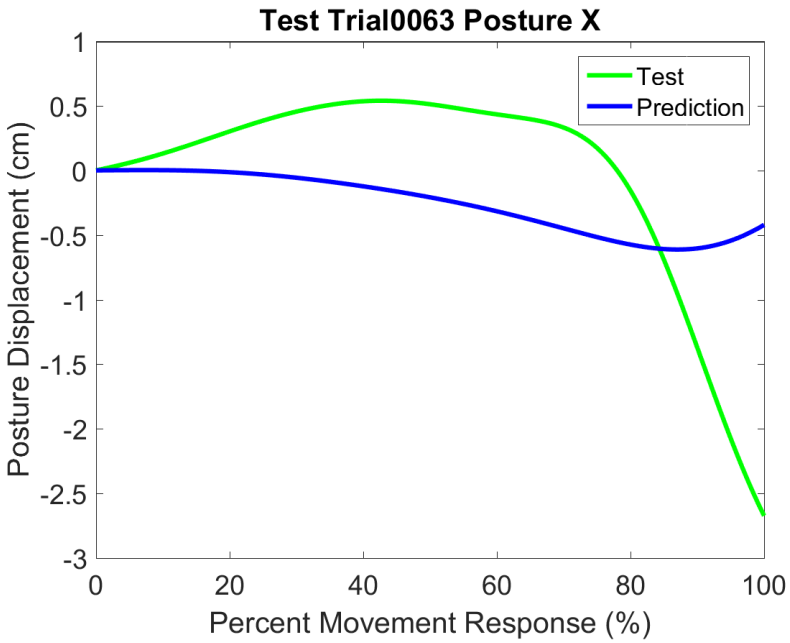

Figure 70: Displacement of posture in the x-direction from its initial position. Test line (green) represents experimental data collected from the subject during Trial 0063. Prediction line (blue) represents the system response to the same perturbation input.

C4: Trial 0075

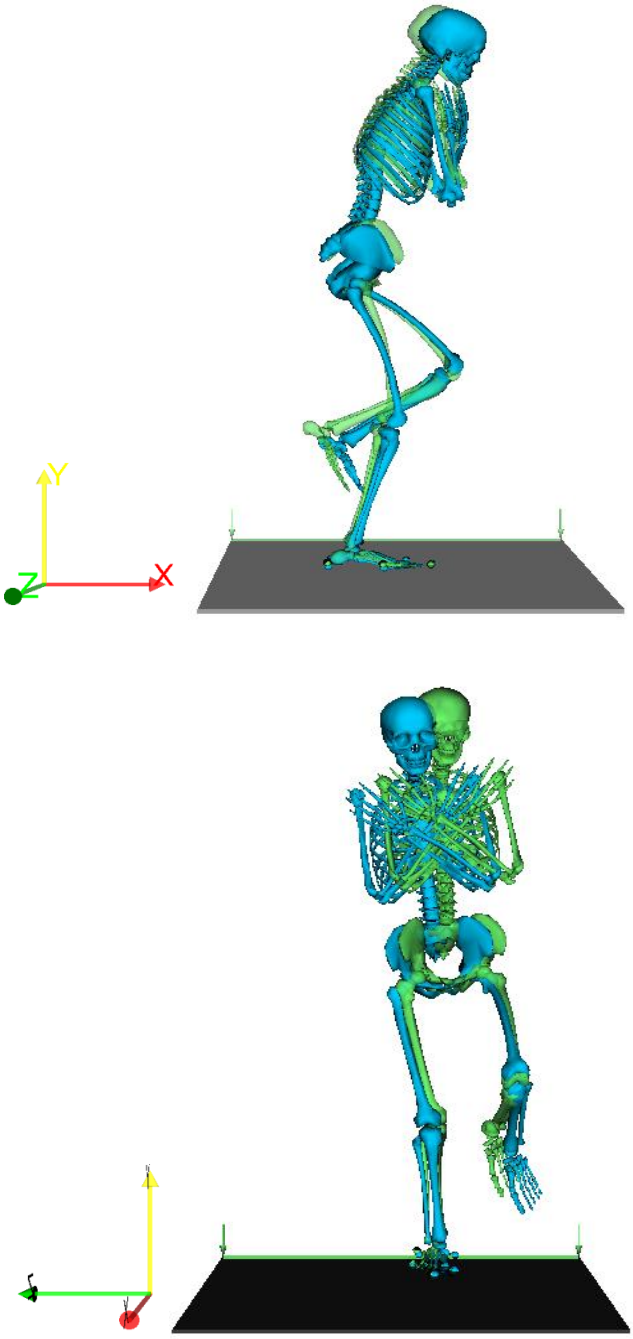

Figure 71: Depiction of the lateral (top) and front (bottom) view of the predicted response (blue) to the 6 cm posterior perturbation experienced by the subject in Trial 0075 and their experimental response (green).

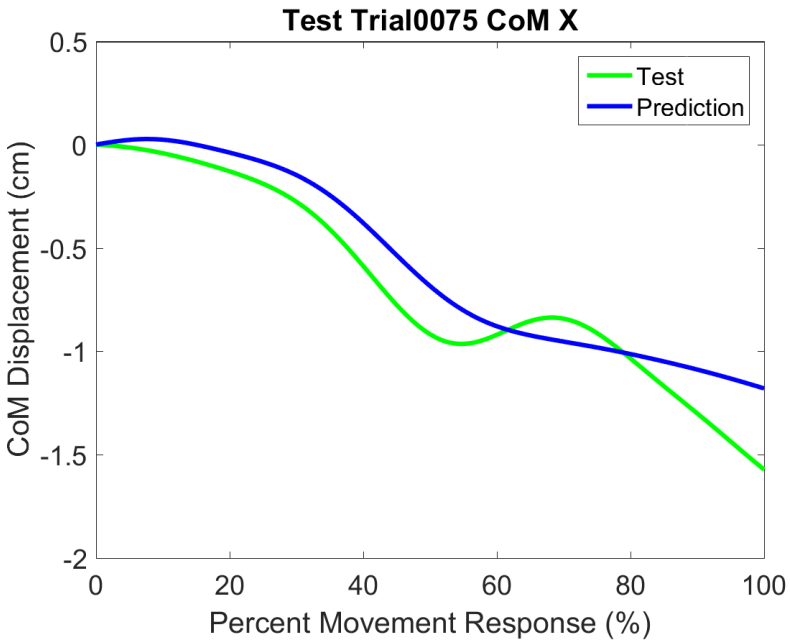

Figure 72: Displacement of center of mass in the x-direction from its initial position. Test line (green) represents experimental data collected from the subject during Trial 0075. Prediction line (blue) represents the system response to the same perturbation input.

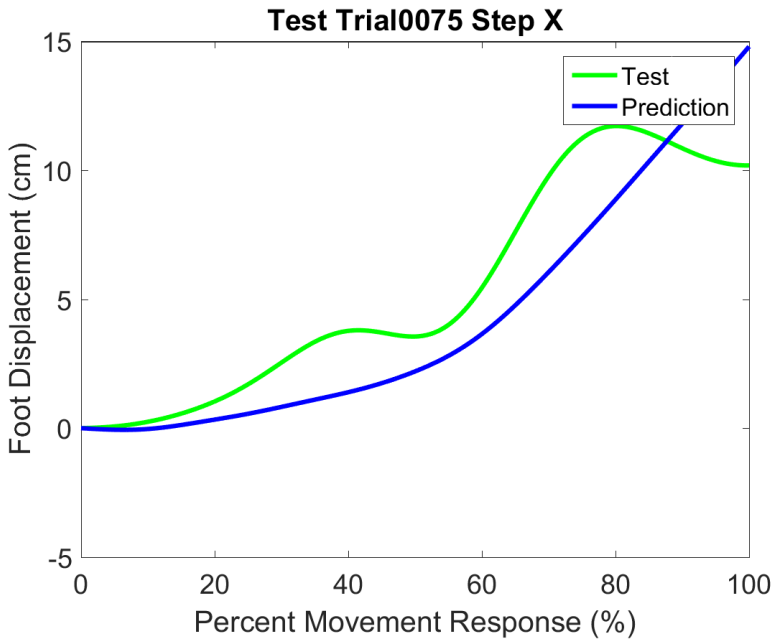

Figure 73: Displacement of step foot in the x-direction from its initial position. Test line (green) represents experimental data collected from the subject during Trial 0075. Prediction line (blue) represents the system response to the same perturbation input.

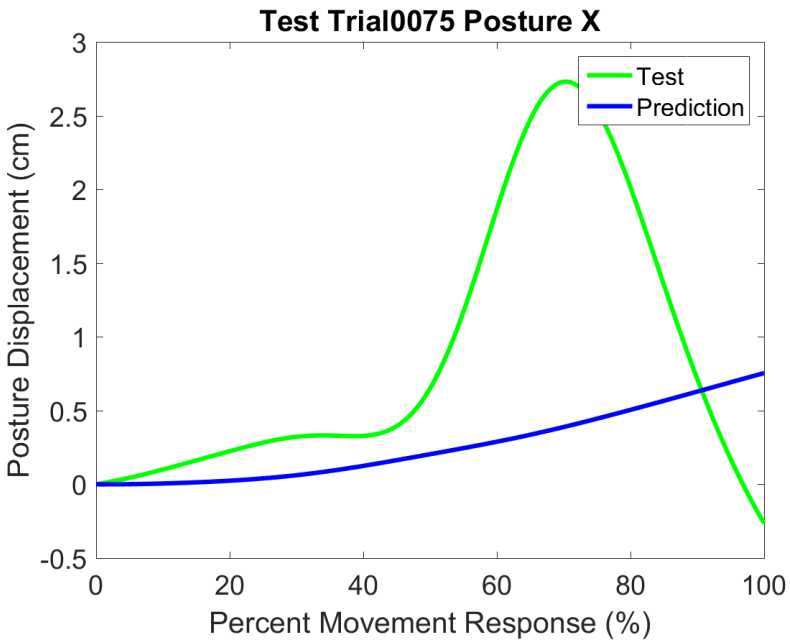

Figure 74: Displacement of posture in the x-direction from its initial position. Test line (green) represents experimental data collected from the subject during Trial 0075. Prediction line (blue) represents the system response to the same perturbation input.

C5: Trial 0077

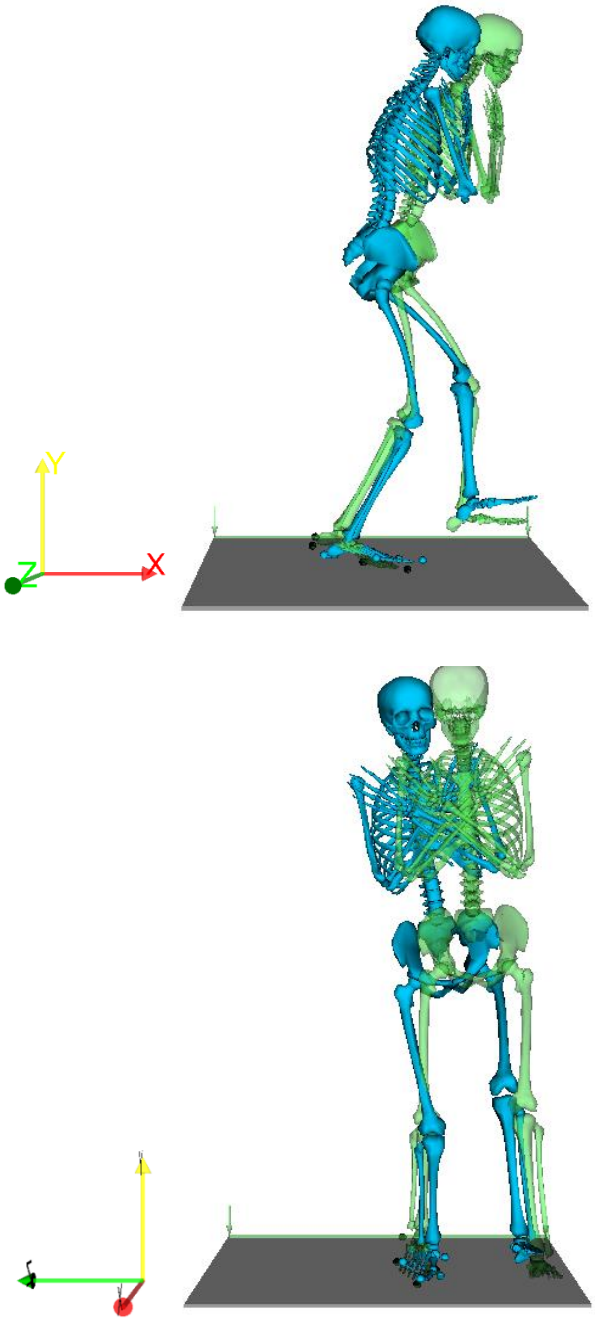

Figure 75: Depiction of the lateral (top) and front (bottom) view of the predicted response (blue) to the 12 cm posterior perturbation experienced by the subject in Trial 0077 and their experimental response (green).

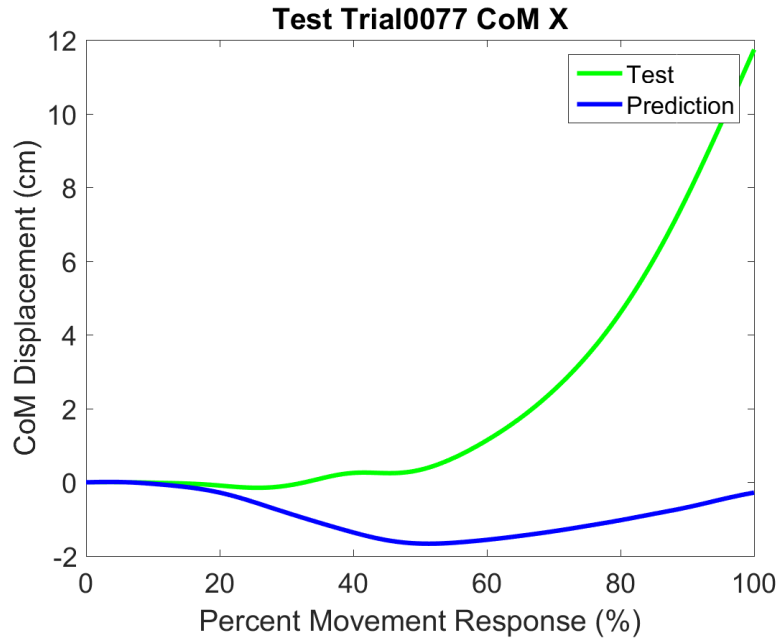

Figure 76: Displacement of center of mass in the x-direction from its initial position. Test line (green) represents experimental data collected from the subject during Trial 0077. Prediction line (blue) represents the system response to the same perturbation input.

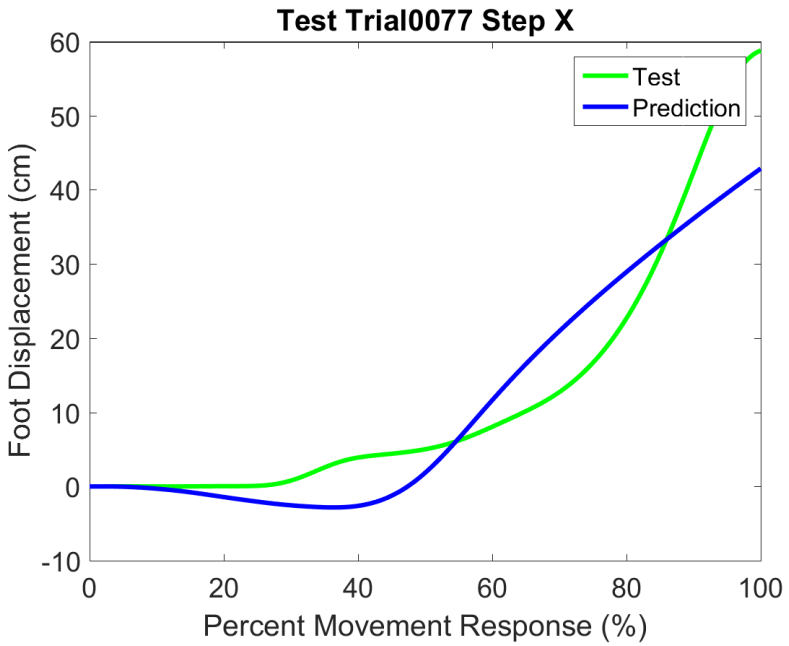

Figure 77: Displacement of step foot in the x-direction from its initial position. Test line (green) represents experimental data collected from the subject during Trial 0077. Prediction line (blue) represents the system response to the same perturbation input.

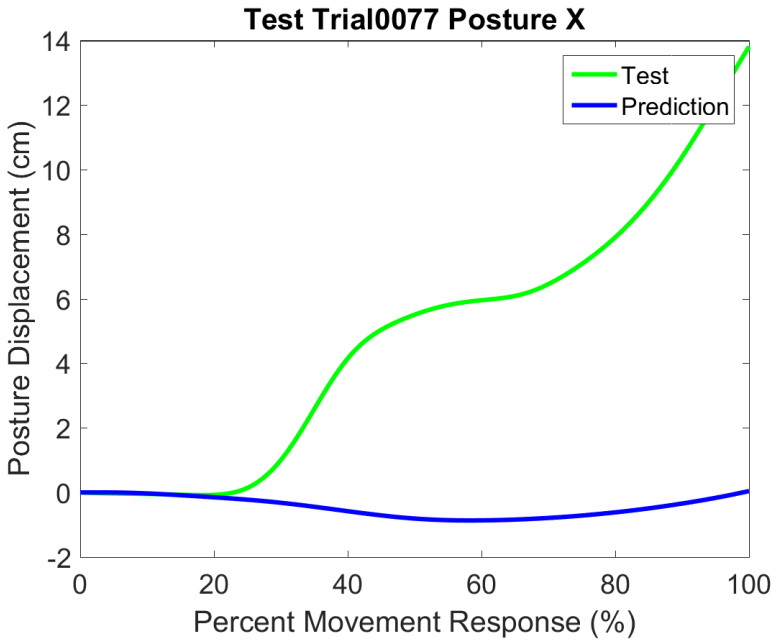

Figure 78: Displacement of posture in the x-direction from its initial position. Test line (green) represents experimental data collected from the subject during Trial 0077. Prediction line (blue) represents the system response to the same perturbation input.

C6: Trial 0085

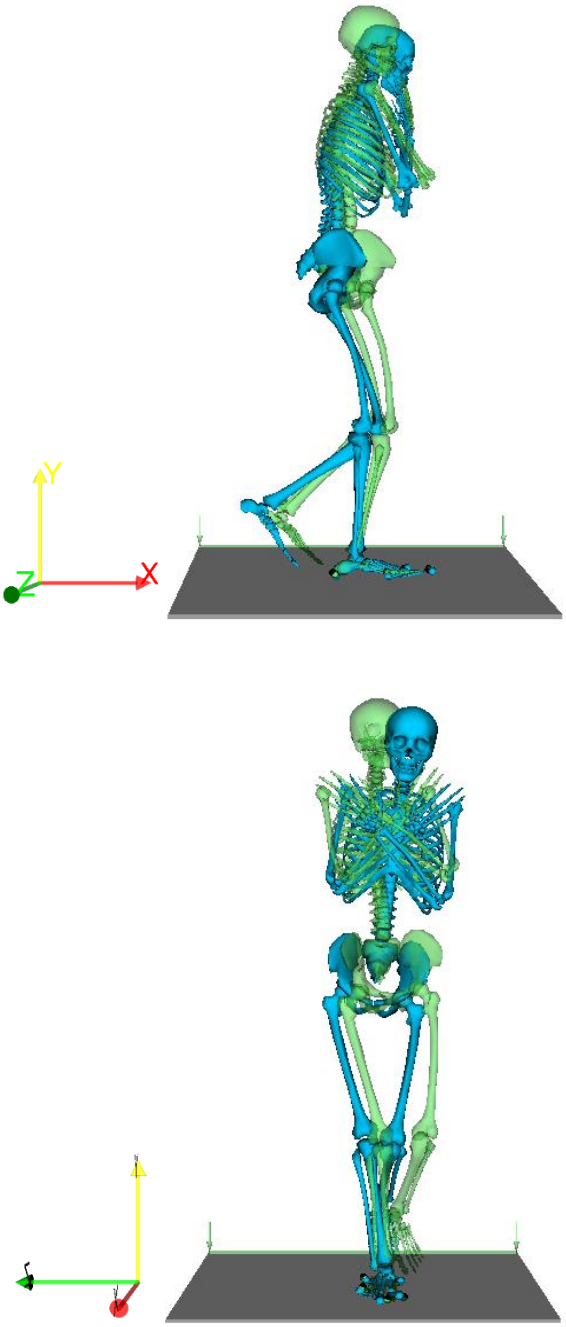

Figure 79: Depiction of the lateral (top) and front (bottom) view of the predicted response (blue) to the 6 cm anterior perturbation experienced by the subject in Trial 0085 and their experimental response (green).

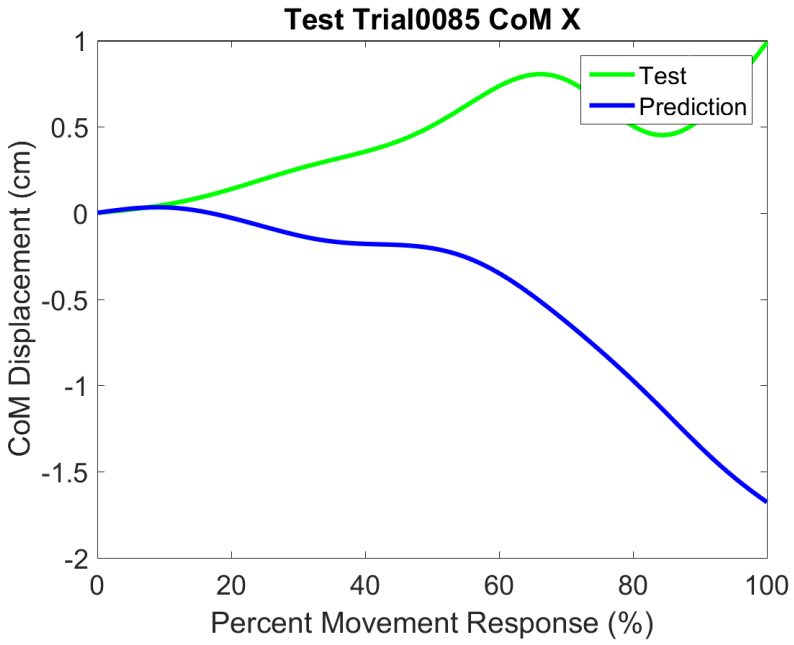

Figure 80: Displacement of center of mass in the x-direction from its initial position. Test line (green) represents experimental data collected from the subject during Trial 0085. Prediction line (blue) represents the system response to the same perturbation input.

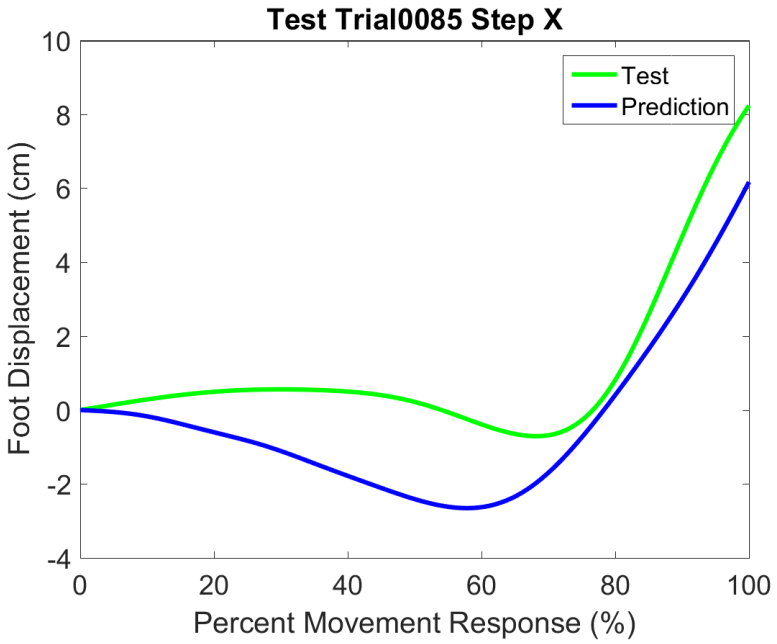

Figure 81: Displacement of step foot in the x-direction from its initial position. Test line (green) represents experimental data collected from the subject during Trial 0085. Prediction line (blue) represents the system response to the same perturbation input.

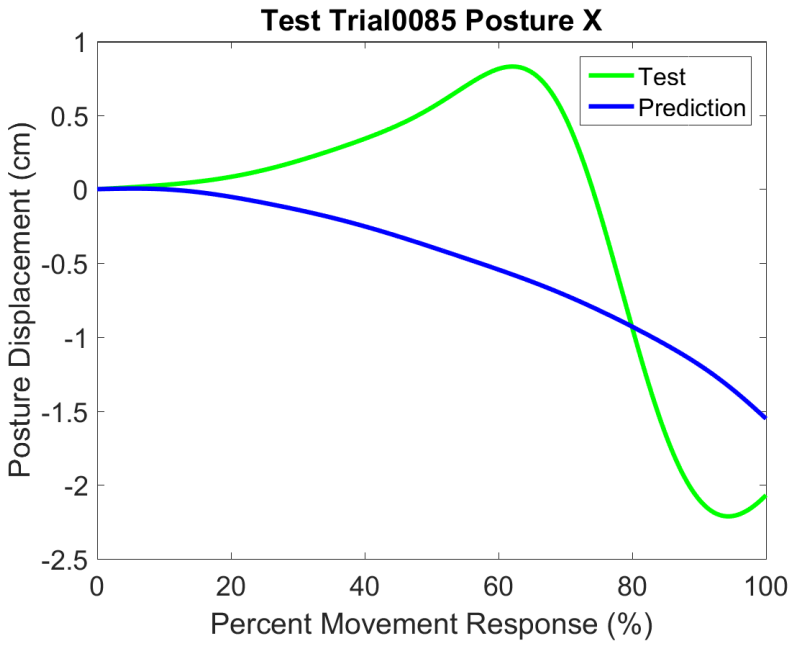

Figure 82: Displacement of posture in the x-direction from its initial position. Test line (green) represents experimental data collected from the subject during Trial 0085. Prediction line (blue) represents the system response to the same perturbation input.

Vita

Nicolas Vivaldi was born December 16, 1991 in Ft. Campbell, TN. He grew up in South Riding, VA where he graduated from Freedom High School and the LCPS Academy of Science in 2010. He received his Bachelor of Science in Biomedical Engineering with minors in Mechanical Engineering and Biophysics from The George Washington University, Washington, DC in May 2014. He then went on to pursue biomechanics research with the Reinbolt Research Group in the Neuromuscular Biomechanics Lab at the University of Tennessee, Knoxville where he finished his Master's Degree in Mechanical Engineering in December 2017, and his Doctor of Philosophy in May 2018.